Alma Mater Studiorum – Università di Bologna

DOTTORATO DI RICERCA IN

BIOLOGIA CELLULARE E MOLECOLARE

Ciclo 33

Settore Concorsuale:05/I1 – GENETICA

Settore Scientifico Disciplinare: BIO/18 GENETICA

Multi-omic analyses of the MYCN network unveil new potential vulnerabilities in childhood neuroblastoma

Presentata da: Roberto Ciaccio

Coordinatore Dottorato

Prof. Vincenzo Scarlato

Supervisore

Prof. Giovanni Perini

Esame finale anno 2021

Abstract

Neuroblastoma is the first neurogenic-extracranial solid cancer occurring in infancy and childhood. The genetic aberration most commonly associated with a poor prognosis is MYCN gene's amplification, which befalls in almost 20% of all cases. The MYCN gene encodes the N-MYC transcription factor, one of the three MYC gene family members recognized to impact tumorigenesis significantly. When gene amplification occurs and its activity is unleashed, N-MYC drives the development of many human cancers. We hypothesize that effective anti-MYC therapeutics can be developed by understanding the regulation and function of N-MYC in neuroblastoma. The MYC-targeted therapy could be of great relevance in neuroblastoma, considering the standard strategies' weakening approach in treating high-risk patients. Since N-MYC is an intrinsically disordered protein, it is still challenging to target this transcription factor; however, the model is shifting significantly after discovering novel therapeutic targets that impact MYC-driven tumorigenesis in various cancers. The following work explores how MYCN expression affects the induction and maintenance of neuroblastoma. By using different multi-omic approaches and many promising innovative techniques (RNA-seq, ChIP-seq, BioID coupled with LC-MS analyses, RNAi), we were able to identify and characterize new potential vulnerabilities of this pathology, which may work in concert with N-MYC for the instruction of a high-risk neuroblastoma phenotype. In this context, my studies' first objective was to investigate whether and how N-MYC can regulate transcription of lncRNAs by comparing transcriptional profiles between non-amplified and MYCN-amplified neuroblastoma cell lines. Among the several lncRNAs stimulated by N-MYC, we singled out lncNB1, which is selectively higher expressed in high MYCN cells only and it is also firmly and almost uniquely transcribed in neuroblastoma among all types of cancers. Our data showed that N-MYC directly activates transcription of lncNB1, instructing a complex network of molecular interactions, ultimately resulting in increased N-MYC protein stability, reinforcing the N-MYC oncogenetic program.

The second objective of this thesis was to assess how high N-MYC expression may cooperate to establish a dynamic regulatory axis through the interaction with the E2F3 transcription factor, impacting the development of the high-risk cancer phenotype. To better understand how E2F3 works as a function of the MYCN status and to consider the contribution of the two known E2F3 isoforms (E2F3a and E2F3b), we examined the complexity of their protein interactome by using the proximity-dependent biotin labelling technology (BioID) in both high and low MYCN expression conditions. These analyses revealed respectively 96 and 99 protein candidates belonging to the comprehensive proteomics map of both E2F3a and E2F3b proteins, underlining for the first time the mutual dependency of MYCN status and the proteomic profiling of these two transcription factors in neuroblastoma.

Taken together, our unbias screenings uncovered potential candidates that help to fill the knowledge gap in understanding what is the impact of N-MYC in childhood neuroblastoma, providing new opportunities for the development of specific treatments able to target the function of MYC oncoproteins in a context of MYCN gene amplification, shedding light on potential novel therapeutic applications for the treatment of this pathology.

Table of contents

INTRODUCTION 5

- *Epigenetics, an overview* 5
- *The "histone code", DNA methylation and chromatin organization* 6
- *Looking deeper at the histone acetyltransferases (HATs)* 8
- *Histone-DNA-RNA methylation* 9
- *Epigenetics in cancer* 11
- *Long non-coding RNAs (lncRNAs): new characters of the epigenomic era* 12
- *lncRNAs as potential novel targets for cancer therapy* 14
- *Neuroblastoma* 15
- *lncRNAs in neuroblastoma* 17
- *The MYC genes: new insights in cancer biology* 19
- *MYCN in neuroblastoma* 20
- *MYCN and epigenetic dysregulation in neuroblastoma* 21
- *MYCN in cell cycle progression* 23
- *E2F proteins, an overview* 24
- *E2F3a and E2F3b* 25
- *E2F proteins in neuroblastoma* 27
- *Promising therapeutic approaches in neuroblastoma* 29
- *Inhibition of the N-MYC/MAX interaction* 30
- *Targeting N-MYC stability* 30
- *Targeting N-MYC and its regulatory networks* 31

AIM 34

ABSTRACT SUMMARY 36

RESULTS (Part I) 37

- *Identification and functional characterization of the novel long non-coding RNA lncNB1 to promote N-MYC stabilization in high-risk neuroblastoma.* 37
- *LncNB1 is highly expressed in MYCN-amplified neuroblastoma cells* 37
- *High levels of lncNB1 correlate with patients' poor prognosis and bad outcomes* 42
- *lncNB1 downregulation reduces cell proliferation of MYCN-amplified neuroblastoma cells by diminishing N-MYC protein levels.* 43
- *lncNB1 regulates DEPDC1B expression to induce N-MYC protein stabilization* 45
- *lncNB1 upregulates E2F1 expression to increase DEPDC1B transcription* 46
- *lncNB1 is localized in the cytoplasm and binds the ribosomal protein L35 (RPL35)* 48

DISCUSSION (Part I) 50

RESULTS (Part II) 53

- *The role of the E2F3a and E2F3b proteins and their interactomes for the instruction of a novel functional axis with N-MYC in neuroblastoma.* 53

- *E2F3: a novel prognostic biomarker of neuroblastoma pathology* 53
- *E2F3a but not E2F3b is prognostic in neuroblastoma* 56
- *N-MYC increases E2F3a but not E2F3b expression in neuroblastoma* 58
- *N-MYC and E2F3a may instruct a synergic feed-forward loop to regulate transcription* 60
- *N-MYC and E2F3a genome-wide occupancy on chromatin* 62
- *N-MYC and E2F3a may physically interact* 64
- *BioID analyses revealed the huge complexity of E2F3s interactome* 66
- *High MYCN expression expands the protein interactome of E2F3a and E2F3b* 71

DISCUSSION (Part II) 74

THESIS CONCLUSIONS 77

MATERIALS & METHODS 79

- *BioID in cell culture* 79
- *BioID: Mass spectrometry analysis* 79
- *Cell culture* 80
- *Chromatin immunoprecipitation (ChIP) and ChIP-seq assays* 80
- *ChIP-seq (high-throughput data) from Gene Expression Omnibus – GEO -* 82
- *Clinical validation of E2Fs, MYC and MYCN genes* 82
- *Clonogenic assays* 82
- *Gene reporter assays* 83
- *GO analysis.* 84
- *GTEx RNA sequencing data analysis* 84
- *Immunoblot* 84
- *Immunoblot densitometry* 85
- *Immunofluorescence* 85
- *Lentiviral production and infection for stable cell lines generation* 86
- *Patient tumour sample analysis* 87
- *Plasmid transfection* 87
- *Proximity ligation assay (PLA)* 88
- *Real-time reverse transcription PCR (RT-qPCR)* 88
- *RNA fractionation assays* 90
- *RNA sequencing* 92
- *siRNA transfection* 92
- *TCGA RNA sequencing data analysis* 92
- *GST pull-down assay* 92
- *Statistical analysis* 93

REFERENCES 94

INTRODUCTION

Epigenetics, an overview

The Human Genome Project (HGP) has been a critical conquest in science's modern history, piloting the scientific community in a new life research era. Aside from the plethora of striking new findings regarding genome organization and function, several discoveries lead to the understanding that the information carried by the DNA sequence is not enough per se to justify most phenotypic variations. The system by which DNA is translated into proteins is not merely dependent on the nucleic acid sequence but also on a refined and complex regulatory mechanism that interplays between genetic and environmental factors. These processes mainly include the science of epigenetics and the control of gene expression through numerous biological interactions.

The term "epigenetics," which means "above genetics" is well-adapted to describe the study of stable alterations in gene expression that potentially arise during development and cell proliferation (Waddington, 2012). Epigenetic regulation is a crucial point during the broad spectrum of life, particularly during the development of the embryo or of the differentiation processes (Martello and Smith, 2014). It similarly arises in mature humans and mice, either by random changes or under environmental pressure (Issa, 2000). The fast increasing understanding of the epigenetic processes pinpoints post-synthetic modification of either the DNA itself or proteins intimately associated with DNA as essential mediators. These modifications are interpreted by proteins skilled in identifying specific changes and facilitating the appropriate downstream biological effects. The cells of a living multicellular organism are genetically unvarying biological entities containing the same genomic DNA that is processed and expressed differentially, due to the existence of molecular support known as nucleosome, an octamer of positively charged proteins called histones, available as two functional copies apiece of histone type H2A, H2B, H3, and H4 proteins. The 6 billion bases of coding and non-coding human DNA, wrapped in ~146 base pairs of DNA around histone octamers, are enfolded in about 30 million nucleosomes. This organization shapes an exquisitely regulated macromolecular complex termed chromatin, forming a tightly packed "molecular barrier" that limits the factor access to the genome (Luger, Dechassa and Tremethick, 2012; Flavahan, Gaskell and Bernstein, 2017).

The "histone code", DNA methylation and chromatin organization

Chromatin represents the "soil" through which transcription factors (TFs), pathways controlling cell growth and differentiation, and other signals can change gene activity and cellular phenotypes (Allis and Jenuwein, 2016). Eukaryotic cells can modify this barrier by dynamically changing DNA and histones at the specific nucleotide or amino acid residues, forming genomic areas selectively exposed for cellular machinery modifications. The specific functional consequences of the epigenetic alterations are associated with different gene expression levels, thus revolutionizing the modern concept of genetics and molecular biology.

The information was adapted to hypothesize the presence of a "histone code," which assumes that the existence and combination of specific DNA and histone modifications are linked to the regulation of transcriptional programs and gene expression phenomena by changing the chromatin structure or by inducing the recruitment of non-histone protein effectors to chromatin (Strahl and Allis, 2000; Kouzarides, 2007).

Looking deeper at the molecular organization, chromatin can be arranged into two different groups based on their physical and biochemical traits: the heterochromatin, characterized by a high level of condensation, which results in transcriptional inactivation and the decondensed, actively transcribed euchromatin.

The arrangement of heterochromatin and euchromatin is determined by the presence of a plethora of epigenetic modifications that were extensively linked to a massive variety of molecular processes. Histone phosphorylation and acetylation are the most common markers of euchromatin. While phosphorylation introduces negative charges, acetylation neutralizes the modified lysine residue's positive charge. Thus, both modifications can disrupt the interaction between histone and DNA, generating an open chromatin structure that facilitates transcriptional initiation/elongation.

On the other hand, heterochromatin is usually characterized by trimethylation of histone 3 lysine 9 (H3K9me3), which stimulates chromatin condensation together with the HP1 protein, resulting in a molecular barrier adept at avoiding the reprogramming of the cell identity (Becker, Nicetto and Zaret, 2016). Heterochromatin maintenance can be similarly mediated by a different mechanism known as DNA methylation, characterized by the inclusion of methyl groups to specific cytosines (5mC) or adenines (N6-mA) nucleotides (Wu *et al.*, 2016). DNA methylation is of particular interest for embryonic development; however, it is also associated with actively transcribed gene bodies and, in specific contexts, with gene activation. This epigenetic mark can be mitotically inherited and is required to boost

transcriptional repression when found at the start sites of mammalian genes. Some common examples are the classical epigenetic phenomena of genomic imprinting and X-chromosome inactivation (XCI), which work in concert with histone modifications for the epigenetics' truthful maintenance state (Greenberg and Bourc'his, 2019). The increasing list of histone post-translational modifications (PTMs) and the functional heterogeneity of DNA methylation have expanded in the latest years due to the substantial novelties in multi omics-approaches (Greenberg and Bourc'his, 2019). The majority of the histone PTMs are localized on the evolutionary conserved N-terminal or C-terminal tails of the histone sequence or their globular domains that physically interact with DNA through chemical modifications including acetylation, methylation, phosphorylation, and ubiquitylation but also the newer acylation, hydroxylation, glycation, serotonylation, crotonylation, glycosylation, sumoylation and ADP-ribosylation (Chan and Maze, 2020)**.** Overall, PTMs control the chromatin-binding affinities of many proteins like transcription factors, chromatin remodelers, and the transcriptional machinery's apparatuses. The model was confirmed by demonstrating the presence of chromatin-binding modules, such as the *chromodomains* and PHD fingers, which recognize and bind to methylated histones and *bromodomains* and *Yeats domains,* which bind to acetylated histones (Musselman *et al.*, 2012; Verdin and Ott, 2015).

Based on their functions, epigenetic modifiers and modulators can be classified into three different subgroups: *writers*, *readers*, and *erasers*. The functional interactions between these three classes form a regulatory network to trigger a specific transcriptional event by working on the dynamic regulation and stabilization of chromatin condensation/decondensation (Soshnev, Josefowicz and Allis, 2016). Histone writers, erasers, and readers are among the key components for comprehending the epigenetic landscape in several mammalian cell types. Writers and erasers are enzymes proficient in tagging and removing PTMs at specific histone residues, respectively, while histone readers like histone deacetylases (HDAC), histone phosphatases, deubiquitinating enzymes (DUBs), histone and DNA demethylase (Atanassov, Koutelou and Dent, 2011; Cheng, 2014; Gil and Vagnarelli, 2019; Wong *et al.*, 2019; Milazzo *et al.*, 2020) are proteins that can recognize and decipher specific post-translational modifications (Gillette and Hill, 2015)

Looking deeper at the histone acetyltransferases (HATs)

The extraordinary richness of PTMs define a complex mixture of epigenetic combinations that can be associated explicitly with chromatin when prone or refractory to transcription. A detailed type of histone modifications characterizes the open chromatin. Indeed, the acetylation of the lysine 27 at Histone 3 (H3K27ac) and the monomethylation of the lysine 4 of the same protein (H3K4me1) are associated with active enhancers (Creyghton *et al.*, 2010), while the enrichment in H3K4me3 and H3/H4 acetylation are specific at the proximal promoters of active genes (Barrera *et al.*, 2008), generally along with with H3K79me3 (Ng *et al.*, 2003), H2BK120u1 (Batta *et al.*, 2011), and H3K36me3 close to the 3′ end (Pokholok *et al.*, 2005). H3K4me3 and H3/H4 acetylation generally co-occur at the start sites of active genes. In particular, H3K4me3 can stimulate the recruitment of specific histone acetyltransferase complexes (HATs) to increase H3/H4 acetylation levels. By definition, HATs are enzymes capable of acetylating core histones, leading to essential effects on chromatin structure, assembly, and gene transcription. HATs are evolutionarily conserved in eukaryotic cells (Kimura, Matsubara and Horikoshi, 2005), and embrace several components that drastically influence the functions of the catalytic core subunits of the complex (Utley and Côté, 2003). This class of proteins can be clustered into two large canonical and one non-canonical groups (Kimura, Matsubara and Horikoshi, 2005) based on the catalytic domain:

1. GNATs (GCN5 N-acetyltransferases): This group comprises KAT2A (GCN5), KAT2B (PCAF), Elp3, Hat1a, Hpa2, and Nut1a proteins;
2. The MYST HATs: this group is composted by Morf, Ybf2 (Sas3), Sas2, and Tip60;
3. CBP/p300: non-canonical histone acetyltransferases

HAT complexes are characterized by several subunits, which confer exclusive characteristics after the assembly. A key example is the dichotomy between the SAGA/STAGA (Spt-Taf9-Ada-Gcn5-Acetyltransferase) and ATAC (Ada-Two-A-Containing) HAT complexes. The GCN5-containing SAGA complex was first identified in yeast as a multi-modular HAT complex (Grant *et al.*, 1997). This complex is highly conserved (Spedale, Timmers and Pijnappel, 2012) and is composed of 19 subunits structured in 4 different modules (G. Liu *et al.*, 2019; Papai *et al.*, 2020; Wang *et al.*, 2020). On the other hand, the ATAC complex appears to be exclusively expressed in multicellular eukaryotes (Spedale, Timmers and Pijnappel, 2012), and it includes specific elements like the ZZZ3 DNA-binding protein and the reader YEATS2, which are essential for the assembly of the complex (Mi *et al.*, 2017). Although they share several components – including the catalytic HAT protein KAT2A or KAT2B – they can target distinct genomic loci to exert differential functions. Indeed, SAGA

is principally found at the proximal promoters, while ATAC is engaged to both promoters and enhancers, depending on the cell type and context (Krebs *et al.*, 2011).

GCN5 is required for H3K9 acetylation (H3K9ac), which correlates to active promoters (Brownell *et al.*, 1996), but it was recently demonstrated to catalyze both succinylation and crotonylation; two different PTMs related to transcriptional activation (Wang *et al.*, 2017; Kollenstart *et al.*, 2019).

In pathological contexts, such as cancer, HATs displayed both tumour suppressive and oncogenic activities, which can trigger tumour initiation and cancer development. Histone acetylation increases the chromatin availability, leading to a higher level of gene transcription (Strahl and Allis, 2000). Histone hyperacetylation is considered a negative prognostic marker in several types of cancer like hepatocellular carcinoma, prostate cancers, and glioma (Bai *et al.*, 2008; Liu *et al.*, 2010; Bianco-Miotto *et al.*, 2016). However, HATs can also display tumour suppressive effects even in the same tumour variety, like KAT3B in colorectal cancer (Gayther *et al.*, 2000; Ishihama *et al.*, 2007).

HATs can also induce transcriptional initiation of specific genes through the interaction with transcription factors like CREB, nuclear hormone receptors, and oncoprotein-related activators such as c-Fos, c-Jun, c-Myb (Sterner and Berger, 2000) E2F1 and C-MYC (Lang *et al.*, 2001; Patel *et al.*, 2004) by generally increasing their protein stability.

Histone-DNA-RNA methylation

Although it is clear how chromatin organization can influence gene expression regulation, there is still little evidence about the mechanisms for setting up and maintaining these epigenetic marks during various biological processes like DNA replication and cell division.

Methylation plays a crucial role in exerting these functions: It is borne by both DNA, RNA and proteins through the action of specific chemical reactions and different sets of enzymes, which interplay together for the modulation of numerous gene expression programs in several organisms (Michalak *et al.*, 2019).

While DNA methylation arises predominantly at the palindromic CpG islands (Jin, Li and Robertson, 2011), histone methylation principally occurs on the side chain of lysines and arginines (Clarke, 1993). This scenario is more intricate for RNAs, which can expose more than 100 different types of methyl-modifications that can occur post-transcriptionally or co-transcriptionally, many of which are still not fully understood (Xuan *et al.*, 2018).

From a functional perspective, the silencing of the repetitive DNA elements through DNA methylation is significant to preserve genome integrity (Guenatri *et al.*, 2004). DNMT1, DNMT3A and DNMT3B were identified as the three active DNA methyltransferases in mammals (Robertson and Wolffe, 2000). DNMT1 works as a maintenance methyltransferase, while DNMT3A and DNMT3B are primarily de novo methyltransferases (Cheng, 2014). However, some new lines of evidence suggests that these peculiarities are not absolute, as determined by the type of repetitive elements taken into consideration (Arand *et al.*, 2012).

Regarding histones, three families of enzymes have been shown to catalyze the addition of methyl groups:

1. SET-containing domain as SUV39H1, SUV39H2, G9A, GLP, and SETDB1;
2. DOT1-like proteins;
3. The N-methyltransferase (PRMT) protein family that has been shown to methylate arginine residues.

Heterochromatin contains decreasing values of acetylation and, on the other hand, it is characterized by high levels of H3K27me2/3, H3K9me2/3, and H4K20me3 (Trojer and Reinberg, 2007).

Some methylated histone residues can additionally work as open chromatin markers to instruct specialized transcriptional programs: one of the most common examples is the post-translational modification of H3K4, which can be mono-/bi- or three methylated.

H3K4me3 is a marker of both enhancers and promoters of actively transcribed genes, and correlating with the recruitment of the pre-initiation complex and the RNA polymerase II (Santos-Rosa *et al.*, 2002; Wang *et al.*, 2008). This PTM works as an anchor to recruit multicomponent complexes like SAGA, which help transcriptional activation (Pray-Grant *et al.*, 2005)**.**

Differently, H3K4me1 is highly enriched at enhancers (Cheng *et al.*, 2014), while H3K4me2 can be generally found at the active gene bodies (Pokholok *et al.*, 2005).

The distinctions between global and local methylation levels upon histones and DNA are crucial new research focuses on cancer research.

Many mutations in cancer genomes occur in various enzymes capable of exerting methyl- and dimethyl- catalytic activities, revealing novel strategies used by cancer cells to change DNA methylation patterns and induce the malignant transformation (You and Jones, 2012).

The widespread loss and gain of H3K27me3 is a clear example to elucidate how the deregulation of histone methylation pathways reflects changes in gene expression and genome integrity.

This process can occur in different ways, including recurrent gain- or loss- of function mutations in the EZH2 gene, the catalytic subunit of the Polycomb repressive complex 2 (PRC2) which is crucial for this modification (Piunti and Shilatifard, 2016).

Epigenetics in cancer

Over the last few years, it has become clear how mutations on genes encoding proteins and RNAs that control epigenetic alterations are prevalent in human cancers. Several mutations stimulate tumour induction, whereas others affect cell growth, immune invasion, metastasis, heterogeneity, and drug resistance. Therefore, targeting epigenetic mutations is increasingly recognized as an outstanding therapeutic strategy for several diseases like neurological disorders, autoimmune and cardiovascular pathologies, and cancer (Arrowsmith *et al.*, 2012).

The expanding epigenomic revolution allowed us to shed light on the relationship between epigenetic alterations on oncogenes and the possibility that they may be required to trigger tumour progression, thus helping elucidate several driving effects in different cancer pathologies. This model was later confirmed and strongly supported by several pieces of evidence, particularly in paediatric tumours, for which it has been possible to establish the role of the epigenetic alterations in driving cancer development and progression .

At the light od these findings, the traditional classification of cancer-related genes as oncogenes or tumour suppressors has been re-interpreted by introducing new larger classes comprising the suggested epigenetic functional classification. These novel categories resulted in the identification of new emerging protein functions that are known as epigenetic *modulators*, *modifiers*, and *mediators* (Feinberg, Ohlsson and Henikoff, 2006; Feinberg, Koldobskiy and Göndör, 2016).

The intrinsic properties of tumour stemness are required during malignant transformation to regulate cellular self-renewal and multiple proliferating-pathways. The mediators are encoded by genes that are hot spot of epigenetic modifications, and are charcterized by rare mutatios that are critical for the formation of cancer stem cells. Some key examples are the pluripotency factors NANOG (Fischedick *et al.*, 2014), OCT4 (Lengner *et al.*, 2007), and the WNT signalling members (Serman *et al.*, 2014; Poli *et al.*, 2018). Epigenetic-mediator-driven modifications in the chromatin landscape of the cells and of their altered functions, often result in cancer development. These examples are essential to understand how cancer cells can instruct a set of commands within the expanding tumour and between the tumour and its microenvironment (Medema, 2013).

The activation of cell reprogramming is closely-dependent on the activity and localization of several epigenetic modifiers, which can subvert specific epigenetic states under the control of epigenetic modulators. That activation usually results in a change in the chromatin architecture of pro-tumourigenic genes and in the acquisition of stem-like features of the cancer cell (Feinberg, Koldobskiy and Göndör, 2016).

Long non-coding RNAs (lncRNAs): new characters of the epigenomic era

The recent signs of progress in the field of epigenomic allowed the identification of a new pivotal discipline of study known as "epitranscriptome" or "RNA epigenetics" that is responsible for the study of novel RNA molecules and the various chemical modifications of cellular RNAs that implies new layers of regulation on gene expression and diseases (Wang and He, 2014; Dominissini *et al.*, 2016; Helm and Motorin, 2017). Advances in RNA sequencing technologies revealed the complexity of our genome (Costa *et al.*, 2010). The HGP has shown that at least 75% of DNA is transcribed into RNAs, while protein-coding genes comprise only 1% of the whole human genome (Harrow *et al.*, 2009). Formerly, many genomic regions that are transcribed into non-coding RNAs (ncRNAs) had been viewed as 'junk' DNA without biological meaning (Feingold *et al.*, 2004; Doolittle, 2013). In the last years, however, there has been an incredible expansion in the functional studies on these transcripts. Several chromatin signatures such as H3K4me3, H3K9ac or H3K36me and DNAse hypersensitive support evidence of non-coding transcription in the intergenic regions. These improvements allowed the discovery of many types of ncRNAs that appear to be essential for proper cell development. Long non-coding RNAs (lncRNAs), which consist of non-protein-coding transcripts longer than 200 nucleotides, have received much attention for their abundance and tissue-specific expression in physiological and pathological processes (Rinn and Chang, 2012). Many studies demonstrated the central relevance of these molecules in protein synthesis, RNA maturation, RNA transport, gene silencing, chromosome conformation, and translation control, although most of these transcripts are functionally not fully characterized. The majority of the lncRNAs are transcribed by the RNA polymerase II and later capped at the 5'end, spliced, and poly-adenylated. We can distinguish lncRNAs as signals, decoys, guides, and scaffolds (Balas and Johnson, 2018).While some lncRNAs are just sub-products of transcription, many others have essential regulatory functions, thereby suggesting new signal mechanisms of cell regulation independent from protein translation. Several experimental shreds of evidence suggest that lncRNAs can work as molecular signals due to their specific cell and tissue expression, leading to the activation of precise pathways in response to various stimuli (Kim and Sung, 2012; Schmitz, Grote and Herrmann, 2016).

They may also work as decoys by taking away proteins from specific genomic loci, thus acting as a molecular competitor to negatively regulate gene transcription. The RNA-binding proteins (RBPs) are usually transcription factors, chromatin modifiers, or other regulatory factors. For this reason, lncRNAs would presumably act by depressing the mechanism of an effector (Kugel and Goodrich, 2013). These molecules have been demonstrated to interact with chromosome-modification complexes and guide them to specific target genes. The guiding lncRNAs are essential for the proper localization of the chromosome-modification complexes and can carry several gene expression changes acting in cis (in the nucleus) or trans (in nucleus or cytoplasm). The binding protein complexes can work as repressors or activators and have essential roles in gene expression modifications. Their functions seem to be directly connected to the activity of the tether effector complexes (Kugel and Goodrich, 2013)(Khalil *et al.*, 2009; Gupta *et al.*, 2010; Kugel and Goodrich, 2013).

LncRNAs can also work as scaffolds upon which relevant molecular components are assembled. This class of lncRNAs possesses different domains capable of binding effector molecules with transcriptional activating or repressive activities (Tsai *et al.*, 2010; Yoon *et al.*, 2013)

All the processes described above are dependent on the subcellular context in which they are.

LncRNAs can be localized both in the nucleus and in the cytoplasm and affect the cell's ability to express specific genes by direct or subsidiary strategies (Engreitz, Ollikainen and Guttman, 2016).

In particular, cytoplasmic lncRNAs regulate RNA expressions at the post-transcriptional level by helping mRNA decay, mRNAs stabilization, and promoting or inhibiting target mRNAs' translation through extended base-pairing. They can influence gene regulation by acting, for example, as decoys for miRNAs and proteins involved in translational processes. Conversely, in the nucleus, the role of lncRNAs is different: they play a predominant part in the organization of nuclear domains and, in general, they can be classified into two subgroups based on their cis or trans-regulatory mechanisms. Cis-acting lncRNAs are close to the site of transcription and can directly influence the expression of neighbour genes. In contrast, trans-acting lncRNAs need to be relocated from their synthesis sites to impact gene regulation, functioning either globally or in a gene-specific manner (Engreitz, Ollikainen and Guttman, 2016).

lncRNAs as potential novel targets for cancer therapy

Many types of malignancies are caused by genetic mutations leading to the deregulation of gene networks responsible for maintaining cellular homeostasis. These DNA alterations are contained in genome regions that codify for proteins and also non-coding RNAs (Schmitt and Chang, 2016).

Several lncRNAs have active roles in gene regulation and are controlled by important tumour suppressors and oncogenes. For these reasons, they are found with different expression levels and are linked to the malignant transformation for their implication in cell cycle regulation, proliferation, survival, immune response, and pluripotency. In particular, genome-wide studies reveal that many lncRNAs are direct targets of several transcription factors involved in tumour progression as p53, MYC, signalling cascade proteins (such as Notch) and many others (Hamilton *et al.*, 2015; Huarte, 2015; Kim *et al.*, 2015; Diaz-Lagares *et al.*, 2016)

Today, childhood and paediatric cancers are among the leading causes of death in children under the first years of life (Siegel, Miller and Jemal, 2016). Although researchers are investigating several possible risk factors that can discriminate cancer development in children and adolescents, their causes are mostly unknown. There are no widely recommended screening tests able to define its formation and evolution complicated by methodological difficulties and problems related to these diseases' biological properties and clinical behaviour (Pui *et al.*, 2011). Childhood cancers are characterized by short latency periods, rapid growth and strong invasiveness, although, unlike adult tumours, they are usually more responsive to treatments and therapies. On this topic, research is focusing on the investigation of new possible molecular targets able to define and discriminate cancer formations in the early phases of development to prevent their foundation and progression. Long non-coding RNAs take hold as new aspects that can influence cellular physiology and pathogenesis from the genome-wide revolution (Wilusz, Sunwoo and Spector, 2009; Bartonicek, Maag and Dinger, 2016). On this basis, it's not surprising that alterations in lncRNAs expression emerged as new possible targets for therapeutic intervention due to their extremely specificity and oncogenic roles in multiple diseases, including childhood cancers.

Neuroblastoma

Neuroblastoma (NB) is the most common extracranial solid tumour identified in childhood, with 25-50 cases per million individuals. It is the first cause of death for children between one and five years old, representing 13% of overall paediatric cancer mortality (Matthay *et al.*, 2016).

It differs from other solid tumours by its biologic and clinical heterogeneity, which spans from spontaneous regression to overly aggressive metastatic disease unresponsive to standard and experimental anticancer treatments.

In 1999, the International Neuroblastoma Pathology Classification (INPC) was established to standardize the criteria and terminology for the description of all neuroblastic tumours (NTs). Based on those criteria, neuroblastoma can be classified in:

• Immature: cells are largely undifferentiated with small cytoplasm (Neuroblastoma, malignant).

• Partially mature: neuroblasts are differentiated into ganglion cells - neuron cells that typically reside in the adrenal medulla – that can create metastasis.

• Mature: ganglion cells organized in cluster and surrounded by a stroma of Schwann cells (ganglioneuroma, benign).

Since 1994, the majority of the cancer centers are using the categorization made by the International Neuroblastoma Staging System (INSS) to distinguish all the different kinds of neuroblastoma; these stages are divided into six different classes (table1).

Stage 1	Localized tumour with grossly complete resection with or without microscopic residual disease; negative ipsilateral lymph nodes
Stage 2A	Localized tumour with grossly incomplete resection; negative ipsilateral non-adherent lymph nodes
Stage 2B	Localized tumour with or without grossly complete resection with positive ipsilateral nonadherent lymph nodes; negative contralateral lymph nodes
Stage 3	Unresectable unilateral tumour infiltrating across the midline with or without regional lymph node involvement, OR Localized unilateral tumour with contralateral regional lymph node involvement, OR Midline tumour with bilateral extension by infiltration (unresectable) or by lymph node involvement
Stage 4	Any primary tumour with dissemination to distant lymph nodes, bone, bone marrow, liver, skin or other organs (except as defined for stage 4S)
Stage 4S	Localized primary tumour (as defined for stages 1, 2A or 2B) with dissemination limited to skin, liver and bone marrow (limited to infants)

Table1: International Neuroblastoma Staging System (INSS) classification

Neuroblastoma originates from the peripheral sympathetic nervous system, with 30% of the tumours arising within the adrenal medulla, 60% from abdominal paraspinal ganglia, and 10% from the sympathetic ganglia in the chest, neck, and pelvis (Louis and Shohet, 2015). All these structures derive from the ventrolateral neural crest cells, which move from the neural tube during early embryogenesis (Betters *et al.*, 2010). Neural crest maturation is a complex process that involves a satisfactory arrangement of signalling pathways into an exact outline (Prasad, Sauka-Spengler and LaBonne, 2012). The earliest neural crest precursors display a pluripotent-like differentiation potential and acquire an embryonic stem cell-like self-renewing capacity through the expression of pro-survival factors such as FOXD3, C-MYC, and N-MYC, which make these cells resistant to apoptosis (Rogers, Saxena and Bronner, 2013). Therefore, the observed clinical heterogeneity of neuroblastoma is ascribed to the disruption of the meticulously arranged process of neural crest maturation through the connection to several molecular components at different stages. For this reason, neuroblastoma tumour-initiating cells of disparate backgrounds may yield various tumour phenotypes (Howk *et al.*, 2013).

A bilateral organization based on the origin of the genetic mutations allowed neuroblastoma distribution into two main classes: familial and sporadic. Familial neuroblastoma only represents approximately 2% of overall cases and the germline mutations usually predisposing to disease development are in PHOX2B and, mainly, in the ALK gene. The remaining 98% entirely comprises sporadic neuroblastoma, with various somatic mutations promoting the onset of this malignancy. The most common genetic aberration in sporadic cases is the amplification of the *MYCN* gene, which is found in approximately 22% of all patients and in 50% of high risk neuroblastoma, thus, representing a relevant hallmark of this tumour (Cheung and Dyer, 2013).

Today, no genetic or epigenetic aberrations in common by all the neuroblastoma phenotypes have been established yet. However, a few numbers of genomic alterations (like 1p and 11q deletion, the 17q gain and MYCN amplification) are known to be related to tumourigenesis, which may be fruitful for the identification of some subtypes of neuroblastoma and, consequently, for survival odds (Theissen *et al.*, 2014; Matthay *et al.*, 2016).
Therefore, this neoplasia is a spectrum of diseases that clarifies the motivations for which morphologically very similar tumours usually display contrasting responses to treatments.

lncRNAs in neuroblastoma

The discovery of lncRNAs represented a new frontline for understanding the aetiology, pathogenesis and treatment of neuroblastoma. A significant number of lncRNAs have been functionally involved in many cellular processes, and, when their expression is not well-regulated, they can influence the courses of tumour initiation and progression (Pandey and Kanduri, 2015). Several studies indicated that lncRNAs could act differently based on their structure, genomic location and cellular background.

As previously described, chromosomal aberrations characterized a wide-range of neuroblastoma. Indeed, these abnormalities are frequently observed and generally correlate with the worst pathological scenarios. The chromosome arms that mostly share these types of mutations are 17q, 1q, 11q, 7q, and, in many cases, they became prognostic of poor outcome (Castel *et al.*, 2007). A fascinating data is that these gained regions are characterized by many sequences encoding for lncRNAs, which seem significant in tumour development.

The evaluation of different expression patterns in patients with chromosomal gains allowed the identification of many non-coding transcripts. A representative example is ncRAN (non-coding RNA expressed in Aggressive Neuroblastoma), which show oncogenic properties and contribute to a robust and aggressive behaviour in high-risk neuroblastoma. ncRAN is overexpressed in patients with 17q gain and correlates with the bad outcome and aggressive phenotype, although its mechanism is still unknown (Yu *et al.*, 2009).

In the past 30 years, it has been amply demonstrated how 2p24 amplification represents one of the most significant causes of neuroblastoma development. MYCN, which maps in this region, is probably not only the single cause leading to tumour formation, but co-amplified lncRNAs could also contribute to this purpose. In agreement with this hypothesis, our lab recently reported a 14kb lncRNA named lncUSMycN that maps on chromosome 2p. This ncRNA's silencing resulted in MYCN downregulation - both at mRNA and protein levels – with the NonO protein's help, an RNA binding molecule that works as a bridge between lncUSMycN and MYCN mRNA, for the stabilization of the codifying transcript (Liu *et al.*, 2014). On the other hand, many allelic deletions are also common in neuroblastoma, particularly on chromosomes 1 and 11(Bown, 2001). The absence of many tumour suppressive proteins and lncRNAs encoded by these genes appears to be crucial for developing a more aggressive phenotype NDM29 (Neuroblastoma Differentiation Marker 29) maps on one of these regions that are usually deleted. The overexpression of this transcript led to a better prognosis, as showed by in vitro and in vivo analyses. It can promote differentiation in cells with neuron-like features (including marker expression, morphology,

anchorage-dependent growth and excitatory properties) and reduces the ability of the cells to express pluripotency's factors (Castelnuovo *et al.*, 2010; Vella *et al.*, 2015).

Several data support the indication that various lncRNAs can work as oncogene too. These molecules' ability to drive malignant transformation has been widely documented in several types of tumours, including neuroblastoma.

Epidemiological studies have shown that some genomic regions called T-UCR (transcribed ultra-conserved regions) can transcribe lncRNAs, which are highly conserved in mammals and have functional roles, and apparent deleterious effect when they are deregulated. Indeed, T-UCRs are functionally linked to carcinogenic pathways as cell proliferation, differentiation, cell cycle, apoptosis, DNA repair and replication. For these reasons, their deregulation drives tumour development (Ling *et al.*, 2015).

RT-qPCR analyses demonstrated a relationship between 28/481 T-UCRs and neuroblastoma in 34 high-risk patients. In particular, 15 upregulated T-UCRs distinguished long and short-term survivors with high specificity (Scaruffi *et al.*, 2009). Interestingly, a part of these lncRNAs is overexpressed only in MYCN amplified cells and shows a similar expression pattern (Mestdagh *et al.*, 2010). Among all these groups of molecules, the downregulation of T-UC 300A (a component of the T-UCR family) resulted in a significant decrease in cell proliferation and invasive capacities (Watters *et al.*, 2013).

MYCN can directly regulate the transcription of numerous lncRNAs, but it can also improve the expression of some of these transcripts through the activation of chromatin remodelling proteins. Recent studies showed how MYCN activates MALAT1 expression through JMJD1A, an H3K9-specific histone demethylase. The higher levels of JMJD1A, due to MYCN amplification, can downstream regulate MALAT1 expression through the demethylation of histone H3K9me3 modification at the MALAT1 gene promoter (Tee *et al.*, 2014). MALAT1 can induce cell proliferation, cell migration and cell invasion in neuroblastoma cell lines, consistently with its metastatic property in lung cancer (Tee *et al.*, 2016).

These different pathways support the idea that lncRNAs can act as an oncogene and can be used as potential therapeutic targets for novel treatments.

The MYC genes: new insights in cancer biology

The new multidisciplinary approaches allowed making great strides in cancer research in the last years. These studies permitted not only to identify new molecules to be used as novel therapeutic targets but elucidate the roles of some specific factors already known for their ability to induce tumourigenesis.

In this regard, it is not surprising that MYC research has always been booming over the years, but it is still fascinating how the studies on this well-known transcription factor always have a lot to say. Many new insights into MYC's regulation and function have pushed the boundaries of our understanding of the fundamental mechanisms of normal and neoplastic cell growth, death, and development (Meyer and Penn, 2008).

Indeed, it is essential to highlight how the brand-new MYC researches confirmed the fundamental importance of this protein in changing more intimately the broad concept of cell physiology (Clavería *et al.*, 2013; Levayer, Hauert and Moreno, 2015; Poli *et al.*, 2018) confirming that the MYC factors, composed by C-MYC, N-MYC and L-MYC proteins, are more than just simple oncogenic drivers. The broad spectrum of genetic aberrations concerning both the MYC genes, their regulatory elements, and co-regulatory proteins reflect the presence of a comprehensive molecular signature that could be found in a large number of cancers (~50%), elucidating the complexity of the MYC functions and their regulatory networks (Schaub *et al.*, 2018).

In the last decade, several extensive studies shed lights on the ability of MYC to potentially bind all cell promoters that are prone to transcriptional activation (Lin *et al.*, 2012; Nie *et al.*, 2012; Sabò *et al.*, 2014) however, the MYC-driven tumours are generally characterized by the deregulation of a specific set of genes, resulting in both the activation or repression of essential expression programs (Walz *et al.*, 2014), which dramatically influence the overall survival of the patients by driving, for example, autonomous proliferation and self-renewal (Seruggia *et al.*, 2019; Bywater *et al.*, 2020).

The classic description of the MYC protein combines the structural properties with its functional traits, giving a unique example of its kind: MYC is a nuclear intrinsically disordered protein, with a C-terminal basic helix-loop-helix/leucine zipper (bHLH/LZ) that functions as a transcription factor (bHLH/LZ), can dimerize with the partner MAX (MYC-associated factor X) to finally interact with the "CACGTG" DNA consensus sequence known as E-box (Blackwell *et al.*, 1990; Blackwood and Eisenman, 1991). Also, MYC regions known as MYC homology boxes (MBs) are highly conserved across species and within the MYC family of transforming oncogenes. Six MBs have been described (MB0, MBI, MBII,

MBIIIa, MBIIIb, MBIV), which have been shown to mediate interactions with ~50% of the MYC interacting protein interactome.

Over the years, the mechanisms supporting MYC to trigger the transition from the non-cancerous to the tumourigenic phenotype were deeply investigated using experimental and computational approaches to better appreciate how this protein works. It's now clear how MYC can establish multifarious crosstalk with the transcriptional machinery and with a plethora of regulatory proteins that drastically influence the oncogenic program, driving the cell towards the malignant transformation (Kalkat *et al.*, 2018). Moreover, MYC can bind both low-affinity (non-canonical) and high-affinity (canonical) E-box regions, properties that are intrinsically connected to the presence of high or low levels of MYC respectively, which can drive significant transcriptional alterations when its expression is deregulated, like in cancer (Walz *et al.*, 2014; Lorenzin *et al.*, 2016; De Pretis *et al.*, 2017).

MYCN in neuroblastoma

The expression of the MYCN gene –encoding for the N-MYC protein- and the other members of the MYC family are finely organized in physiological conditions (Charron *et al.*, 1992; Davis *et al.*, 1993). MYCN displays a distinct spatiotemporal expression pattern: high-levels of MYCN can be found in the forebrain, hindbrain and kidneys of newborn mice. On the other hand, MYCN shows low or null expression in the adult tissues, confirming its crucial role during the early developmental stages of neural tissues (Zimmerman *et al.*, 1986).

MYCN is considerably involved in maintaining the proliferative phenotype and in blocking differentiation pathways in neural precursors, as demonstrated by in vitro and in vivo experiments. Accordingly, MYCN is now considered, like C-MYC, a proto-oncogene, and, owing to their marked homology, the vast majority of the general findings about C-MYC are usually applied to MYCN as well and viceversa.

The high frequency of MYC dysregulation in cancer is not surprising, as oncogenic MYC confers a strong selective advantage to tumour cells by enabling their growth and survival.

Besides, some established functional domains within MYC, including the basic region (BR) and helix-loop-helix leucine-zipper (HLH-LZ) at the C-terminus, share homology with other transcription factors, thereby creating additional challenges for the development of specific MYC inhibitors (Chen, Liu and Qing, 2018).

As neuroblastoma typically occurs in early childhood, genetic mutations are not accumulated like in adult tumours and, thus, epigenetic modifications have a significant role in promoting transformation. MYCN directs this tumorigenic epigenetic programme, thereby mediating the

expression regulation of multiple genes simultaneously. It can activate miRNAs and long non-coding RNAs, but it also affects DNA methylation and global histone methylation and acetylation (Knoepfler *et al.*, 2006; Buechner and Einvik, 2012).

Reports of its amplification soon resulted in the original characterization of MYCN in approximately 20-25% of cases of neuroblastoma and the observation that the degree of amplification correlated with advanced stage, unfavourable biologic features, and a poor outcome. Patients with MYCN amplification are stratified for more aggressive treatment. Aberrant amplification and overexpression of MYCN is not only a neuroblastoma hallmark but has also been described in several other types of tumours. The presence of MYCN alterations has been associated with aggressive tumour behaviour and suggests a similar driving role in MYCN–amplified and overexpressed tumours as medulloblastoma, glioblastoma, retinoblastoma and correlates with worse clinical outcomes (Rickman, Schulte and Eilers, 2018).

MYCN and epigenetic dysregulation in neuroblastoma

Some of the most relevant activating complexes involved in chromatin organization that appeared to play a role in MYC-driven tumours are the Spt-Ada-Gcn5-Acetyltransferase (SAGA) complex, the ADA Two A Containing (ATAC) complex and the NuA4 complex (Rickman, Schulte and Eilers, 2018; LM *et al.*, 2020). Many components of these complexes, especially including TRRAP, KAT2A and Tip60, are known to interact with c-MYC, serving as coactivator or affecting its protein stability (S and M, 2005; L and SY, 2014; LM *et al.*, 2020). Despite the lack of studies about these complexes' role in neuroblastoma, some evidence allows the scientific community to speculate on their role also in a neuroblastoma context. Firstly, the homology among the sequences of MYC proteins is widely known and, in particular, the MYC Box II -a stretch of amino acids highly conserved among MYC proteins- represents the site where these complexes interact with MYC, commonly via TRRAP (S and M, 2005). Secondly, the interaction of SAGA and ATAC's components with c-MYC have been largely demonstrated through protein crosslinking assays, co-immunoprecipitation and pull-down assays (N *et al.*, 2014): these data might be important knowing that MYCN-amplified neuroblastoma stand for only the 20% of all cases and MYCN non-amplified neuroblastoma are driven by c-MYC, whose levels are inversely correlated with N-MYC ones (F *et al.*, 2008). Lastly, despite the interaction between these proteins and N-MYC has been only barely validated (J *et al.*, 2001), a CRISPR-Cas9 screening, performed by Durbin et al. in MYCN-amplified neuroblastoma cell lines, detected 147 gene dependencies selective for this tumour, involved in cell growth and survival. Among these, they also found genes coding for

SAGA and ATAC's components, notably different ADA proteins. All these findings support the idea that these activating complexes may have a crucial role also in neuroblastoma tumours. All functioning as transcriptional coactivators, SAGA, ATAC and NuA4 complexes contain a "writer" acetyltransferase (HAT) module which can be recruited via TRRAP transcription factor (SB, MA and MD, 2000; SR *et al.*, 2003). The Tip60 enzyme carries out NuA4's catalytic activity. On the other hand, the ATAC and SAGA's one is performed by human GCN5/PCAF (KAT2A/KAT2B) proteins. The latter's KAT activity is deemed modulated by a specific member of the ADA protein family, a component of the HAT module itself (Krebs *et al.*, 2011; LM *et al.*, 2020). KAT2A, whose expression is usually increased in cancer, has been shown to regulate significantly overlapping transcriptional programs with N-MYC in neural stem cells (V *et al.*, 2012). Furthermore, protein crosslinking assays identified an interaction between TRRAP and MYC in cancer cells (SB *et al.*, 1998; N *et al.*, 2014) with consequent recruitment of KAT2A. Likewise, YEATS2 (ATAC) directly interacts with MYC and appears to play a critical role in promoting MYC-driven cancers (N *et al.*, 2014; LM *et al.*, 2020). Finally, MYC can also induce the remodelling of the nucleosome's topography by recruiting the SWI/SNF complex through the interaction with INI1, one of its components (SW *et al.*, 1999). TFs can also recruit chromatin-remodellers-containing repressive complexes to their target loci. Above all, N-MYC can exert repressive functions interacting with the basal transcription factor 1 (SP1). This dimeric complex requires the sequence-specific transcription factor MIZ-1 to bind targets' promoter regions and recruit other chromatin modifiers such as the "eraser" histone deacetylases (HDAC) (K *et al.*, 1990; S *et al.*, 2014). The most well-characterized repressive complexes that are known to have a role in neuroblastoma development are the PRC2 (Polycomb repressive complex 2), Sin3, NuRD (Nucleosome Remodelling and Deacetylase complex), SMRT (Silencing Mediator for Retinoid and Thyroid Hormone Receptors), CtBP (C-terminal binding proteins) and CoREST (REST co-repressor) complexes all sharing one or more protein of the HDAC family (Milazzo *et al.*, 2020). These complexes have been widely investigated in a cancer landscape, even though just a few studies have drawn attention to their behaviour in neuroblastoma and how they differentially work in this context. Providing some examples, Gajer et al. (JM *et al.*, 2015) showed that inhibition of HAT activity in vitro and in vivo blocked neuroblastoma cells growth; Chen et al.(L *et al.*, 2018) demonstrated that shRNA-mediated knockdown of the PRC2 component EZH2 or its depletion upon inhibitors treatment resulted in markedly decreased neuroblastoma cells viability; Yang et al. (H *et al.*, 2014) proved that the silencing of the histone demethylase LSD1, a component of CoREST complexes, resulted in a reduction in cell proliferation, colony formation, migration, and invasion of neuroblastoma

cell lines. Despite the lack of information regarding how these complexes work and influence the initiation and maintenance of neuroblastoma, the fact that the tumorigenic phenotype is reduced or inhibited after depletion of some of these complexes' components is a great suggestion of their importance in neuroblastoma. Interestingly, these machineries show a high level of interconnection in terms of shared members, similar binding sites on chromatin and downstream effects. Further investigations on these potentially druggable regulators might be fundamental for developing new therapeutic strategies to tackle one or more critical pathways in keeping a tumorigenic profile in the neuroblastoma landscape.

MYCN in cell cycle progression

One of the leading programs through which MYC proteins exert their oncogenic functions is the activation of proliferation by cell cycle and the downregulation of the activity of a set of proteins that act as cell-cycle brakes.

MYCN regulates several aspects of cell cycle progression by activating or repressing gene expression. Indeed, checkpoint kinase 1 (CHK1) may establish a significant relationship with MYCN. CHK1 is a regulator of S-phase and G2/M checkpoints, whose inhibition induces chemosensitization in different tumours (Zhang *et al.*, 2009). Interestingly, N-MYC upregulates CHK1, which may increase resistance to standard chemotherapy (Cole *et al.*, 2011). MYCN mainly operates between G1 and S phase progression; significantly, MYCN-amplified neuroblastoma does not arrest in G1-phase in response to irradiation and DNA damage (Tweddle *et al.*, 2001). Conversely, the downregulation of MYCN expression displays a reduction in S-phase (Bell, Lunec and Tweddle, 2007; Woo *et al.*, 2008).

One of the main MYCN's functions proposed on this topic is the repercussion in G1-checkpoint overriding by down-regulating the TP53 inducible nuclear protein 1 (TP53INP1) and by upregulating ID2, CDK6, CDK4 and SKP2, thus allowing CDK2 to escape p21 inhibition (Bell, Lunec and Tweddle, 2007; Woo *et al.*, 2008; Muth *et al.*, 2010). Moreover, N-MYC may mediate the activation of the WNT/β-catenin pathway, which can trigger the upregulation of Cyclin D (Bell, Lunec and Tweddle, 2007).

All these pathways converge on the pRB inactivation, which releases E2F family transcription factors which are crucial components of the cell cycle regulation (Kent and Leone, 2019).

E2F(s) activation does not merely result from inhibition of the RB sequestering action, but it is also achieved through up-regulation of those factors. For instance, high-MYCN cells have been shown to correlate with high E2F1 expression and with a quicker entry in the G1/S

transition state as compared to low MYCN cells (Ryl *et al.*, 2017). Hence, the relationship between MYCN and E2F factors has been subjected to studies for a few years but needs to be further investigated to understand the precise mechanisms linking each E2F factor to MYCN in the context of neuroblastoma.

E2F proteins, an overview

The E2F story began in 1986 when a cellular transcription factor with a prominent role in early events of adenoviral replication was identified. Today, E2Fs have been efficiently described as cell cycle major transcriptional regulators, but new functions in preserving genomic stability are only emerging. Yet, the exact general mechanism by which E2Fs help control cellular physiology is still partially unclear (Kent and Leone, 2019). Eight genes encode E2F family members. Moreover, their complexity is further increased for the presence of transcriptional variants (like E2F3 and E2F7), derived either from alternative splicing or the use of alternative promoters (Iaquinta and Lees, 2007; Araki *et al.*, 2019).

E2Fs are traditionally classified into three sub-groups: Activators: (*E2F1, E2F2, E2F3A and E2F3B*) that are at high levels during the G1/S phase transition, canonical repressors (*E2F3B, E2F4, E2F5 and E2F6*) expressed more or less constitutively, and atypical repressors (*E2F7 and E2F8*) generally in higher amount at the late S phase (Kent and Leone, 2019).

From a structural perspective, these proteins contain similar DNA binding domain sequences thanks to a distinctive protein motif called "winged helix" (WH)(Leone *et al.*, 2000).

Winged helix is a subtype of helix-turn-helix (HTH) motif-containing two characteristic loops (the so-called "wings"). All E2Fs (excluding E2F7 and E2F8) bind the so-called E2F consensus sequence TTTCC/GCGC by engaging with one of the transcription factor DP family members, which includes TFDP1, TFDP2 and TFDP3 (DeGregori and Johnson, 2012). E2F–TFDP1 and E2F–TFDP2 heterodimers have similar effects on E2F targets, whereas E2F–TFDP3 show reduced DNA binding ability, generally preventing its interaction with the E2F DNA consensus site (Qiao *et al.*, 2007; DeGregori and Johnson, 2012). Conversely, E2F7 and E2F8 bind DNA in a TFDP independent manner.

Regulation of E2F factors through their direct binding to pocket proteins has been extensively detailed over the years. Pocket proteins include:

- pRB (encoded by RB1 gene);
- p107 (also known as RBL1);
- p130 (also known as RBL2).

The interactions are mainly controlled by cyclin-CDK complexes, which phosphorylate pocket protein, leading to the release of E2Fs and resulting in activation of E2F targets transcription after mitogenic signalling (Henley and Dick, 2012).
E2Fs show robust self-regulation at the transcriptional level, in fact, they regulate each other during cell-cycle progression. The model just described, however, is already incomplete. Recent works shed light on previously undisclosed functions and regulation pathways of some E2F factors. For example, despite the general assumption that all E2Fs share the same DNA targets, receht studies have shown a specific DNA sequence binding selectivity among E2Fs. (Kent and Leone, 2019).

E2F3a and E2F3b

E2F3 human gene is localized into the short (p) arm of chromosome 6 at position 22.3 (6p22.3), and it is composed of only seven exons. Although its superficial genetic simplicity, to date, four isoforms deriving from this genomic locus have been discovered (E2F3a, E2F3b, E2F3c and E2F3d) (Araki *et al.*, 2019), with some peculiarities that make them distinct from the other.

E2F3a belongs to the winged-helix subtype of helix-loop-helix (HLH) class of transcriptional factors. This protein is mainly localized in the nucleus, and it is extensively implicated in cell cycle regulation and response to growth stimuli. As an activating E2F, E2F3a is inhibited by pRb binding in quiescent cells, but in the late G1-phase, it escapes from the physical sequestering and activates E2F-responsive genes necessary for G1-S transition. Its transcription is high at the early S-phase and declines while the cell heads towards G2-phase entry. Moreover, its promoter is E2F-responsive (Danielian et al., 2008).

In 2000, Gustavo Leone's lab discovered a different transcript encoded by the E2F3 locus, named E2F3b. The latter is transcribed from an alternative promoter localized into E2F3a's first intron. The resulting protein contains the same primary sequence of E2F3a protein except for N-terminal region encoded by the first exon, which determines the difference between E2F3a and -3b (Leone et al., 2000). Indeed, all the well-characterized domains of E2F3a are conserved in E2F3b as well, including the cyclin A regulatory domain and the NLS (He & Douglas Cress, 2002).

E2F3b has always been placed at the juncture between E2F activator (E2F1, E2F2 and E2F3a) and canonical repressor (E2F4 and E2F5). It shares sequence homology with E2F1-3a, and binds pRb as a pocket protein. However, it is constitutively activated in quiescent and

cycling cells like E2F4-5 (Adams et al., 2000). In contrast to the ablation of both E2F3a and E2F3b, which resulted in embryonic lethality, inactivation of either isoform alone had no measurable effect on mouse embryonic development. Otherwise, loss of E2F3a or E2F3b significantly rescued selected phenotypes observed in *Rb* mutant embryos. Some data suggested that E2F3a and E2F3b proteins contribute to the control of proliferation in *Rb* mutant embryos in a tissue-specific manner, with E2F3a playing a major role in the placenta and nervous system and with E2F3a and E2F3b having critical roles in the lens. To date, it is currently thought that E2F3a acts as a transcription activator by accumulating maximally at the G1/S transition. Given that E2F3b complexes specifically with Rb in quiescent cells, it has been assumed that E2F3b functions as a repressor (Adams et al., 2000).

Taken in their whole complexity, E2F3 is essential in early development as most KO mice homozygous for a not functional E2F3 gene (both E2F3a and E2F3b) die in uterus or just immediately after birth. In particular, loss of E2F3 in MEFs (mouse embryonic fibroblasts) results in the impairment of mitogen-induced cell cycle re-entry (Humbert et al., 2000). However, single knocking-out of either E2F3a or E2F3b, suggest a certain redundancy between the two isoforms. When the expression of only one of the two isoforms is disrupted, MEFs cell cycle re-entry is not affected, and mice reach adulthood without exhibiting any pathology. The presence of either isoform thus compensates for the other's absence and avoids the impairment of normal cell proliferation and organism development.

While the loss of E2F1 and E2F3b does not produce relevant defects both in MEFs and mice, the absence of E2F1 and E2F3a results in the impairment of cell cycle re-entry and E2f-responsive genes regulation in MEFs and post-natal lethality for mice.

These data suggest that E2F3a and E2F3b have only partial overlapping functions and can differently contribute to cell cycle regulation (Danielian et al., 2008) . Other studies, however, claim that in MEFs, both E2F3a and E2F3b can compensate for the concomitant absence of E2F1, E2F2 and either E2F3, preventing cell proliferation defects (Chong et al., 2009). This would place E2F3a and E2F3b on an equal footing, with the latter predominantly or uniquely acting as a transcriptional activator able to induce E2F responsive genes in the G1-S transition. Hence, the presence of E2F3b-pRb complex on promoters of E2F targets in G0 (quiescent cells) could be seen as a cell strategy meant to guarantee a quicker activation of the mitogenic signal and subsequent dissociation from phosphorylated pRb. Then, the rapid increase of E2F3a levels in the G1-phase would allow us to reach the E2F3 threshold activity necessary to pass through the G1-S restriction point (Chong et al., 2009). Moreover, a role for

E2F3a/b in maintaining proliferation has been suggested in RB1 KO mouse embryos. In doing this, E2F3a seems to play a more dominant role than E2F3b in most RB1 KO tissues (Chong et al., 2009). All these shreds of evidence contribute to outline a predominant activating role for E2F3b, which would cooperate with other E2F activators (especially E2F3a) to activate the E2F-mediated transcriptional programme necessary for G1-S transition. However, it does not rule out the E2F3b repressing role, which should not be neglected as it is likely to be equally critical. This dual nature allowing E2F3b to have opposing roles in different contexts might make it a balancer for E2F total activity. E2F3 locus acquired increasing attention over the last fifteen years as it was found to be amplified in several human tumours, including retinoblastoma and bladder, lung and prostate cancer (Cooper et al., 2006; Foster et al., 2004; Hurst et al., 2008; Orlic et al., 2006). However, E2F3a/b overexpression has also been noticed in tumours not carrying its gene amplification. For example, high E2F3a/b are detected in breast cancer, where E2F3a/b silencing results in milder proliferative phenotype (Vimala et al., 2012). E2F3 overexpression is also associated with poor prognosis hepatocellular carcinoma and with advanced cases of clear cell renal cell carcinoma (Gao et al., 2017; Zeng et al., 2014), Interestingly, in the latter, E2F3 has been found to transcriptionally activate HIF-2α (hypoxia-inducible factor 2α), thus boosting proliferation and invasion capacity of cancerous cells (Gao et al., 2017). Strikingly, Wilms tumour, a paediatric tumour affecting kidneys, exhibits E2F3 overexpression, especially in metastatic tissues (Kort et al., 2008)

E2F proteins in neuroblastoma

Several studies have demonstrated that E2F activators are required for cell proliferation in tumours characterized either by MYC overexpression or by functional inactivation of pRb. For example, E2F1 and E2F3 have been found to have penetrating oncogenic activities in Myc-mediated mammary tumourigenesis, while E2F2 seems to have tumour suppressive capacities (Wu *et al.*, 2015).

Interestingly, almost all neuroblastoma cases show RB1 wild-type, suggesting an expected minor dysregulation of cell cycle and apoptosis pathways. Nevertheless, the subset of neuroblastoma characterized by MYCN-amplification does not offer a mild phenotype, but rather great aggressiveness and uncontrolled proliferation. Interestingly, the absence of mutations in RB1 is also surprisingly found in some cases of retinoblastoma. Such discovery clashes with the deep-rooted belief that RB1 gene mutations initiate retinoblastoma. Of this

restricted subset of Rb wild-type retinoblastomas, an even smaller percentage characteristically shows MYCN-amplification (RB1+/+MYCNA) (Rushlow *et al.*, 2013).

Notably, this feature is also shared by MYCN-amplified neuroblastomas (Mosse *et al.*, 2007). In RB1+/+MYCN^{A} retinoblastoma, pRb protein is strongly expressed in the nucleus, and it also seems to be functional, as it coimmunoprecipitated with E2F1. Moreover, the large majority of the cases of RB1+/+ retinoblastoma display MYCN-amplification (Ewens *et al.*, 2017). Such evidence suggests that, in RB1+/+MYCNA retinoblastoma, N-MYC might have a crucial role in inducing tumourigenesis, somehow overriding the tumour-suppressing action of pRB (Rushlow *et al.*, 2013). As a consequence, E2F-mediated gene expression is inferred to increase, thus promoting cell cycle progression. Hence, the parallelism with MYCN-amplified neuroblastomas could be established. A relevant role played by E2F activators has already been pointed out in neuroblastoma, especially related to MYCN. N-MYC, for example, promotes and represses transcription of E2F1 and miR-93-5p, respectively. Most importantly, E2F1-3 seems to considerably upregulate MYCN expression levels by directly activating its transcription, even if only in an MYCN-amplified context (Strieder and Lutz, 2003). E2F3 gene is only recently emerging as an essential player in neuroblastoma. First of all, E2F3a/b is considerably overexpressed in human MYCN-amplified neuroblastomas, together with other cell cycle-related genes such as FOXM1 and MYBL2 (Olsen *et al.*, 2017). Indeed, a strong correlation with MYCN has been noticed since ChIP experiments have shown the capacity of E2F3 to bind the MYCN promoter in MYCN-amplified rather than in MYCN-nonamplified neuroblastoma cell lines (Strieder and Lutz, 2003). Yet, beyond this link with MYCN, which is one of the critical oncogenes characterizing neuroblastoma , E2F3 appears to be implicated in other deregulated aspects of neuroblastoma. For example, E2F3 usually is post-transcriptionally regulated by miRNA-34a, but the latter's levels considerably decrease in primary neuroblastoma tumours, thus driving a parallel increment of E2F3 levels (Welch, Chen and Stallings, 2007). In addition to this, protein degradation is also an element that appears to be deregulated for E2F3 in neuroblastoma. When APC/C ubiquitin ligase complex is impaired in neuroblastoma cells induced to differentiate, E2F3 protein accumulates, and this suggests the presence of this alteration in this tumour (Ping *et al.*, 2012). Yet, knowledge of the E2F3 role in neuroblastoma is still fragmented and thus, additional studies are needed to better outline the mechanisms in which this transcriptional factor may be involved. To date, the relationship between E2F3 and MYCN is still not well understood, both in physiological and in pathological contexts. The reasons for this considerable difficulty in unveiling the mechanisms underlying the E2F3-MYCN axis can be reasonably attributed to the redundancy and the still not wholly characterized roles of E2Fs,

as well as to the broad range of processes involving MYCN and to the tremendous genetic heterogeneity typical of the central disease where this axis is studied, which is neuroblastoma. Nevertheless, some works released in the last twenty years have provided insights into the connection between E2F factors and MYC genes (including MYCN and C-MYC) and fragmented data E2F3-MYCN relationship are present.

Promising therapeutic approaches in neuroblastoma

The description of the neuroblastoma landscape through advances in DNA, RNA and epigenetic profiling reveals the complexity of this pathology (JJ *et al.*, 2012; H *et al.*, 2013; JL *et al.*, 2017). In this regard, it is not surprising that neuroblastoma research has always been booming over the years, showing how the extreme variety of genetic and epigenetic backgrounds, mixed with multiple levels of regulatory networks regulations, reflect a challenging tumour to investigate. To date, treatment of neuroblastoma high-risk patients includes intensive chemotherapy regimen with cisplatin, vincristine, carboplatin, etoposide, and cyclophosphamide (COJEC), followed by resection surgery and myeloablative therapy in combination with hematopoietic stem cell reinfusion and local radiation therapy (AD *et al.*, 2008). The relevance of specific targeted therapy in neuroblastoma could be crucial considering the standard strategies weakening approach in treating high-risk patients and the extreme cancer heterogeneity, which spans from spontaneous regressions to metastatic and aggressive diseases (Luo *et al.*, 2018). Several biological and genetic markers of this tumour have been understudied to help diagnosis and prognosis, giving relevant insights on the molecular landscape of neuroblastoma and attention to specific factors. Indeed, the dysregulation of gene expression programs, biochemical cascades and metabolic pathways control the aggressiveness of neuroblastoma, shedding light on some crucial components capable of being directly or indirectly targeted. Activating ALK mutations and N-MYC overexpression were shown to be the most influential de novo oncogenic drivers. In particular, the regulatory networks dependent on N-MYC is considerably involved in maintaining the proliferative phenotype and blocking differentiation pathways in neural precursors, as demonstrated by in vitro and in vivo experiments (M and WA, 2013). For instance, the MYCN-dependent regulatory network drives the malignancy and maintenance of stem-like state by activating the expression of genes involved in metastasis like integrins α1 and β1, the FAK protein and metalloproteinases (D *et al.*, 2002; CM *et al.*, 2003), self-renewal and pluripotency as KLF2, KLF4, and LIN28B (R and PS, 2009), survival, angiogenesis and cell cycle progression as previously described. Thus, novel efforts

are converging on the investigation of new methods to target MYC in order to achieve anti-tumour effects by disrupting its oncogenic program's key components.

Inhibition of the N-MYC/MAX interaction

N-MYC is a nuclear intrinsically disordered protein that can exist in distinct complexes within the same cell by interacting with hundreds of components to keep the cell identity (Kalkat *et al.*, 2018; A, E and M, 2020; C *et al.*, 2021). All the MYC proteins are basic helix-loop-helix/leucine zipper (bHLH/LZ) transcription factors capable of dimerizing with the partner MAX (MYC-associated factor X) to regulate up to 10–15% of all genes (Meyer and Penn, 2008). This data assumes additional relevance within MYCN biology in neuroblastoma models, considering how MAX can instruct transcriptional programs that either reinforce or weaken the oncogenic process enacted by N-MYC (F *et al.*, 2020). Thus, the N-MYC/MAX heterodimer's-controlled inhibition is an attractive approach to counteract the oncogenic regulatory network triggered by MYCN. In 2002, a 7000 peptidomimetic compounds screening was performed to select novel candidates capable of preventing the dimerization between MYC and MAX. This analysis identified IIA6B17 and IIA4B20, two small molecules that exert a strong inhibitory effect on MYC-MAX dimerization and DNA binding, characterized by a lower IC50 for MYC compared to the homologous transcription factor Jun (T *et al.*, 2002). The ground-breaking work of Berg et al. gave the start to the development of novel therapeutic interventions to inhibit the oncogenic program MYCN-mediated. The identification of new drugs like 10074-G5, 10058-F4 (X *et al.*, 2003; I *et al.*, 2014; GT *et al.*, 2017), KJ-Pyr-9 (JR *et al.*, 2014), the MYC inhibitor 361 (MYCi361) and the novel Peptomyc's Omomyc-based therapy (OMO-103) (D and L, 2020) brought new hope for the fight against neuroblastoma disease. Remarkably, just in March 2021, OMO-103 was announced to have obtained approval from the Spanish Agency of Medicines and Medical Devices for conducting a phase I/II clinical trial, proving the efficacy of this innovative approach (NCT04808362).

Targeting N-MYC stability

As for c-MYC, the N-MYC protein degradation is mainly induced by the ubiquitin-proteasome system (AS and RC, 2014). The discovery of new components affecting the N-MYC protein stability aroused great interest concerning the possibility of developing novel treatments against many MYC-driven tumours. In this framework, AURKA inhibition is making inroads as a promising alternative approach in preclinical models of neuroblastoma. N-MYC is usually stabilized by direct interaction with AURKA, preventing proteasomal

degradation dependent on the SCF-FBXW7 E3 ubiquitin ligase (T *et al.*, 2009). Confirming the importance of this topic, the AURKA inhibitor MLN8237 (also known as alisertib) combined with irinotecan and temozolomide chemotherapy is under clinical assessment for multiple cancers relapsed neuroblastoma (NCT01601535) (SG *et al.*, 2016). The characterization of a new class of conformation-disrupting inhibitors of AURKA that destabilize interactions between AURKA and N-MYC is enjoying great popularity (WC *et al.*, 2014), proving to be another promising strategy in the next future operations. As for AURKA, WDR5 is emerging as a novel promising MYC vulnerability in cancers . Following this approach, many other drugs like the PLK1 inhibitor BI 2356, the HAUSP inhibitor P22077, and the PA2G4 inhibitor WS6 (S *et al.*, 2011; O *et al.*, 2016; J *et al.*, 2019) are providing together with the basis for drug design of small molecules targeting MYC and N-MYC binding partners in malignancies driven by MYC family oncoproteins, representing new alternative forms for the treatment of high-risk neuroblastoma.

Targeting N-MYC and its regulatory networks

The potential of selectively inhibiting N-MYC would be the most effective approach to counteract advanced forms of neuroblastoma. Indeed, since the high frequency of MYCN amplification in cancer and its role in driving and promoting tumorigenesis, as well as its space-temporal restricted expression during embryo development, precise N-MYC targeting would certainly result in successful therapeutics to support neuroblastoma treatment (G, FW and P, 1988; M and WA, 2013). However, the extreme variability in cancer mutations and the presence of homologous forms of MYC proteins are still profoundly affecting the process of selective drug design. Specific N-MYC inhibitors therapy still remains poorly explored (S and EV, 2015). To overcome this issue, the scientific community is focusing on alternative approaches that aim to control N-MYC mediated transcriptional activation and its regulatory networks. N-MYC mediated transcriptional regulation is promoted mainly by the association with Bromodomain and extra terminal (BET) containing proteins, which work as chromatin "readers" by binding to acetylated lysine residues and helping transcription. The bromodomain-containing protein 2 (BRD2), BRD3 and BRD4 are of great relevance. Several analyses showed that the application of the BET inhibitor JQ1 downregulates N-MYC transcriptional signatures, lowering MYCN expression, thus increasing the survival percentage in both xenograft and transgenic murine models of neuroblastoma (Puissant *et al.*, 2013). Although not yet approved by the American agency of Food and Drug Administration (FDA), the application of BETi seems to be one of the most promising approaches to treat neuroblastoma patients with MYCN amplification. Further proof of this was provided by

developing new drugs like birabresib (MK-8628) - formerly known as OTX015 - an orally bioavailable small molecule that prevents BRD2/3/4 from binding to acetylated histones. Recently, Henssen et al. showed that BRD4 specifically occupies N-MYC targets and other genes associated with super-enhancers and that OTX015 specifically disrupts BRD4 binding to chromatin and murine models MYCN driven neuroblastoma, leading to significant survival advantage compared with untreated controls (A *et al.*, 2016). This study established the therapeutic efficacy of the BET inhibitor OTX015 in preclinical neuroblastoma studies. Also, it confirmed the effectiveness of this drug in phase I trials in adult hematological malignancies (NCT01713582) and solid tumours (NCT02259114) as well as for GSK525762, another BETi under phase I clinical trial for solid tumours including neuroblastoma (SA *et al.*, 2019). As an amplifier of active transcription, the modern concept of MYC proteins is constantly evolving compared to the commonly held conclusion that MYC coordinates the transcription of distinct groups of genes (Sabò *et al.*, 2014; Walz *et al.*, 2014; Zeid *et al.*, 2018). This event can be possible since N-MYC can interact with a plethora combination of multiple proteins, allowing the regulation of several central control points of gene transcription like promoter binding, epigenetic modifications, initiation, elongation, and post-transcriptional processes (C *et al.*, 2021). RNA polymerase II (RNA Pol II) transcriptional activation is regulated by a specific set of cyclin-dependent kinases (CDKs), including CDK7 (Cyclin-Dependent Kinase 7), a crucial component of the transcription initiation factor TFIIH phosphorylates RNA Pol II to start transcription. In 2014, Chipumuro et al. report that a covalent inhibitor of cyclin-dependent kinase 7 (CDK7), THZ1, was found to disrupt the transcription of MYCN-amplified neuroblastoma cells selectively, leading to global repression of N-MYC dependent transcriptional amplification and induction of tumour regression in mice models (E *et al.*, 2014). The substantial selectivity of this compound for cells with MYCN amplification may be attributable to the reduced expression of super-enhancer-associated oncogenic drivers, including the same N-MYC. Combinatorial therapy with THZ1 and the tyrosine kinase inhibitor (TKi) ponatinib and lapatinib (AE *et al.*, 2020), as well as with the HDACi Panobinostat (Wong *et al.*, 2019), synergistically induced neuroblastoma cell apoptosis leading to neuroblastoma tumour regression. These novel therapeutic approaches are gaining ever greater importance considering the effect on the regulation on the core regulatory circuitry (CRC) and global gene expression, confirming how particularly JQ1 and THZ1 injection can rapidly decrease the expression of CRC mRNA levels after just one hour of treatment in MYCN-amplified neuroblastoma cells. The expression level of each of the six transcription factor genes was dramatically downregulated by the combination of JQ1 and THZ1, with more restricted consequences regarded either drug

alone. These results underlined the impact of JQ1 and THZ1 combination treatment in MYCN-amplified neuroblastoma, although the broad implication of combining transcriptional disruption is still not fully understood (AD *et al.*, 2018). In line with these novel pharmacological strategies, recent studies shed light on the CDK9/2 inhibitor CYC065 (fadraciclib) contribution, resulting in selective loss of nascent MYCN transcription. MYCN loss sensitizes cells to apoptosis following CDK2 inhibition by selectively targeting neuroblastoma cells characterized with MYCN amplification (E *et al.*, 2020), confirming the pivotal role of the crosstalk between the components of the transcriptional machinery. On the other hand, N-MYC dysregulation can influence cell cycle progression by upregulating genes like cyclin D2 (C *et al.*, 2001), E2F proteins, CDK4/6, CDC2 (Woo *et al.*, 2008), resulting in the inactivation of genes involved in the G1 phase and DNA replication. These data assume additional relevance in preclinical studies and clinics considering the promising effects of CDK4/6 inhibitors on NB and other paediatric cancers such as Palbociclib, Ribociclib (LEE011) and Abemaciclib, shedding lights on the potential role of these molecules for the development of new effective therapeutic approaches (J *et al.*, 2013; B *et al.*, 2017; LS *et al.*, 2017).

AIM

Neuroblastoma is the most common neurogenic-extracranial solid cancer occurring in childhood and infancy. The genetic aberration most prominently associated with a poor prognosis for patients affected by this pathology is the amplification of the MYCN gene.

The latter encodes the N-MYC protein, a basic helix-loop-helix leucine zipper (bHLH-LZ) transcriptional regulator belonging to the MYC protein family (C-MYC, N-MYC and L-MYC). Over the years, many lines of evidence suggested that all MYC family members are tightly correlated with cancer development. As a matter of fact, they activate transcription of several potentially pro-tumorigenic coding and non-coding genes that finely orchestrate the mechanisms underlying cell proliferation, but that, if deregulated, can pave the way for cancer onset (Meyer and Penn, 2008).

Expression of the MYCN proto-oncogene is tightly controlled in normal cells. Still, when the MYCN gene is amplified and its activity unleashed, it drives the development of many human cancers. We hypothesize that by understanding the regulation and function of MYCN in neuroblastoma, we can develop effective anti-MYC therapeutics. Such inhibitors of MYC would have a significant impact on cancer patient care and outcome. Traditional therapeutics rely on small molecular inhibitors to bind to enzymatic pockets or defined structures within their target.

As MYC proteins have no enzymatic activities and have very few defined structures, these approaches have not been fruitful, making MYC's modern paradigm almost undruggable. Fortunately, some new evidence underscores the complexity of many new oncogenic regulatory networks dependent by N-MYC in this pathology. These further information pave the way for new multi-target therapies against these hallmarks, showing how novel approaches together with chemotherapy, surgery, or radiotherapy can play substantial anti-neoplastic effects, disrupting a wide variety of tumorigenic pathways through combinations of different treatments. Moreover, discovering the functionality of novel strategies like the peptidomimetic approach (Omomyc peptide), molecules able to affect both protein stability and/or DNA-binding gives hope and provides crucial novel mechanistic insights and clues for promising approaches (SK *et al.*, 2021).

The significance of a MYC-targeted therapy in neuroblastoma could be of great importance considering the standard strategies' weakening approach in treating high-risk patients, distinguished by metastatic and aggressive tumours, leading to poor outcome (Luo *et al.*,

2018). Some therapies are already under assessment, and these include clinically verified treatments, such as the application of 13-cis-retinoic acid, JQ1 and pioneering approaches, like immunotherapy (Puissant *et al.*, 2013; Veal *et al.*, 2013; Morandi *et al.*, 2018). However, relative inefficacy of the current systems and variable response of neuroblastoma to therapy leads research to discover alternative methods.

My research during the last three years as a PhD student was particularly focused on exploring how MYCN expression can influence the induction and maintenance of the tumorigenic phenotype in neuroblastoma. Using different multi-omic approaches and many promising innovative techniques (RNA-seq, ChIP-seq, BioID coupled with LC-MS analyses, RNAi), we were able to identify and characterize novel vulnerabilities of this pathology, which can work in concert with MYCN for the development of a high-risk cancer phenotype. For simplicity, my thesis results will be divided in two different parts, depending on the object of study:

PART I: The identification and functional characterization of the novel long non-coding RNA lncNB1 to promote N-MYC protein stabilization in high-risk neuroblastoma;

Project in collaboration with Children's Cancer Institute of Sydney – Australia.
Research team: *Tao Liu research group*

PART II: The role of the E2F3a and E2F3b proteins and their interactomes for the instruction of a novel functional axis with N-MYC in neuroblastoma.

Project in collaboration with University Health Network of Toronto – Canada.
Research team: *Linda Z. Penn research group*

ABSTRACT SUMMARY:

PART I: The identification and functional characterization of the novel long non-coding RNA lncNB1 to promote N-MYC protein stabilization in high-risk neuroblastoma

Abstract (Part I): *Our study investigated whether and how N-MYC can regulate transcription of lncRNAs by comparing transcriptional profiles between non-amplified and MYCN-amplified neuroblastoma cell lines. Among the several lncRNAs stimulated by N-MYC, we singled out lncNB1. LncNB1 is selectively higher expressed in high MYCN cells only and it is also firmly and almost uniquely transcribed in neuroblastoma among all types of cancer. Our data showed that N-MYC directly activates transcription of lncNB1, which accumulates in the cytoplasm to interact with the ribosomal protein L35 (RPL35). This interaction enhances translation of the E2F1 transcription factor, whose accumulation in the nucleus up-regulates, particularly the expression of the DEPDC1B gene, a GAP protein that stimulates ERKs to phosphorylate N-MYC at Ser62 to increase N-MYC half-life. Overall, our findings show that N-MYC can instruct a complex network of molecular interactions through transcriptional stimulation of lncNB1, ultimately resulting in increased stability of the N-MYC oncoprotein to reinforce N-MYC oncogenetic program. The regulatory levels, herein identified, are novel and become relevant targets for therapeutic interventions.*

PART II: The role of the E2F3a and E2F3b proteins and their interactomes for the instruction of a novel functional axis with N-MYC in neuroblastoma

Abstract (Part II): *Neuroblastoma (NB) is the most common neurogenic-extracranial solid cancer of infancy and childhood. The most aggressive subtype of NB, which carries the worst overall prognosis, occurs where the MYCN gene is amplified. Many questions remain concerning what discriminates MYCN-amplified from non-amplified tumours. Our data provide new insights about how high N-MYC may establish a dynamic regulatory axis through the interaction with the E2F3 transcription factor, impacting the development of the high-risk cancer phenotype. High E2F3 expression is consistently associated with poor survival across different NB datasets regardless of MYCN expression, thus highlighting its crucial role in NB progression. To better understand how E2F3 works despite MYCN status and to assess the contribution of the two known E2F3 isoforms (E2F3a and E2F3b), we examined the complexity of their protein interactome by using the proximity-dependent biotin labelling (BioID) in both high and low MYCN expression conditions. These analyses revealed respectively 96 and 99 protein candidates belonging to the comprehensive proteomics map of both E2F3a and E2F3b proteins, underlining for the first time the mutual dependency of MYCN status and the proteomic profiling of these two transcription factors in NB disease. Our unbiased screen uncovered many potential candidate proteins that help to fill the knowledge gap in understanding what is the impact of MYCN on E2F3 biology, shedding light on the molecular principles that leads the MYCN/E2F3 axis to foster the oncogenic programme.*

RESULTS (Part I):

Identification and functional characterization of the novel long non-coding RNA lncNB1 to promote N-MYC stabilization in high-risk neuroblastoma.

LncNB1 is highly expressed in MYCN-amplified neuroblastoma cells

Long non-coding RNAs (lncRNAs) are emerging as crucial regulators of cell biology involved in several molecular mechanisms, many of which are today not fully understood. Recent investigations better defined the association between lncRNA expression and disease progression; in particular, these molecules have been linked to the modulation of many oncogenic pathways crucial for neoplastic formation and development. N-MYC modulates the expression of several lncRNAs, which strongly contribute to oncogenesis in neuroblastoma disease, a paediatric cancer characterized by MYCN gene amplification in 22% of all cases. To better investigate how N-MYC can influence transcription of lncRNAs in neuroblastoma samples, we performed in collaboration with Tao Liu's research group (CCIA-Sydney) RNA-sequencing analyses (RNA-seq) by comparing the expression profiles between two MYCN non-amplified (SK-N-AS and SH-SY5Y) and four MYCN-amplified neuroblastoma cell lines (SK-N-BE(2)C, SK-N-DZ, CHP134 and KELLY) (**Fig. 1a**). These analyses revealed 459 differentially expressed genes among all the six samples (data not shown). The MYCN amplified cells displayed high RNA expression of MYCN, IGF2BP1 and MYCNOS, consistent with literature evidences (J. L. Bell et al., 2015; Breit & Schwab, 1989; Suenaga et al., 2014). Moreover, the RNA levels of the MYC gene and other known targets like DKK2 and TFIP2 were lower expressed in MYCN amplified cells and more elevated in MYCN non-amplified context, confirming the analysis's reliability. We focused our studies on lncNB1, a novel functionally unreported non-coding RNA, also known as RP1-40E16.9 or linc02525, since our analyses showed a high consistent expression in all MYCN amplified cells and patients affected by high-risk neuroblastoma. The lncNB1 gene, located at chromosome 6: 3182817–3195767, encodes a lncRNA of 1472 nucleotide (NCBI Ref_Seq: NR_038295.1), transcribed by RNA polymerase II, spliced and latter polyadenylated. To validate the RNA-seq analyses, RT-qPCR experiments were performed on five MYCN amplified and three MYCN non-amplified cell lines, confirming the positive correlation between N-MYC and lncNB1 expressions (**Fig. 1b**). Additionally, we decided to make use of the Maris-41-FPKM-rsg001 RNA sequencing dataset to better support our hypothesis; this dataset contains 39 human neuroblastoma cell lines publicly available on the R2 genomics website [http://r2.amc.nl]. The correlation between lncNB1 and MYCN RNA levels was

evaluated using two-sided Pearson's (R) coefficient, which measured the strength of the association of their expression pattern. This parameter showed a statistically significant R-value of 0.503, confirming the relationship (**Fig. 1c**). Once again, the dataset analysis revealed that lncNB1 expression was significantly higher in a subset of MYCN amplified neuroblastoma samples compared to MYCN non-amplified (**Fig. 1d**).

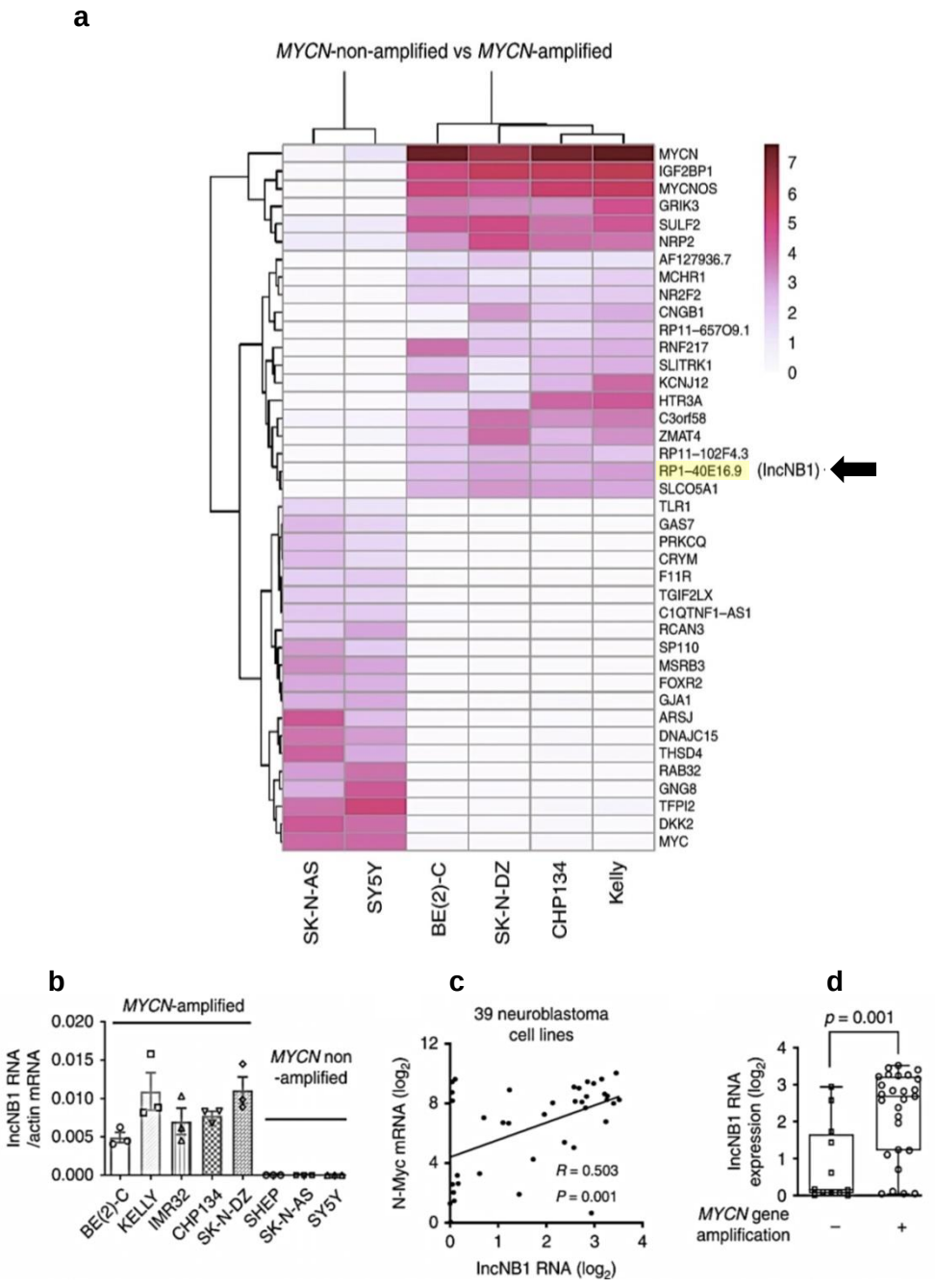

Figure 1. (**a**) RNA samples from four MYCN gene-amplified [MYCN (+)] [BE(2)C, Kelly, CHP134 and SK-N-DZ] and two MYCN gene non-amplified [MYCN(-)] (SY5Y and SK-N-AS) human neuroblastoma cell lines were sequenced. Heatmap showed the top 40 genes most differentially expressed between the two groups of cell lines. Black arrow indicates lncNB1 expression. (**b**) RT-qPCR analyses performed on MYCN-amplified and MYCN-non-amplified human neuroblastoma cell lines, followed by lncNB1 RNA expression analyses. Data were shown as the mean ± standard error of three independent experiments. **(c-d)** lncNB1 and N-MYC RNA expression was evaluated using the publicly available Maris-41-FPKM-rsg001 RNA sequencing dataset from 39 human neuroblastoma cell lines downloaded from R2 microarray analysis and visualization platform [http://r2.amc.nl]. Correlation between lncNB1 and N-MYC RNA expression was analyzed by two-sided Pearson's correlation. *Copyright associated to (P. Y. Liu et al., 2019)*

Several lncRNAs show high specificity in various tissues, and sometimes their expression may be deregulated in tumours. To verify if lncNB1 expression is tissue-specific, we assessed the RNA levels using datasets from the Genotype-Tissue Expression (GTEx) project [https://gtexportal.org/], which contains the records of 53 non-disease tissues from different sites of the human body across approximately 1000 people. These analyses revealed that lncNB1 is higher expressed in brain, pituitary, testis, uterus, and nerve tissues, while it is somewhat detectable in the other samples (**Fig.2a**). Importantly, pan-cancer analysis using the Cancer Genome Atlas (TCGA) datasets demonstrated that lncNB1 is not only expressed in cancer but it appeared to be highly transcribed in patients affected by neuroblastoma (**Fig.2b**).

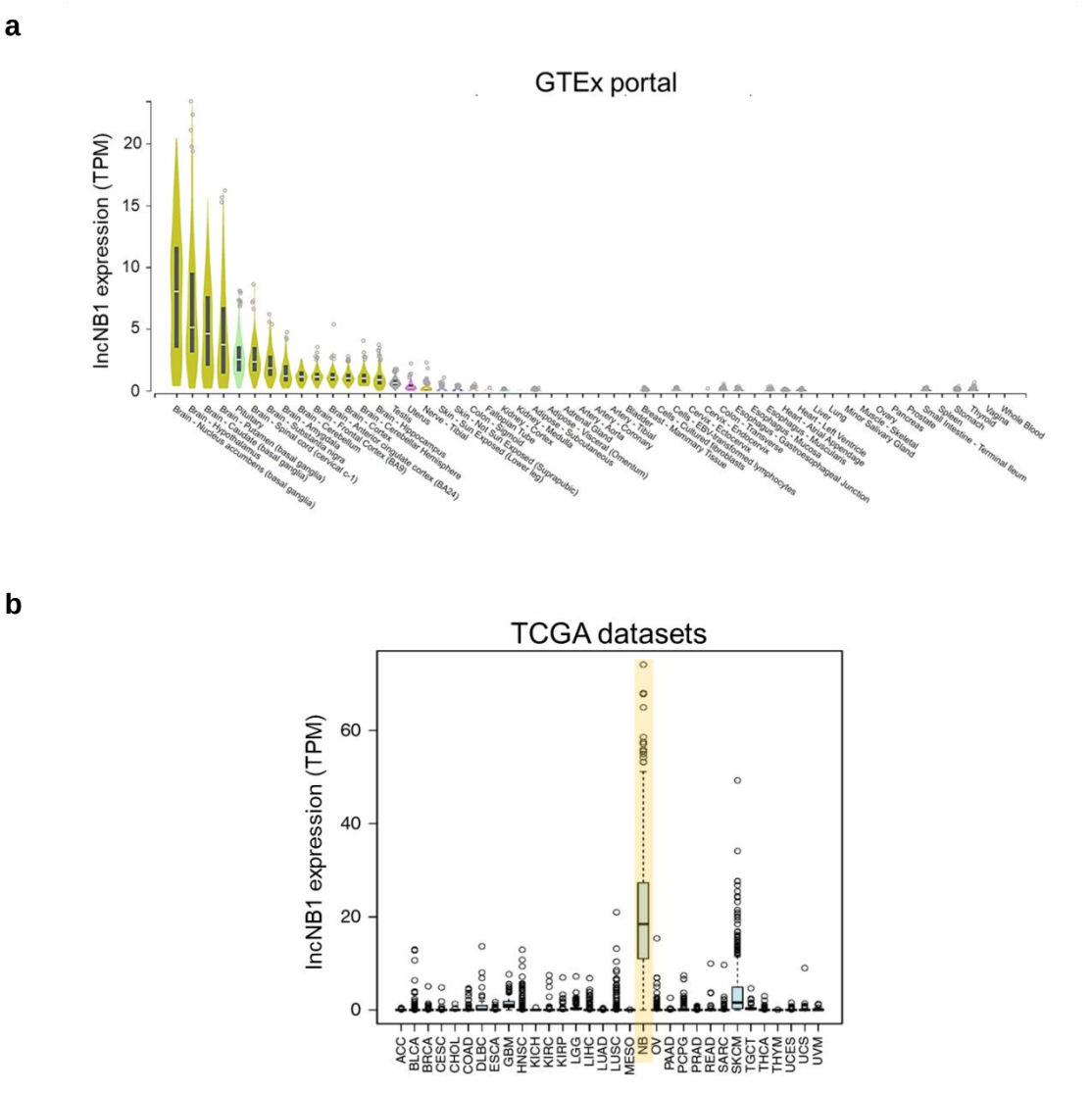

Figure 2. (**a-b**) lncNB1 expression levels on 53 normal tissues evaluated using GTEx portal [https://gtexportal.org/] and 32 cancer samples with the TCGA portal [https://portal.gdc.cancer.gov/]. Expression values are shown in TPM (transcript per million) calculated from a gene model with isoforms collapsed to a single gene. Violin and bar plots are shown as a median and 25th and 75th percentiles. Neuroblastoma samples are highlighted in yellow in figure 2b. *Copyright associated to (P. Y. Liu et al., 2019)*

To further investigate if N-MYC can directly bind lncNB1 promoter and regulate its expression, we took advantage of the ChIP-seq data, available on the Gene Expression Omnibus (GEO) accession GSE80154, performed on the SK-N-BE(2)C MYCN-amplified cell line. These analyses confirmed that the N-MYC protein (MYCN ChIP-seq) binds the promoter of lncNB1. Moreover, to comprehensively examine the extent and genomic localization of the histone modifications, we verified the enrichments in H3K27ac, H3K4me3 (markers of open chromatin) and H3K27me3 (marker of heterochromatin) on the same genomic regions. These assays unveiled the presence of euchromatin in the genomic areas corresponding to the lncNB1 *cis* regulatory elements (**Fig. 3a**). To further explore if N-MYC could directly bind the lncNB1 promoter to regulate transcription, we took advantage of the ChIP-seq data available on the Gene Expression Omnibus (GEO) accession GSE80154, executed on TET21/N cells (TET-off system for MYCN expression) treated with +/- tetracycline for 24 hours, to deeply investigate the transcriptional consequences in relation to N-MYC reduction. These analyses confirmed that N-MYC (MYCN ChIP-seq) directly binds the lncNB1 promoter and that, moreover, the downregulation of MYCN expression results in less binding on the lncNB1 promoter. To comprehensively examine the transcriptional status, we estimated the enrichments in RNA polymerase II on the same genomic region. The analyses indicated a significant decrease in binding capacities when MYCN levels are reduced (**Fig.3b**).

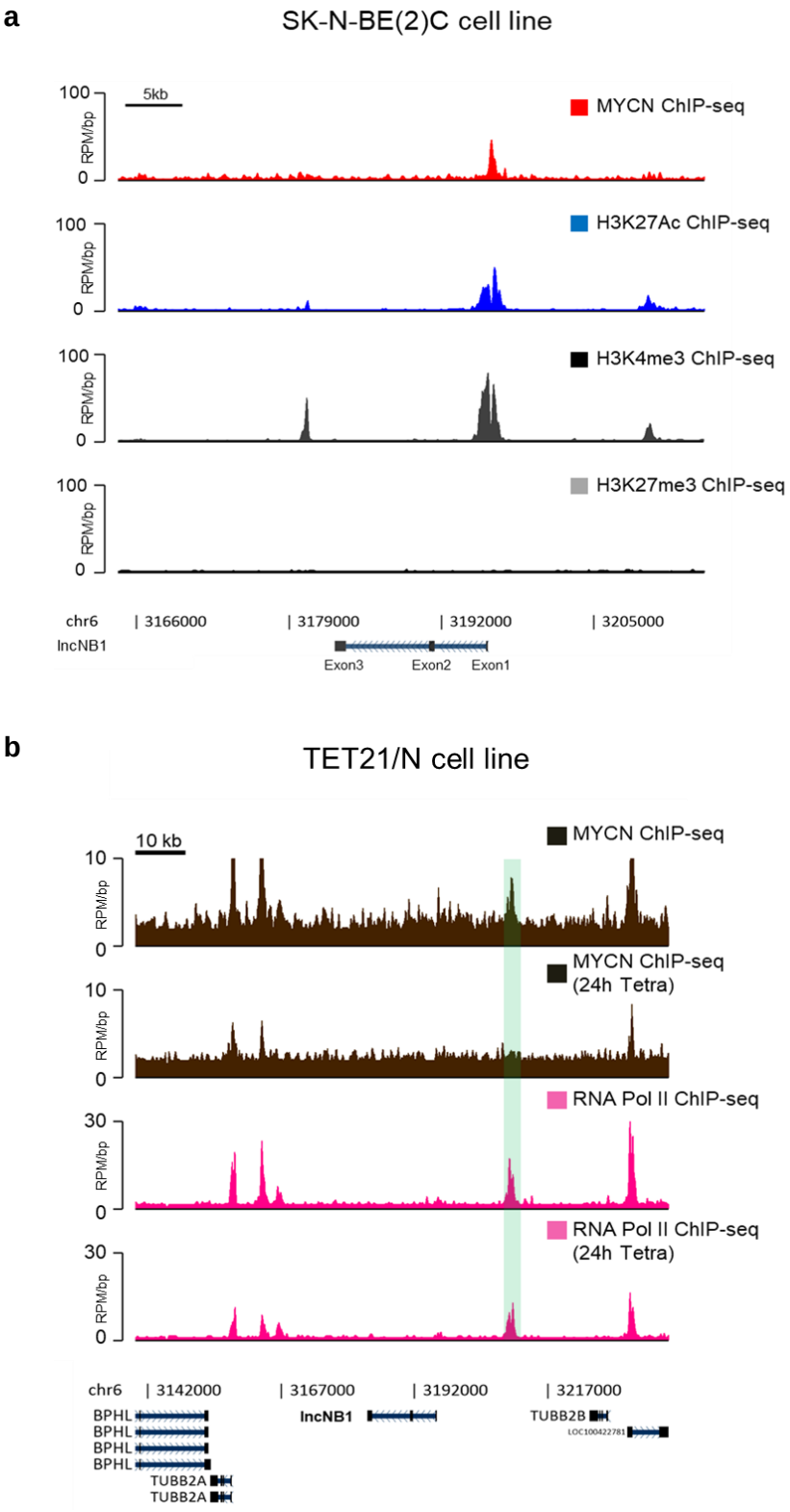

Figure 3. (**a**) ChIP-seq tracks (rpm/bp) of the indicated marks at the *lncNB1* locus across SK-N-BE(2)C neuroblastoma cell line models (MYCN amplified cell lines). Meta track representation across SK-N-BE(2)C neuroblastoma cell lines for MYCN (red), and H3K27ac (blue), H3K4me3 (black) and H3K27me3 (grey). *Copyright associated to (P. Y. Liu et al., 2019).* (**b**) ChIP-seq gene tracks (rpm/bp) showing the protein occupancy of N-MYC (brown) and RNA pol II (fuchsia) at the human lncNB1 gene locus in TET21/N cells (MYCN Tet-off system) after the suppression of MYCN expression through tetracycline injection (24h Tetra).

High levels of lncNB1 correlate with patients' poor prognosis and bad outcomes

The investigation of the clinical significance of lncNB1 in patients affected by neuroblastoma was then evaluated using the publicly available SEQC-RPM-seqcnb1. This RNA-seq dataset contains 493 human neuroblastoma tissues, examined through the R2 genomics platform [http://r2.amc.nl]. Samples derived from patients affected by MYCN amplification displayed significantly higher expression of lncNB1 compared to MYCN non-amplified samples, confirming the previous data (**Fig. 4a**). Moreover, Kaplan–Meier survival curves revealed the association between high levels of lncNB1 and poor patient prognosis (**Fig. 4b**). Interestingly, high lncNB1 expression was also associated with bad outcome by considering the 181 of 493 patients of the same cohort classified as stage 4 (high-risk phenotype) (**Fig. 4c**). The median level of RNA expression was used as a cut-off in all the cases described before.

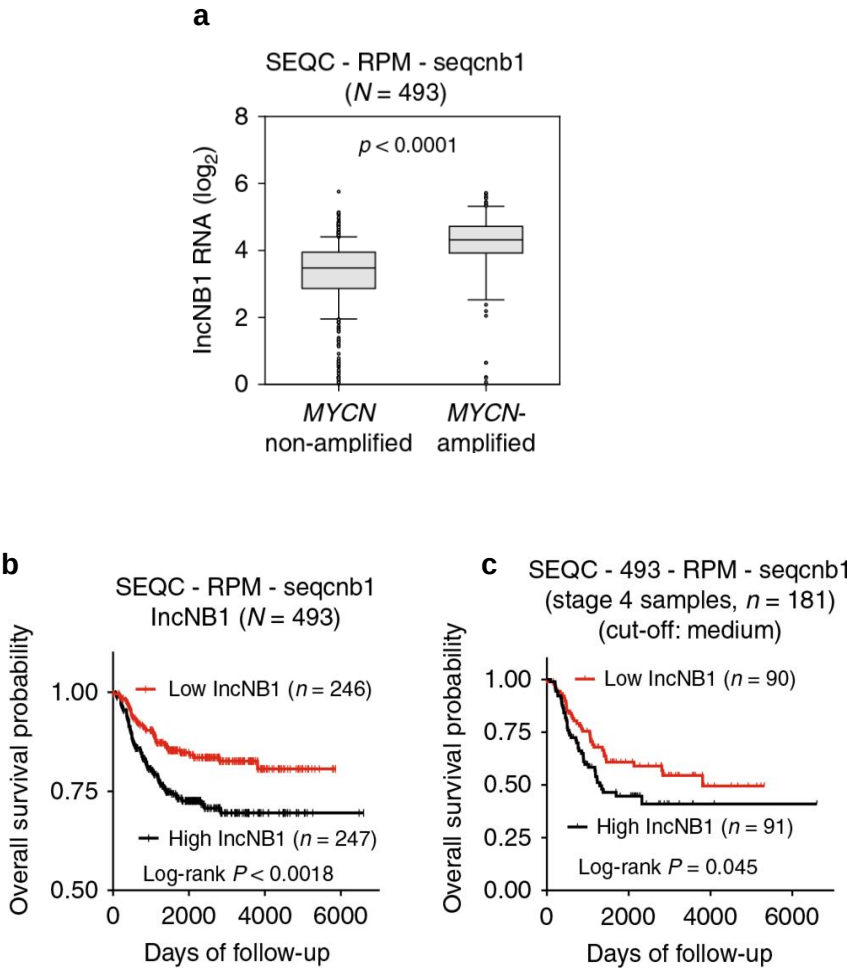

Figure 4. (**a**) Correlation between lncNB1 RNA expression and MYCN gene amplification was analyzed using two-sided unpaired Student's t-test. (**b-c**) Kaplan–Meier curves showed the probability of overall survival of neuroblastoma patients according to the levels of lncNB1(red: high expression; black: low expression) in 493 mixed patients affected by neuroblastoma diseases and 181 patients of the same cohort classified as high-risk neuroblastoma (stage 4). All the data derived from 493 human neuroblastoma tissues in the publicly available RNA sequencing gene expression-patient prognosis SEQC-RPMseqcnb1 dataset, downloaded from the R2 platform [http://r2.amc.nl]. *Copyright associated to (P. Y. Liu et al., 2019)*

lncNB1 downregulation reduces cell proliferation of MYCN-amplified neuroblastoma cells by diminishing N-MYC protein levels.

To better estimate the biological relevance of lncNB1 in neuroblastoma, we evaluated cell response after lncNB1 reduction in order to appreciate how the RNA downregulation could impact cancer behaviour. For this purpose, we generated SK-N-BE(2)C cell lines able to inducibly express lncNB1 shRNAs under doxycycline control (TET/on system). In detail, two different short-hairpin RNAs were designed to specifically target lncNB1 (lncNB1 shRNA-1, lncNB1 shRNA-2) and avoid off-target effects. A scramble shRNA was also used as negative control (Control shRNA).

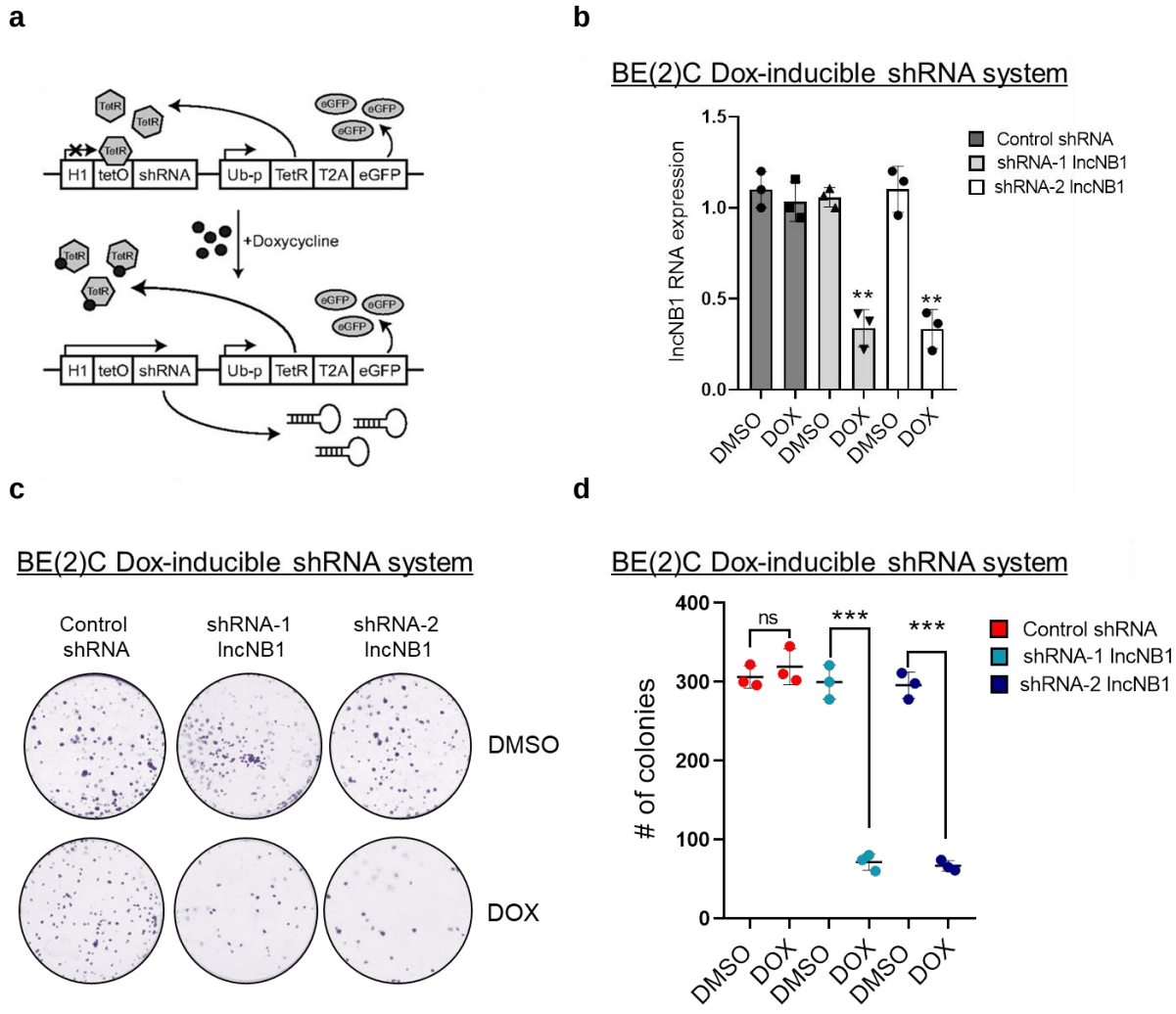

Figure 5. (**a**) The FH1tUTG lentiviral vector system contains an shRNA cassette regulated by the H1 promoter and a tet operator (tetO). A second cassette consisting of the tetR linked to a EGFP by the viral T2A peptide under the ubiquitin C promoter's control (Ub-p) is located downstream. In absence of doxycycline, the tetR protein binds the tetO and blocks shRNA transcription. After the addition of doxycycline, tetR is released, facilitating the onset of shRNA expression. EGFP is constitutively expressed under both conditions. (Herold et al., 2008) (**b**) RT-qPCR analyses concerning lncNB1 levels after 48 hours of +/-doxycycline treatment on SK-N-BE(2)C control shRNA, lncNB1 shRNA-1 and lncNB1 shRNA-2. All the experiments were done in triplicate and plotted with the respective standard deviations. Data were normalized using GUSB housekeeping gene. Data were shown as the mean ± standard error of three independent experiments. Statistical analyses were performed using t-test. Error bars represented SD. *, **, *** indicated P < .05, .01, .001, respectively.(**c-d**) Clonogenic assays performed using BE(2)C Dox-inducible cells. Cells were stained using crystal violet solution after 10 days after seeding. Colony quantification was made using the software ImageJ [https://imagej.nih.gov/]. *Copyright associated to (P. Y. Liu et al., 2019)*

Lentiviral production was completed using a 3rd generation system and FH1tUTG used as transfer backbone for all three conditions (Herold et al., 2008). Briefly, this plasmid is characterized by the presence of the optimized TetR (tetracycline repressor protein), and eGFP (green-fluorescent reporter) coding sequences constitutively expressed under control of the ubiquitin promoter. Conversely, the H1 promoter controls the shRNAs' expression, activated only in response to doxycycline injection (**Fig. 5a**). RT-qPCR analyses were performed to validate the function of the cellular systems. While control samples didn't show any variation of lncNB1 levels under DMSO or doxycyline injection, shRNA-1 and shRNA-2 cells displayed a consistent reduction of the RNA levels after doxycyline treatment (almost 60% of reduced expression in both cases) (**Fig. 5b**). Surprisingly, in vitro clonogenic assays unveil a significant decline in colony-forming capacities when lncNB1 expression was downregulated in both lncNB1 shRNA-1 and shRNA-2 cells treated with doxycycline. In contrast, control shRNA cells didn't show any differences by comparing the two experimental conditions (**Fig.5 c-d**). It is well-known that lncRNAs can work as active players for the regulation of gene expression. Their abundance may be controlled or can control tumour suppressors and oncogenes levels (see introduction). We further investigated whether lncNB1 downregulation may affect N-MYC protein or mRNA expression. While RT-qPCR experiments demonstrated that N-MYC mRNA levels didn't exhibit any variations in all the six samples (**Fig. 6a**), immunoblotting analyses revealed a significant downregulation of N-MYC protein abundance when the expression of lncNB1 was silenced compared to control (**Fig. 6b**).

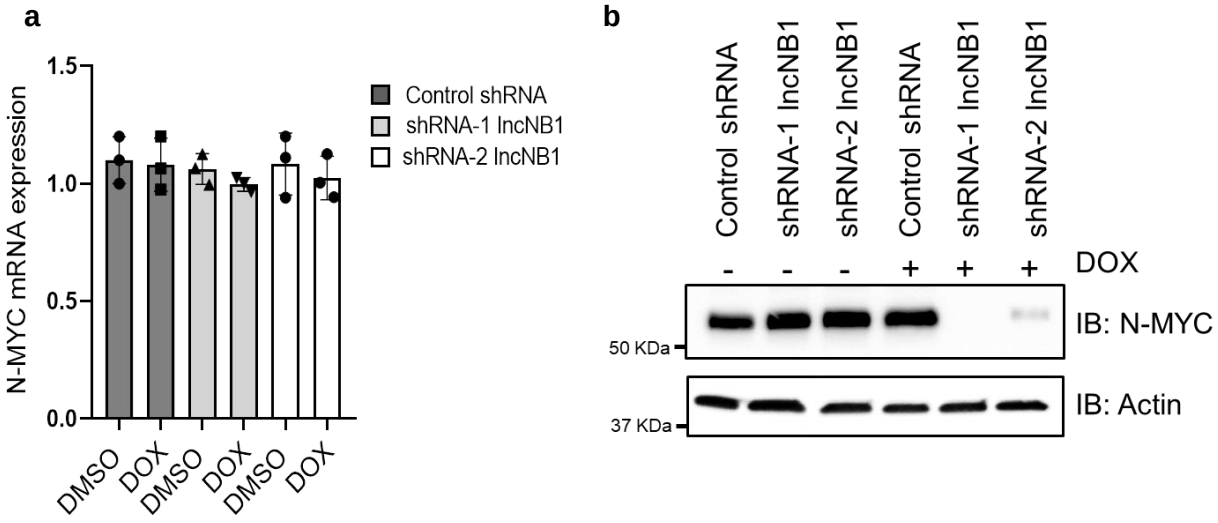

Figure 6. (**a**) RT-qPCR analyses concerning N-MYC mRNA levels after 48 hours of +/- doxycycline treatment on SK-N-BE(2)C control shRNA, lncNB1 shRNA-1 and lncNB1 shRNA-2. All the experiments were done in triplicate and plotted with the respective standard deviations. Data were normalized using GUSB housekeeping gene. Data were shown as the mean ± standard error of three independent experiments. Statistical analyses were performed using t-test. Error bars represented SD. *, **, *** indicated P < .05, .01, .001, respectively.(**b**) immunoblot of N-MYC and Actin protein levels measured in BE(2)C Dox-inducible cells (control shRNA, lncNB1 shRNA-1 and lncNB1 shRNA-2) upon lncNB1 shutdown after 48 hours of +/- doxycycline treatment. Actin was used as housekeeping gene. *Copyright associated to (P. Y. Liu et al., 2019)*

lncNB1 regulates DEPDC1B expression to induce N-MYC protein stabilization

To understand how lncNB1 influences N-MYC protein expression, we performed Affymetrix microarray analyses on SK-N-BE(2)C cells transiently transfected with two different small interfering RNAs (siRNA) that specifically downregulate the expression of lncNB1. A scramble siRNA was also used as a negative control (data not shown). Among the plethora of differently expressed target genes, our attention was focused on DEPDC1B since its expression linearly correlated with lncNB1 levels. This gene encodes a GEF protein, which stimulates the ERK kinases (MAPK3 and MAPK1) by inducing their phosphorylation (Marchesi et al., 2014; Su et al., 2014). Once activated, phosph-ERKs can increase N-MYC protein stability through phosphorylation of the Ser62 residue. This post-translational modification drastically increase N-MYC protein levels, by working on its half-life (Sears et al., 2000).

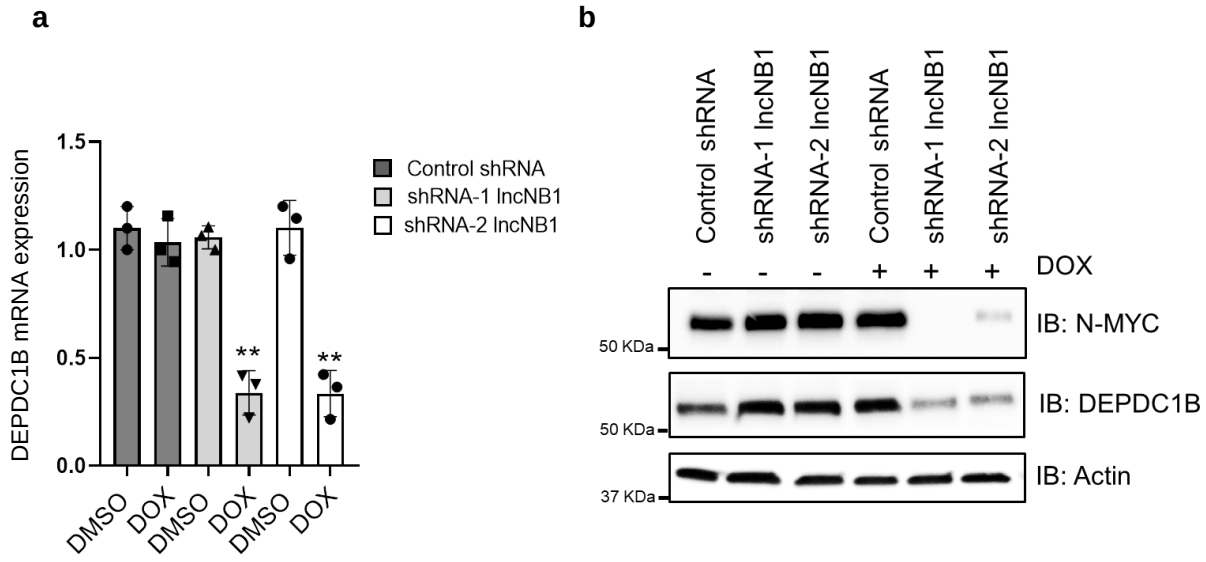

Figure 7. (**a**) RT-qPCR analyses concerning DEPDC1B mRNA levels after 48 hours of +/-doxycycline treatment on SK-N-BE(2)C control shRNA, lncNB1 shRNA-1 and lncNB1 shRNA-2. All the experiments were done in triplicate and plotted with the respective standard deviations. Data were normalized using GUSB housekeeping gene. Data were shown as the mean ± standard error of three independent experiments. Statistical analyses were performed using t-test. Error bars represented SD. *, **, *** indicated P < .05, .01, .001, respectively.(**b**) immunoblot of N-MYC, DEPDC1B, and Actin protein levels measured in BE(2)C Dox-inducible cells (control shRNA, lncNB1 shRNA-1 and lncNB1 shRNA-2) upon lncNB1 shutdown after 48 hours of +/-doxycycline treatment. Actin was used as housekeeping gene. *Copyright associated to (P. Y. Liu et al., 2019)*

To validate the expression data and confirm this hypothesis, we executed RT-qPCR and immunoblotting analyses using the doxycycline-inducible BE(2)C cells, in order to appreciate DEPDC1B expression. The downregulation of lncNB1 resulted in less transcription of the DEPDC1B gene, as showed in **Fig.7a**, thus validating microarray data. Moreover, this event downstream lead to less amounts of DEPDC1B (**Fig.7b**), phosph-ERK but not total ERK protein levels (data not shown). The reduced activity of this pathway results in less pSer62 N-

MYC protein amounts and, consequently, less protein stabilization (**see in addition reference in the figure legend**).

lncNB1 upregulates E2F1 expression to increase DEPDC1B transcription

The effect of lncNB1 on DEPDC1B mRNA expression was further examined using gene reporter assays. Indeed, serial-deleted DEPDC1B promoter sequences were cloned into the basic luciferase reporter vector pGL3b. The resulting constructs [DEPDC1B_1146bp/_545bp/_75bp] were then transfected into doxycycline-inducible control shRNA, lncNB1 shRNA-1, or lncNB1 shRNA-2 BE(2)C cells, and luciferase activity was measured as a function of lncNB1 expression. Results showed that the promoter activities positively correlated with lncNB1 expression, confirming that lncNB1 activates DEPDC1B at transcriptional levels (**Fig. 8a**). Conversely, no changes in the luciferase activities were obtained using constructs containing an extra 20 bp deletion close to the transcriptional start site [DEPDC1B_545bp_Δ20bp /_75bp_Δ20bp] (**Fig. 8a**). Bioinformatic analyses performed on the 20bp promoter region using the PROMO predicting tool (http://alggen.lsi.upc.es/), identified the putative transcription factor binding sites (TFBS) contained in this sequence, thus placing E2F1 as the top candidate (**Fig. 8b**).E2F1 levels were then investigated using immunoblotting analyses, revealing the positive relationship between lncNB1 and E2F1 protein (**Fig. 8c**) but not mRNA expression (data not shown).To further examine if lncNB1 can regulate the E2F1-DNA binding capacities on DEPDC1B promoter, we analyzed whether E2F1 can directly target the transcriptional start site of DEPDC1B in vivo as a function of lncNB1 expression; chromatin immunoprecipitation (ChIP) assays were used to achieve this purpose.

ChIP assays showed that E2F1 protein was highly enriched at the DEPDC1B gene core promoter region, and that the knockdown of lncNB1 significantly reduced E2F1 protein binding at the DEPDC1B gene core promoter in doxycycline-inducible lncNB1 shRNA-1 and shRNA-2 BE(2)-C cells (**Fig. 8d**). Moreover, luciferase assays confirmed that the overexpression of E2F1 and its functional partner DP1 significantly increase wild-type DEPDC1B gene promoter activity, while this effect was completely abolished using the Δ20bp DEPDC1B gene promoter constructs (**Fig. 8e**). Taken together, these data suggest that lncNB1 activates DEPDC1B gene transcription through increasing E2F1 protein expression.

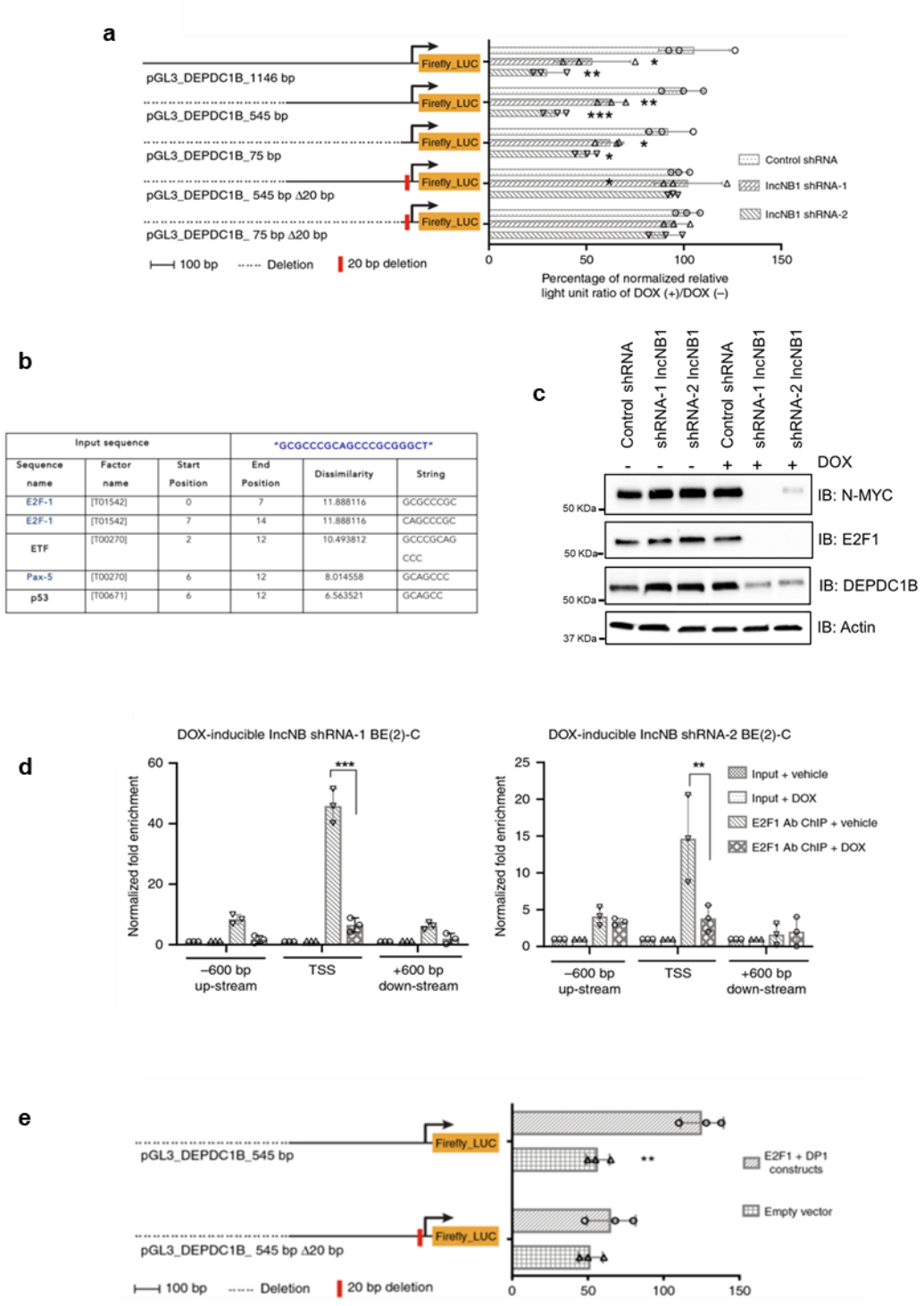

Figure 8. (a) DOX-inducible control shRNA, lncNB1 shRNA-1, and lncNB1 shRNA-2 BE(2)-C cells were transfected with the wild type or Δ20bp deletion mutant DEPDC1B gene promoter pGL3 constructs, followed by treatment with vehicle control or DOX and luciferase assays. Percentage change in luciferase activity, measured as relative light unit (RLU) due to DOX treatment as compared with vehicle control treatment, was normalized by the luciferase activity of DOX-inducible control shRNA cells treated with vehicle control. Data were shown as the mean ± standard deviation, and evaluated by one-way ANOVA. *, **, and *** indicated P < 0.05, 0.01, and 0.001 respectively. **(b)** Bioinformatic analyses of the putative transcription factor binding sites (TFBS) contained in the Δ20bp deleted sequence were performed using the PROMO predicting tool by Alggen (http://alggen.lsi.upc.es/). **(c)** Immunoblot of N-MYC, E2F1, DEPDC1B, and Actin protein levels measured in BE(2)C Dox-inducible cells (control shRNA, lncNB1 shRNA-1 and lncNB1 shRNA-2) upon lncNB1 downregulation after 48 hours of +/-doxycycline treatment. Actin was used as housekeeping gene. **(d)** ChIP assays were performed with a specific anti-E2F1 antibody (Ab) in DOX-inducible lncNB1 shRNA-1 or shRNA-2 BE(2)-C cells after treatment with vehicle control or DOX, followed by PCR with primers targeting different regions of the DEPDC1B gene promoter (−600 bp, transcription start site (TSS) or +600 bp). **(e)** BE(2)-C cells were co-transfected with pCMV14-empty vector or pCMV14-E2F1 plus pCMV10-3 × Flag-DP1 constructs in combination with wild type or E2F1-binding site (Δ20bp) deletion mutant DEPDC1B gene promoter pGL3 Firefly_LUC construct. Data were shown as the mean ± standard deviation, and evaluated by one-way ANOVA. *, **, and *** indicated P < 0.05, 0.01, and 0.001, respectively. Copyright associated to (P. Y. Liu et al., 2019)

lncNB1 is localized in the cytoplasm and binds the ribosomal protein L35 (RPL35)

LncRNAs localization is one of the critical determinants to recognize how they exert their related-cellular functions (Carlevaro-Fita & Johnson, 2019). To determine whether lncNB1 affects the expression of the E2F1 protein, we firstly performed RNA fractionation assays coupled with RT-qPCR analyses in SK-N-BE(2)C cells to assess what is the subcellular compartment in which lncNB1 is mostly enriched. The RNA fractionation method was performed by using several rounds of centrifugation with sucrose density gradient.

As reported in the literature, MALAT1 and GAPDH RNAs displayed a nuclear and cytoplasmic localization, respectively (DANI et al., 1984; Eißmann et al., 2012). This analysis revealed that lncNB1 is mostly abundant in the cytoplasm compared to the nucleus (**Fig. 9a-b**) as then confirmed by RNA FISH analyses (**data not show – see reference figure legend**).

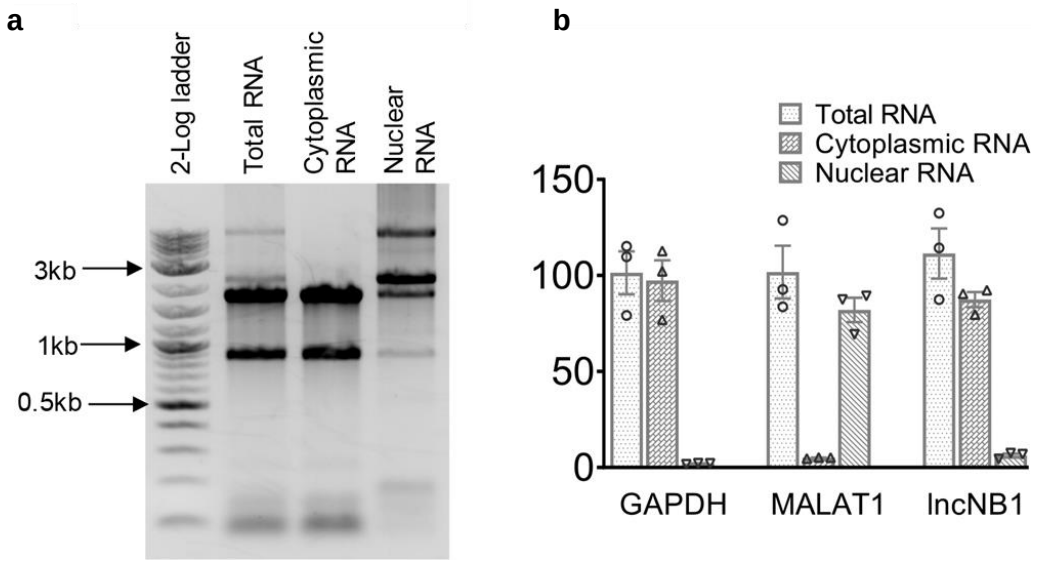

Figure 9. (**a-b**) RNA was extracted from BE(2)C cells with or without cytoplasmic and nuclear RNA fractionation. The RNA samples were run on a 1.5% agarose gel to evaluate their integrity and subjected to qRT-PCR analysis of lncNB1, the cytoplasmic RNA marker GAPDH and the nuclear RNA marker MALAT1. *Copyright associated to (P. Y. Liu et al., 2019)*

To identify the mechanism by which lncNB1 increases E2F1 protein but not mRNA expression, an RNA pull-down was performed by our collaborators using the in vitro-transcribed lncNB1 RNA obtained by the full-length lncNB1 cDNA. The template was transcribed under the control of the T7 promoter in the sense strand (experimental) or SP6 promoter in the antisense strand (negative control) and then biotinylated at the 5'-end of each molecule. The biotin-labelled lncNB1 RNA was then incubated with a total protein extract derived from BE(2)C cells. Mass spectrometry analysis revealed that lncNB1 RNA specifically bound to ribosomal protein L35 (RPL35), the RNA helicase DDX42, the histone protein H1X, interleukin enhancer-binding factor 2 (ILF2), and heterogeneous nuclear

ribonucleoprotein K (HNRPK) proteins but only RPL35 silencing significantly reduced DEPDC1B, N-MYC, and E2F1 protein expression (Table 2).

Protein ID	Protein name	Molecular weight (KDa)	Score *	Matches †	Sequences †	*emPAI* ‡
gi|45446747	ATP-dependent RNA helicase DDX42	102.912	96	4 (4)	4 (4)	0.14
gi|5174449	Histone H1X	22.474	52	4 (4)	4 (4)	0.83
gi| 48145659	Heterogeneous nuclear ribonucleoprotein K	50.944	173	8 (8)	7 (7)	0.61
gi| 392513662	Interleukin enhancer-binding factor 2	43.035	114	5 (5)	5 (5)	0.49
gi| 48145871	60S ribosomal protein L35	14.543	56	3 (3)	3 (3)	0.99

Table 2. lncNB1 RNA-binding proteins identified by RNA-binding protein pull-down assays and mass spectrometry analysis. *Copyright associated to (P. Y. Liu et al., 2019)*

DISCUSSION (Part I)

Childhood and paediatric cancers are among the leading causes of death in children in the first years of life. Since these children' pathologies are mostly unknown, research focuses on developing new treatments that block the critical steps of forming and evolving these malignancies to improve their prognosis. Our understanding of cancer biology was drastically driven by the last decade's genomic revolution, marked by the Human Genome Project's conclusion and the development of novel DNA sequencing technologies. Despite the coding genome accounts for less than 2% of all sequences, transcription of several non-coding regions appears to be a critical hit required in cancer development, which can drastically influence the malignant processes (Ling et al., 2015). Long non-coding RNAs (lncRNAs) take hold as novel aspects from the genome-wide revolution (Bartonicek et al., 2016; Wilusz et al., 2009).

On this basis, it's not surprising that alterations in lncRNAs expression emerged as new possible targets for therapeutic intervention due to their extreme specificity and oncogenic roles in multiple diseases, including childhood cancers. This thematic is of great importance in neuroblastoma, the most common extracranial solid tumour of childhood and infancy, originating from undifferentiated neural crest cells. Despite the latest striking new findings in this field, no genetic or epigenetic aberrations in common by all the neuroblastoma phenotype have been established yet. However, a few genomic alterations are known to be associated with tumorigenesis, which may be fruitful for identifying some subtypes of neuroblastoma and, consequently, survival odds (Matthay et al., 2016; Theissen et al., 2014).

In this background, the amplification of the MYCN gene appears to be one of the best-characterized genetic high-risk markers prognostic for this pathology, found in almost 25% of all cases. When MYCN is amplified and its activity unleashed, the transcriptional regulation MYCN-mediated can spread out beyond its standard capacity to control the expression of a specific set of genes. Indeed, high amounts of N-MYC protein can lead to the activation/repression of multiple transcriptional programs resulting in the stimulation of specific oncogenic signatures generally characterized by the dysregulation of both coding genes but also non-coding RNAs expression, like miRNA, circRNA, eRNA and long non-coding RNA, which drastically impact the tumorigenic process (Buechner & Einvik, 2012).

Our study investigated whether and how N-MYC can regulate transcription of lncRNAs by comparing transcriptional profiles between non-amplified and MYCN-amplified neuroblastoma cells using RNA-sequencing technology. Among the several lncRNAs

stimulated by N-MYC, we singled out lncNB1, a lncRNA expressed at high levels in MYCN-amplified cells only that appears to be firmly and almost uniquely transcribed in neuroblastoma among all types of cancer. Gene expression analyses confirmed the close relationship between lncNB1 and MYCN expression; indeed, N-MYC can directly regulate its expression as demonstrated by ChIP-seq analyses. The evaluation of the clinical significance of lncNB1 expression was further confirmed by analyzing a mixed cohort of neuroblastoma tissues and through the valuation of the overall survival as function of lncRNA expression.

Surprisingly, we discovered that lncNB1 instructs a positive regulatory loop by increasing N-MYC protein stabilization, the best-characterized marker of high-risk neuroblastoma.

As previously showed in the results (part I) paragraph, the reduced expression of lncNB1 didn't affect N-MYC mRNA expression, however, Affymetrix microarray analyses unveil the impact on gene expression regulation when lncNB1 levels were reduced. Among the plethora of differently expressed target genes, our attention was focused on DEPDC1B. This gene encodes a GAP protein, which it is known to stimulate the ERK kinases (MAPK3 and MAPK1) by inducing their phosphorylation (Marchesi et al., 2014; Su et al., 2014). Once activated, phosph-ERKs can increase N-MYC protein stabilization through phosphorylation of the Ser62 residue by working on its half-life (Sears et al., 2000).

lncNB1 positively regulates transcription of DEPDC1B as confirmed by both RT-qPCR and dual reporter assays. Interestingly, the evaluation of the transcriptional activation of DEPDC1B promoter as function of lncNB1 expression revealed the addiction of the system with the E2F1 transcription factor. Subcellular fractionation assays and RNA pull-down experiments coupled with mass spectrometry analyses indicated that lncNB1 is predominantly localized in the cytoplasm and that it can interact with the Ribosomal Protein L35 (RPL35) to increase the E2F1 translational rate (see *P. Y. Liu et al., 2019* reference). Consistently, these data therefore suggest that lncNB1 indirectly induces DEPDC1B gene transcription through increasing protein expression of E2F1, which directly binds to the DEPDC1B gene promoter and enhances DEPDC1B gene transcription, leading to ERK protein phosphorylation and N-MYC protein stabilization.

Several indications suggest that lncRNAs could be, in some cases, new regulators of oncogenes' mRNA stability or cancer suppressor genes. Indeed, this new frontier of gene expression regulation is constantly evolving over the years, shedding light on the functions of novel RNA molecules previously unexplored. Some examples of this type are the urothelial carcinoma-associated 1 (lncRNA UCA1), which can stabilize CDKN2A-p16 mRNA by

sequestering heterogeneous nuclear ribonucleoprotein A1 (hnRNPA1) (Kumar P et al., 2014), or the Programmed cell death 4 (PDCD4)-antisense RNA1 (lncRNA PDCD4-AS1), able to support PDCD4 mRNA stabilization by forming an RNA duplex between PDCD4 mRNA and the ELAV-like protein 1 in breast cancer (Jadaliha et al., 2018).

The identification of lncNB1 in the context of neuroblastoma may be presumably translated into clinical scenarios in a reasonable timeline. Although various questions and challenges remain to be addressed, this discovery offers an exciting chance to develop new treatments for neuroblastoma due the expression specificity and biological impact (**Overview Part I**).

Taken together, the identification of this novel lncRNA provides a new opportunity for the development of specific treatments able to target the N-MYC protein stability in a context of MYCN gene amplification, shedding light on the possible application of silencing of lncNB1 for the treatment of neuroblastoma.

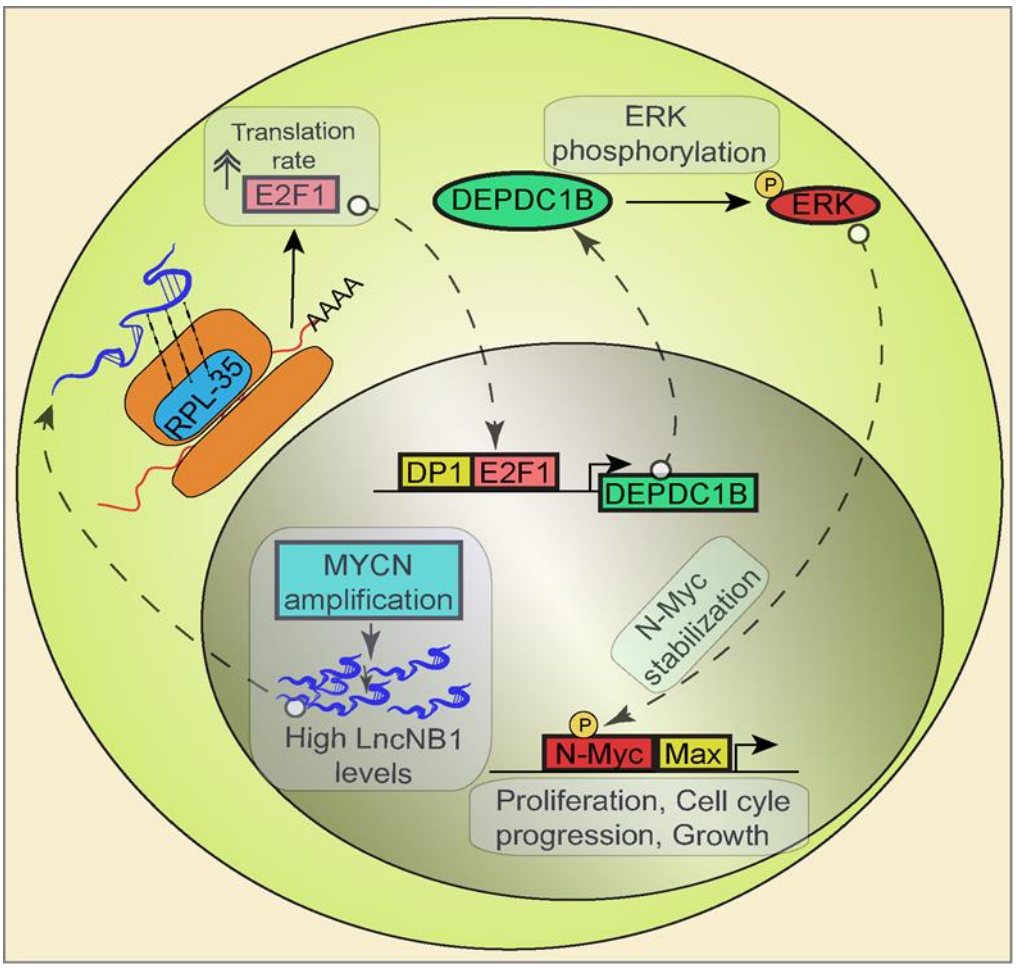

Overview Part I: Schematic representation of the functional characterization of the novel long non-coding RNA lncNB1 to promote N-MYC protein stabilization in high-risk neuroblastoma.

RESULTS (Part II):

The role of the E2F3a and E2F3b proteins and their interactomes for the instruction of a novel functional axis with N-MYC in neuroblastoma.

E2F3: a novel prognostic biomarker of neuroblastoma pathology

A recent pan-cancer analysis of 11,000 tumours, representing 33 different adult malignancies, revealed that the amplification of MYC family oncogenes (MYC, MYCN, or MYCL) occurs in almost 28% of all human cancers (Schaub et al., 2018). MYCN amplification necessarily implies overexpression of the N-MYC protein in cancer cells, perturbing its occupancy distribution in the genome. In addition to that, many studies showed that N-MYC exerts its global activity by physically interacting with a plethora of other proteins involved in all the steps of transcription and epigenetic regulation, making it difficult to narrow down which interactors are the main co-drivers of oncogenesis. Recent studies have listed E2F proteins as possible master regulators, cooperating with N-MYC to drive the oncogenic phenotype (Kalkat et al., 2018; Rajbhandari et al., 2018; P. Y. Liu et al., 2019). This gene family encodes eight different transcription factors (E2F1-8) that work in concert for the accurate regulation of cell cycle progression (Kent & Leone, 2019). Several studies suggest that N-MYC, E2F1 and E2F3 may establish a functional axis that is supposed to be of great relevance to cancer initiation/progression in neuroblastoma diseases characterized by MYCN gene amplification. To outline an overall view on the status of E2F factors in neuroblastoma, we analyzed mRNA expression levels of all E2Fs and assessed their potential role as prognostic markers in four different neuroblastoma datasets: TARGET, NRC/SIOP, Kocak and Versteeg. We took advantage of the Kocak dataset (GSE45547) as a benchmark since it was the largest dataset at our disposal. For each cohort and each gene of interest, we tested the statistical significance of the association with survival *via* a Cox model, based on groups of patients stratified by each gene's median expression level. The statistical significance of the association between high mRNA expression of E2Fs, MYC and MYCN and survival was examined. Our results showed a high correlation degree between the four datasets, reported by positive and significant pairwise Spearman Correlation Coefficient (SCC). Interestingly, among all the E2F family members, high expression of E2F1 and E2F3 are the most prominently associated with bad outcome across the four-neuroblastoma datasets.

Moreover, E2F1 and E2F3 appear to be more predictive of poor prognosis compared to MYC and MYCN expressions too, suggesting a self-reliant function not closely dependent on MYCN amplification status (**Fig. 10**).

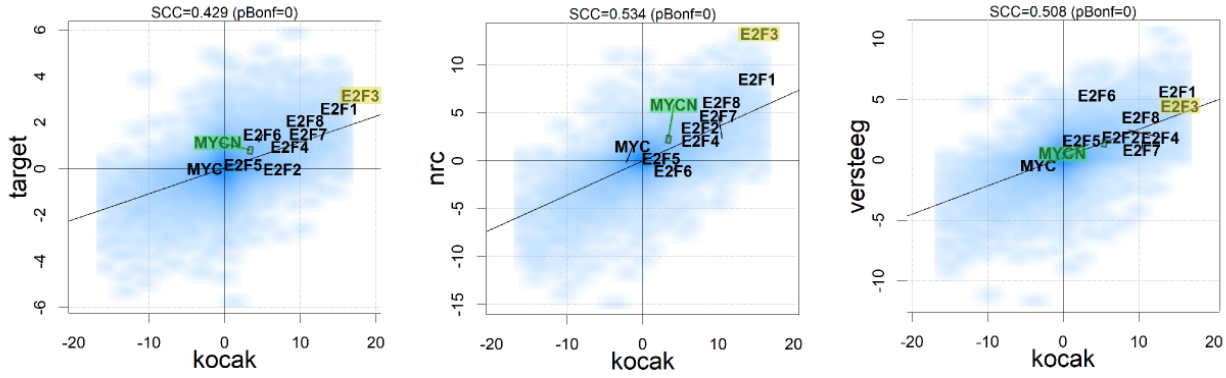

Figure 10. Correlation between mRNA expression and their consequent impact on survival for E2Fs in TARGET, NRC, VERSTEEG and KOCAK datasets of neuroblastoma patients. Cox model based on groups of patients stratified by the median expression level of each gene and by comparing the four datasets two by two. When the log10 (p-value) has a high positive trend the expression profile is connected to poor prognosis, while it is the opposite in case of a negative trend. X and Y axes carry the respective log10 (p-value) of the survival test in NB datasets. E2Fs and MYC and factors were highlighted in black while E2F3 and MYCN expression were highlighted in yellow and green, respectively.

Since our analyses provided evidences that E2F3 is more strongly associated to poor prognosis compared to E2F1 expression, we decided to explore E2F3 role in childhood neuroblastoma. The investigation of the clinical significance of E2F3 was further inspected by comparing the expression profiles between MYCN-amplified and MYCN non-amplified samples using the Kocak dataset, which contains data from 649 human neuroblastoma tissues analyzed through array technology. These analyses unveiled that samples with MYCN amplification displayed a significantly higher amount of E2F3 compared to MYCN non-amplified ones (**Fig. 11a**). The correlation between E2F3 and MYCN RNA levels was then evaluated using two-sided Pearson's (R) coefficient, showing a statistically significant R-value of 0.502, and confirming the linear relationship between their co-expression (**Fig. 11b**). The investigation of E2F3 mRNA expression using the Kocak dataset elucidated that the E2F3 gene is highly transcribed in samples derived from patients with the worst prognosis (stage III and stage IV), presenting a significant association between high levels of E2F3 and short-term survival in neuroblastoma (**Fig. 11c**).

These data have assumed additional relevance after evaluating how the correlation between MYCN and E2F3 expression is associated with survival using a second Cox-model (**Fig. 11d-e)**. Indeed, the percentage of survival for patients characterized by high levels of MYCN and E2F3 expression (red kaplan curve) appears similar to those with high E2F3 but low MYCN expression (green kaplan curve).

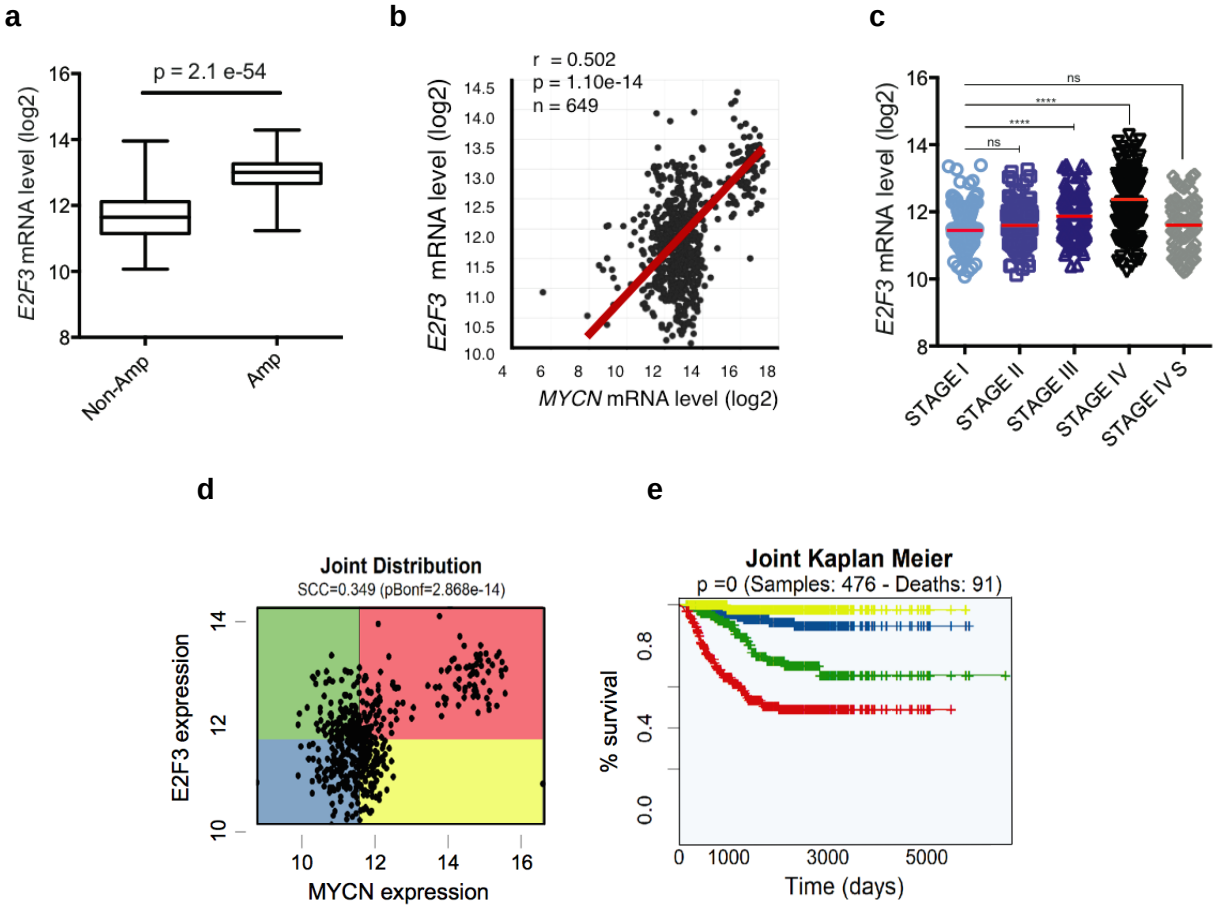

Figure 11. (a) E2F3 RNA expression was evaluated as a function of MYCN amplification status using a total of 643 primary neuroblastoma cases relative to the Kocak cohort, downloaded from the R2 genomics platform [http://r2.amc.nl]. The p-value by the Mann–Whitney test is indicated. **(b)** Scatter plot regarding the correlation between E2F3 and MYCN RNA expression analyzed by two-sided Pearson's association. The entire Kocak cohort (n=649) was examined. MYCN and E2F3 mRNA levels are shown on the x-axis and y-axis, respectively. The p-value by the Mann–Whitney test is indicated. The red line specifies the corresponding R-value of 0.502. **(c)** Scatter dot plot of E2F3 expression levels using the Kocak NB cohort. Data were stratified based on tumour stages according to the INRGSS classification and then evaluated by one-way ANOVA. *, **, and *** indicating P < 0.05, 0.01, and 0.001, respectively. The red line corresponds to the median expression of each group. (**d-e**) Survival analysis of the Kocak NB dataset. E2F3 and MYCN expression were evaluated through Cox model analysis and separated into four coloured quadrants according to median expression levels of MYCN and E2F3. Colours of Kaplan Meier curves match with the colours of the quadrants. The p-value by the Cox model test is indicated.

Interestingly, patients who express high levels of MYCN generally display high levels of E2F3, resulting in the worst scenario (red Kaplan curve). However, a substantially lower survival rate was recognized by comparing samples that express only high levels of E2F3 (green Kaplan curve) with those characterized by high MYCN expression only (yellow Kaplan curve), suggesting that E2F3 may be an independent negative predictor of survival in many types of neuroblastoma.

E2F3a but not E2F3b is prognostic in neuroblastoma

The human E2F3 gene expresses two distinct mRNAs, E2F3a and E2F3b, transcribed from two alternative promoters (Adams et al., 2000) (**Fig. 12a**). As a result, E2F3a and E2F3b have unique first protein-coding exons of 122 and 6 N-terminal amino acids respectively and share the same sequence in all the remaining regions (**Fig. 12b**). To better characterize what are the differences between the two transcriptional variants in terms of expression and impact in childhood neuroblastoma, we evaluated the survival prognosis by perfoming Cox proportional hazards analyses of the two E2F3 isoforms using the TARGET dataset, which includes isoform-level mRNA expression data. Here, we found that the increasing expression of E2F3a but not E2F3b is a negative predictor of patient survival (**Fig. 13a-b**). Examining the TARGET datasets, we also discovered that E2F3a expression is significantly higher in Stage 4 *MYCN*-amplified patients compared to both Stage 4 *MYCN* non-amplified, and Stage 4S patients (KW test. p=0,000878) (**Fig. 13c**). In contrast, no statistically significant differences were found for E2F3b expression between the three groups (KW test. p=0,11) (**Fig. 13d**). Taken together, these data suggest that E2F3a but not E2F3b is a prognostic marker in neuroblastoma.

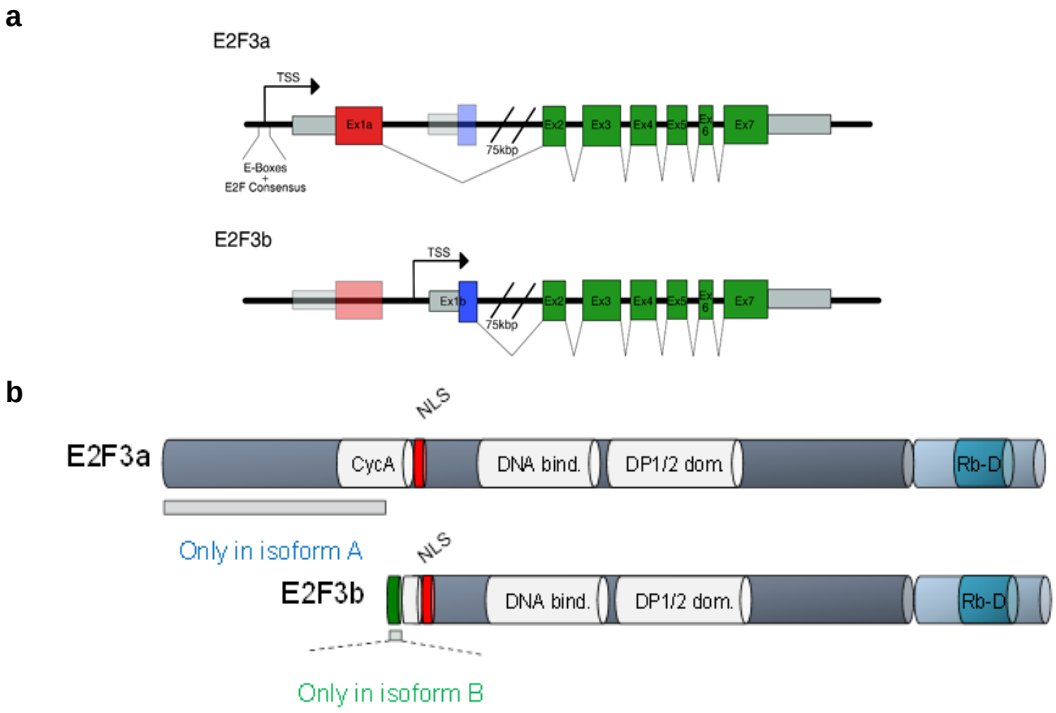

Figure 12. (a) Graphical illustration of the human E2F3 gene. Exon 1a and 1b are represented in red and blue, respectively. The shared remaining exons are coloured in green (Exon 2-7). **(b)** Graphical exemplification of the human E2F3a and E2F3b proteins. E2F3a and E2F3b have unique first protein-coding exons of 122 and 6 N-terminal amino acids respectively and share the same sequence in all the remaining regions.

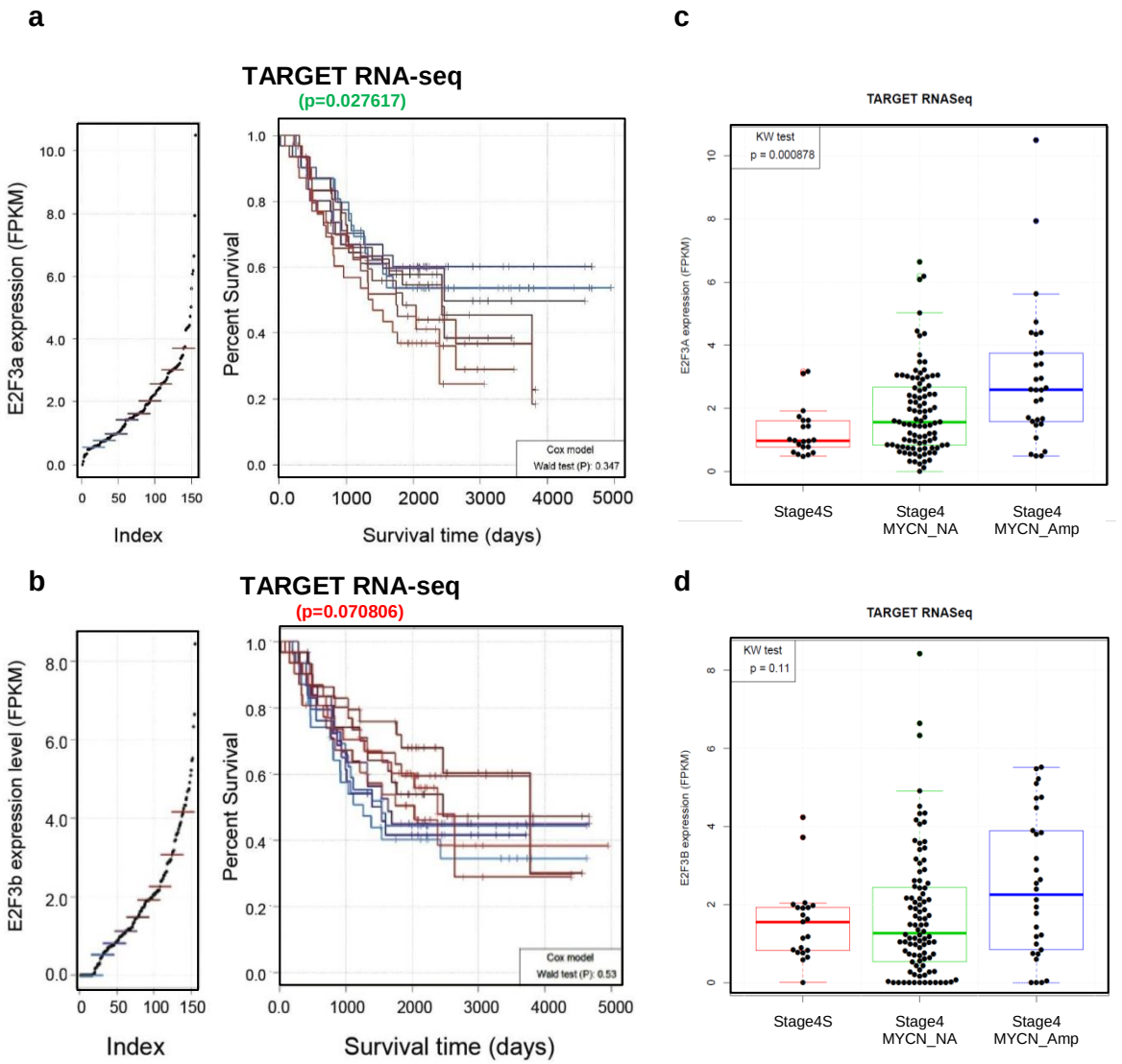

Figure 13. (a-b) Kaplan–Meier curve depicting corresponding increase in poor outcome with increasing expression of E2F3a and E2F3b. Blue and red Kaplan curves indicate low and high E2F3a/b expression, respectively. P-value was calculated using a Cox proportional hazards model. **(c-d)** Box plot of E2F3a and E2F3b expression in stage 4 MYCN-amplified patients (blue), stage 4 non-MYCN-amplified patients (green) and stage 4S tumour regression patients (red). All Expression data derived from NCI TARGET neuroblastoma cohort.

N-MYC increases E2F3a but not E2F3b expression in neuroblastoma

The effect of N-MYC on E2F3a and E2F3b mRNA and protein expression was further investigated by examining five MYCN-amplified (SK-N-BE(2)C, LAN5, KELLY, CHP134, IMR32) and three MYCN non-amplified (SK-N-FI, SK-N-AS, SHEP) cell lines using both RT-qPCR and immunoblotting analyses.

A correlation between MYCN status and E2F3a gene expression was observed, confirming the previous results. Indeed, normalizing on SHEP, SK-N-BE(2)C, LAN5 and CHP-134 display a ~ five-fold increase in E2F3a mRNA levels compared to the control. Conversely, the other cell lines (especially MYCN non-amplified) didn't reveal variations comparable to those previously mentioned (**Fig. 14a-b**). In contrast, E2F3b mRNA levels are quite heterogeneous among all the analyzed cell lines, and no clear correlation with MYCN status was unveiled (**Fig. 14c**).

Protein levels of E2F3a and E2F3b were evaluated as a function of MYCN status. As regards E2F3a, immunoblot analysis broadly reflected gene expression experiments. Interestingly, no E2F3a protein expression was found in SHEP, while SK-N-AS and SK-N-FI exhibit E2F3a signals comparable to MYCN-amplified cell lines. Likewise, E2F3b protein expression is high in both MYCN-amplified and MYCN non-amplified cell lines. Some immunoblot results differ from gene expression experiments; indeed, markedly lower and higher E2F3b protein levels are observed in LAN5 and KELLY compared to mRNA levels, respectively (**fig. 14 d-e**).

To determine whether the expression status of MYCN affects the regulation of E2F3a and E2F3b, we resorted to the TET21/N system. TET21/N is a genetically engineered neuroblastoma cell line derived from SHEP, where the overexpression of the MYCN mini-gene is modulated by a TET-OFF system using tetracycline. TET21/N cells underwent either no tetracycline treatment (+MYCN) or 24 hours/48 hours-treatment (- MYCN). RT-qPCR analyses showed that MYCN mRNA expression was almost totally broken down after only 24 hours of treatment, and this reduction was sustained after 48 hours (**Fig. 14f**).

A similar pattern was observed for E2F3a but not E2F3b expression. In particular, E2F3a expression was reduced by ~ 50%, while E2F3b didn't exhibit statistically significant variations compared to the control.

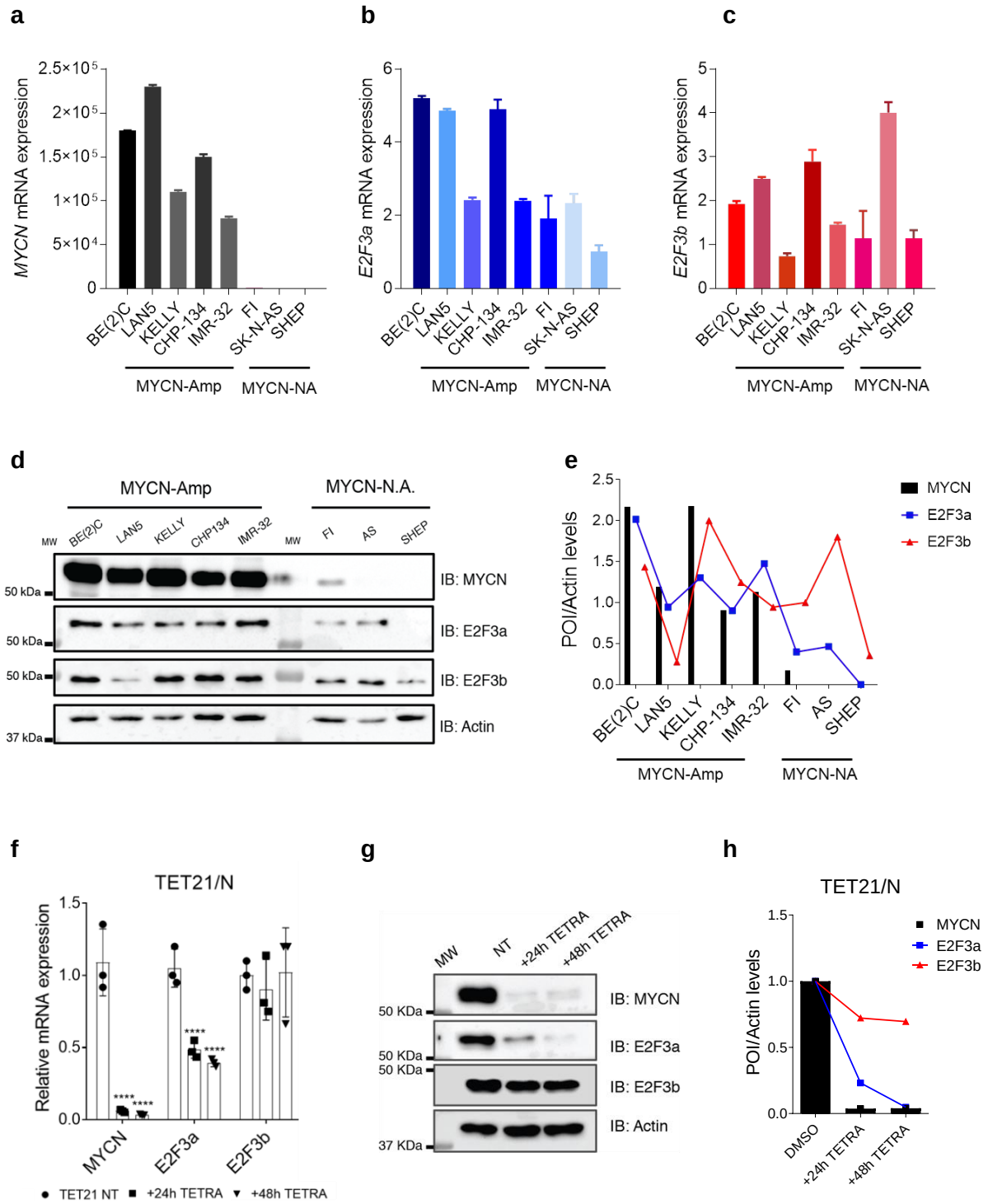

Figure 14. (a-c) mRNA levels of MYCN (black bars), E2F3a (blue bars), and E2F3b (red bars) were evaluated in MYCN amplified (MYCN-Amp) and MYCN-non amplified (MYCN-NA) neuroblastoma cell lines through RT-qPCR analyses. Data were normalized using GUSB and TBP housekeeping genes. SHEP was used as reference control. All the experiments were plotted with their own standard deviations. (**d**) Protein levels of MYCN, E2F3a and E2F3b evaluated in MYCN amplified (MYCN-Amp) and MYCN-non amplified (MYCN-NA) neuroblastoma cell lines through immunoblotting analyses. Actin was used as a loading control (bottom panel). (**e**) Densitometry quantification of a protein of interest (POI) corresponding to figure16d, expressed as a function of the actin levels. Data were normalized using the SHEP cell line. Black bars, blue and red lines correspond to MYCN, E2F3a and E2F3b protein levels. (**f**) Analysis of the MYCN, E2F3a and E2F3b mRNA levels in TET21/N cells (MYCN Tet-off system) after suppression of MYCN expression through tetracycline injection (+24h and +48h TETRA). Data were normalized using GUSB and TBP housekeeping genes. TET21 NT was chosen as reference. All the experiments were performed in triplicate and plotted with their respective standard deviations. Statistical analyses were performed using Two-way ANOVA test. Error bars represent SD. *, **, *** indicate P < .05, .01, .001 respectively. B) Protein analysis of MYCN, E2F3a and E2F3b levels in all three conditions through immunoblotting analysis. Actin was used as a loading control. (**h**) Densitometry quantification of a protein of interest (POI) corresponding to figure16g, expressed as a function of the actin levels. Data were normalized using the vehicle-treated control cells. Black bars, blue and red lines correspond to MYCN, E2F3a and E2F3b protein levels.

The immunoblot analysis confirmed that N-MYC was almost absent in both 24 hours and 48 hours-treated cells. A considerable decrease was also observed in E2F3a protein levels of treated cells, especially in 48h-condition. E2F3b only slightly decreased in treated cells, with no appreciable differences between +24h and +48h-condition (**Fig. 14g-h**). These data corroborate the real-time results, highlighting that the breakdown of MYCN expression correlated with significantly diminished E2F3a.

N-MYC and E2F3a may instruct a synergic feed-forward loop to regulate transcription

To further explore if N-MYC could directly bind the E2F3 promoter to regulate transcription, we took advantage of the ChIP-seq data available on the Gene Expression Omnibus (GEO) accession GSE80154, executed on TET21/N treated with +/- tetracycline for 24 hours, to deeply investigate the transcriptional consequences in relation to N-MYC reduction.

These analyses confirmed that N-MYC (MYCN ChIP-seq) directly binds the E2F3 promoter and that, moreover, the downregulation of MYCN expression results in less binding on the E2F3 promoter. To comprehensively examine the transcriptional status, we estimated the enrichments in H3K27Ac (marker of open chromatin) and RNA polymerase II on the same genomic region. The analyses indicated in both cases a significant decrease in binding capacities when MYCN levels are reduced (**Fig. 15a**).

The effect of N-MYC on E2F3 mRNA expression was further exanimated using gene reporter assays. Indeed, E2F3a promoter sequence (-1081;+182 from TSS) was cloned into the basic luciferase reporter vector pGL3b (**Fig. 15b**). The construct was transiently transfected in the same cell line after +/- injection of tetracycline to control MYCN expression. This experiment defined that the E2F3a promoter construct exhibits a significant reduction in the luciferase activity in absence of MYCN expression (+48H TETRA) compared to control (NO TETRA), indicating that N-MYC activates E2F3a transcription (**Fig. 15c**).

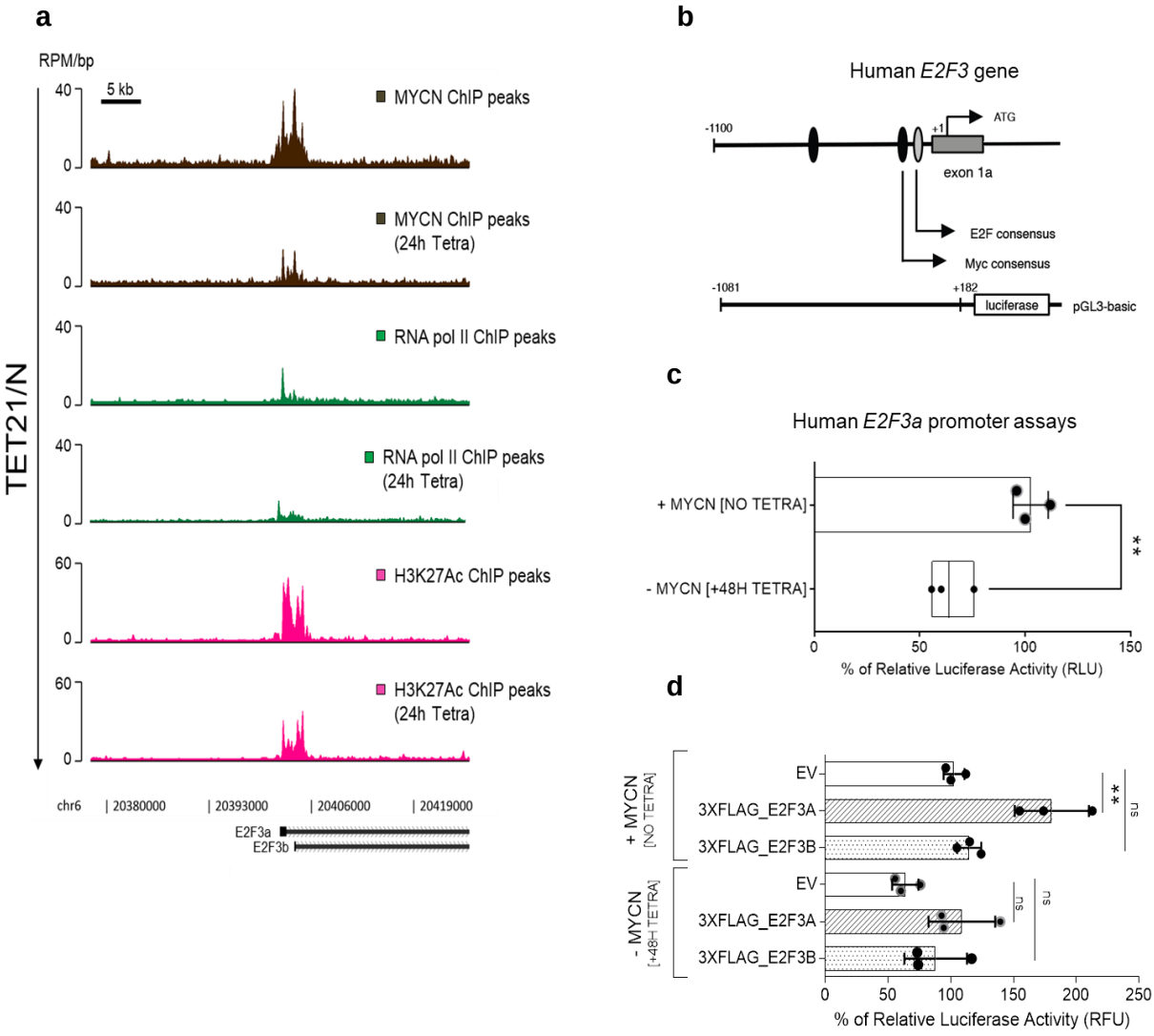

Figure 15. **(a)** ChIP-seq gene tracks (rpm/bp) showing the protein occupancy of N-MYC (brown), RNA pol II (green) and H3K27Ac (fuchsia) at the human E2F3 gene locus in TET21/N cells (MYCN Tet-off system) after the suppression of MYCN expression through tetracycline injection (24h Tetra). **(b)** Schematic representation of the human E2F3 gene promoter. The E2F3a promoter sequence (-1081;+182 from TSS), containing both E2F and MYC binding sites, was cloned into the basic luciferase reporter vector pGL3-basic. **(c)** Gene reporter assays on the E2F3 promoter. Luciferase activity was monitored in TET21/N cells as a function of MYCN expression. Luciferase activity in the (+) MYCN condition was determined as a percentage of the same reporter's activity in the (−)MYCN condition. Percentage change in luciferase activity was measured as a relative light unit (RLU) due to tetracycline treatment compared with vehicle control treatment. Data were shown as the mean ± standard deviation and evaluated by one-way ANOVA. *, **, and *** indicated P < 0.05, 0.01, and 0.001 respectively. **(d)** TET21/N cells (MYCN Tet-off system) after -/+ suppression of MYCN expression through tetracycline injection were co-transfected with either pCMV10-empty vector, pCMV10-E2F3a (3XFLAG_E2F3a) or pCMV10-E2F3b (3XFLAG_E2F3b) constructs in combination with E2F3a promoter pGL3 Firefly_Luciferase construct. Data were shown as the mean ± standard deviation and evaluated by one-way ANOVA. *, **, and *** indicated P < 0.05, 0.01, and 0.001, respectively.

Notably, previous work revealed that c-MYC is required to let on the interaction of the E2F1 protein with the E2F gene promoters, thus providing a link between the action of c-MYC in stimulating cell growth and cell cycle (Leung et al., 2008). Assuming that c-MYC shares a high degree of protein homology with N-MYC as well as E2F1 with E2F3, we performed additional assays in the same system by regulating both N-MYC, E2F3a and E2F3b expressions to assess if cooperation between these factors was present. High-MYCN and low-

MYCN conditions were evaluated separately with either overexpressing E2F3a (3XFLAG_E2F3a), E2F3b (3XFLAG_E2F3b) or the empty vector (EV), the latter used as control. E2F3a promoter activity was considerably affected by low MYCN expression when neither E2F3a and E2F3b were overexpressed, thus confirming our previous result. Interestingly, while E2F3b upregulation didn't affect E2F3a promoter expression in both high and low MYCN context, luciferase assays confirmed that high levels of N-MYC and E2F3a substantially heightened E2F3a promoter activity compared to E2F3a overexpression only (**Fig. 15d**).

N-MYC and E2F3a genome-wide occupancy on chromatin

To explore the relationship between N-MYC and E2F3 in neuroblastoma, we queried genome-wide occupancy on chromatin using ChIP-seq technology. The experiments were performed on SK-N-BE(2)C cells in order to consider the impact of MYCN amplification upon N-MYC expression. Chromatin immunoprecipitation was performed for N-MYC and E2F3a only since no specific IP-grade antibodies are commercially available for E2F3b.

E2F3a and N-MYC DNA-binding narrow and summit peaks were identified using the MACS2 algorithm with a less than 0,5% P-value. 4089 and 24966 peaks were recognized for E2F3a and N-MYC, respectively (**Fig. 16a**). The peak localization analysis using the BedSect algorithm revealed that 15,99% of all E2F3a peaks overlap MYCN peaks using 50 base pairs as overlap size (n=654) (**Fig. 16b**). This result was further examined using the RELDIST algorithm, which measures the relative distances between E2F3a and N-MYC genomic peaks, thus confirming the previous results (**Fig. 16c**). The distribution on the genome of the co-localized peaks is mostly enriched at the proximal promoter elements. Indeed, 446 (68,19%) of those peaks localize around -/+ 5 kb from the transcription start sites (TSS), while a reduced number of peaks were found far from these regions (**Fig. 16d**). Some examples are shown in **Fig. 16e-g** where the cell cycle regulatory proteins *E2F3, MCM3* and *CHAF1A* are presented. Gene enrichment analyses were then performed using the GREAT tool (binomial p value < 5%); in particular, gene ontology biological processes was further retrieved from the intersected ChIP-seq data, revealing high score enrichments in those genes which exert functions for regulating gene silencing by miRNA, chromosome organization, DNA metabolic processes and DNA repair (**Fig. 16i**). Moreover, the same genes appear to be mainly required for DNA packaging and chromosome/chromatin structure, as shown by GO cellular components (**Fig. 16h**).

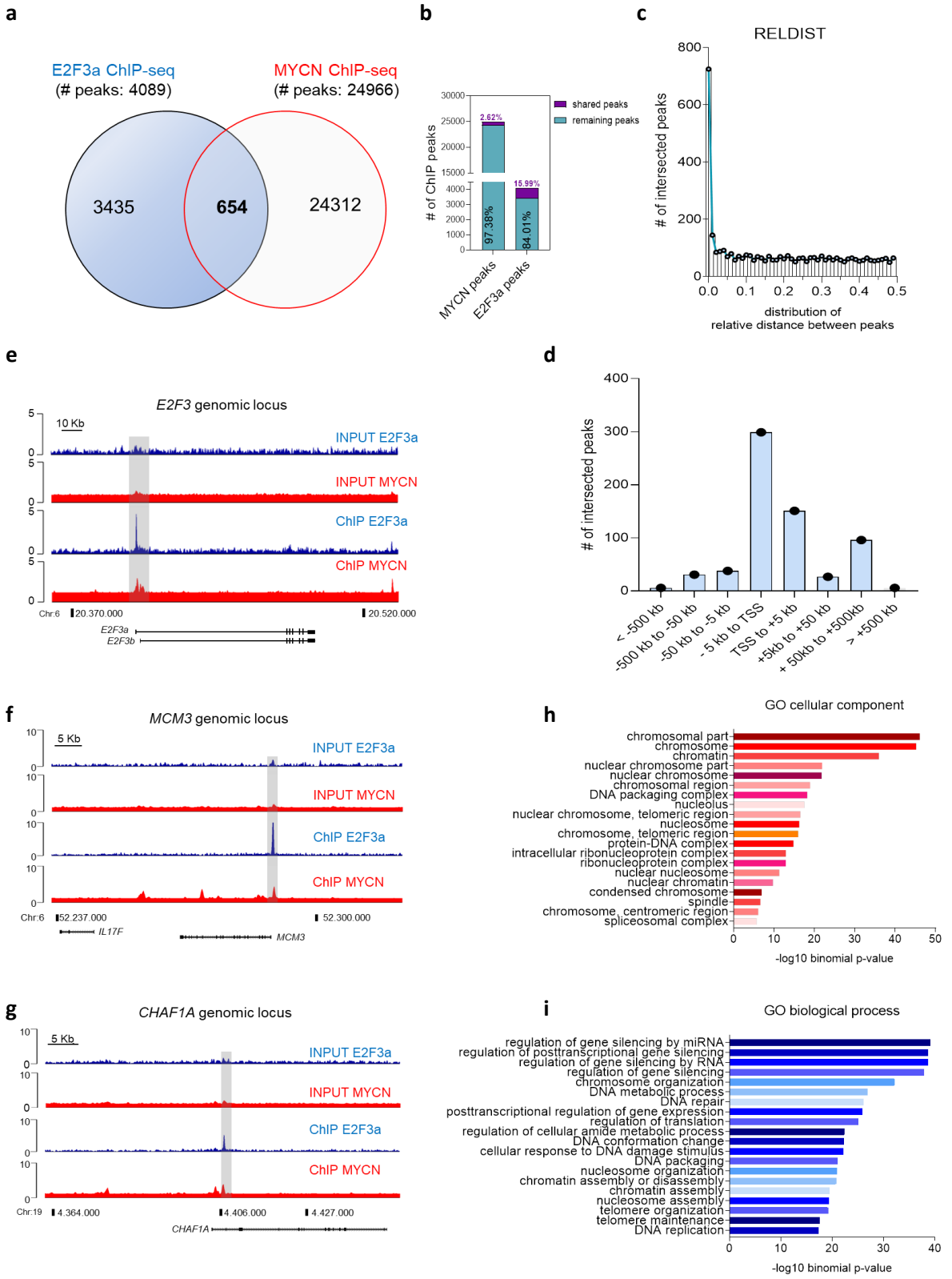

Figure 16. (**a**) Venn diagram representing the overlapped peaks identified by ChIP-seq with E2F3a (in blue) and MYCN (in red) antibodies performed in SK-N-BE(2)C cells (**b**) Percentage quantification of the number of ChIP peaks of E2F3a and MYCN. The overlapping peaks are shown in purple; the remaining peaks are displayed in pearl green. (**c**) Report of the distribution of relative distances between E2F3a and N-MYC peaks using the bedtool RELDIST. The output reports the frequency of each relative distance (ranging from 0.0 to 0.5). If the two sets of intervals are randomly distributed with respect to one another, each relative distance "bin" with be roughly equally represented (i.e., a uniform distribution). (**d**) Distribution of the 654 significant E2F3a/MYCN overlapping ChIP-Seq peaks. The enriched regions were plotted against all known transcription start sites (TSS) of annotated genes within the human genome using the Stanford Bejerano Lab Great Genomic Regions Enrichment Analyses Tool. (**e-g**) ChIP-seq tracks show the occupancy of E2F3a peaks (in blue) and MYCN peaks (in red) close to the TSS of E2F3, MCM3 and CHAF1A genomic loci. Inputs are shown as baseline control. (**h-i**) Gene ontology (GO) terms for putative direct E2F3a/N-MYC activated or repressed genes using the Stanford Bejerano Lab Great Genomic Regions Enrichment Analyses Tool. The statistically significant GO cellular component and biological processes (binomial p value < 5%) are shown in red and blue, respectively.

N-MYC and E2F3a may physically interact

Taken together, these findings suggested possible protein-protein interaction (PPI) between the two factors. The latter hypothesis was corroborated by performing proximity ligation assays (PLA) in SHEP cells stably overexpressing V5_N-MYC proteins under a CMV promoter's control. These cells were separately transfected to either overexpress E2F3a (3XFLAG_E2F3a) or E2F3b (3XFLAG_E2F3b) proteins.

Addition of the mouse V5- or rabbit FLAG- specific antibodies alone yielded almost null background levels of fluorescence in cells; however, a specific fluorescence signal was detected when cells overexpressing V5_N-MYC and 3XFLAG_E2F3a were probed with both V5 and FLAG antibodies (**Fig. 17a**), while only background signal was identified in 3XFLAG_E2F3b transfected cells using the same experimental conditions. Since E2F3a and E2F3b differ for the protein portion encoded by their first exon only, the 1-122aa fragment of E2F3a was assumed as the putative domain important for this interaction. To confirm this data and identify N-MYC's domain crucial for the PPI, we sought to validate these results via GST-pulldown assays.

To achieve this purpose, we generated five MYCN- GST truncation mutants to map the respective interacting protein domain (**Fig. 17b**). 3XFLAG_E2F3a and 3XFLAG_E2F3b constructs were separately transfected in HEK-293T cells due to the high overexpression efficiency. Total protein lysates from either of the conditions were incubated with each of the five different pools of glutathione beads carrying GST-MYCN fragments, plus the pool taking only GST used as control. Interestingly, we found that 82-254aa and 336-400aa MYCN fragments are required for E2F3a interaction and pull down (**Fig. 17c-d**). Once again, no interaction between the MYCN fragments and E2F3b was detected, confirming PLA results.

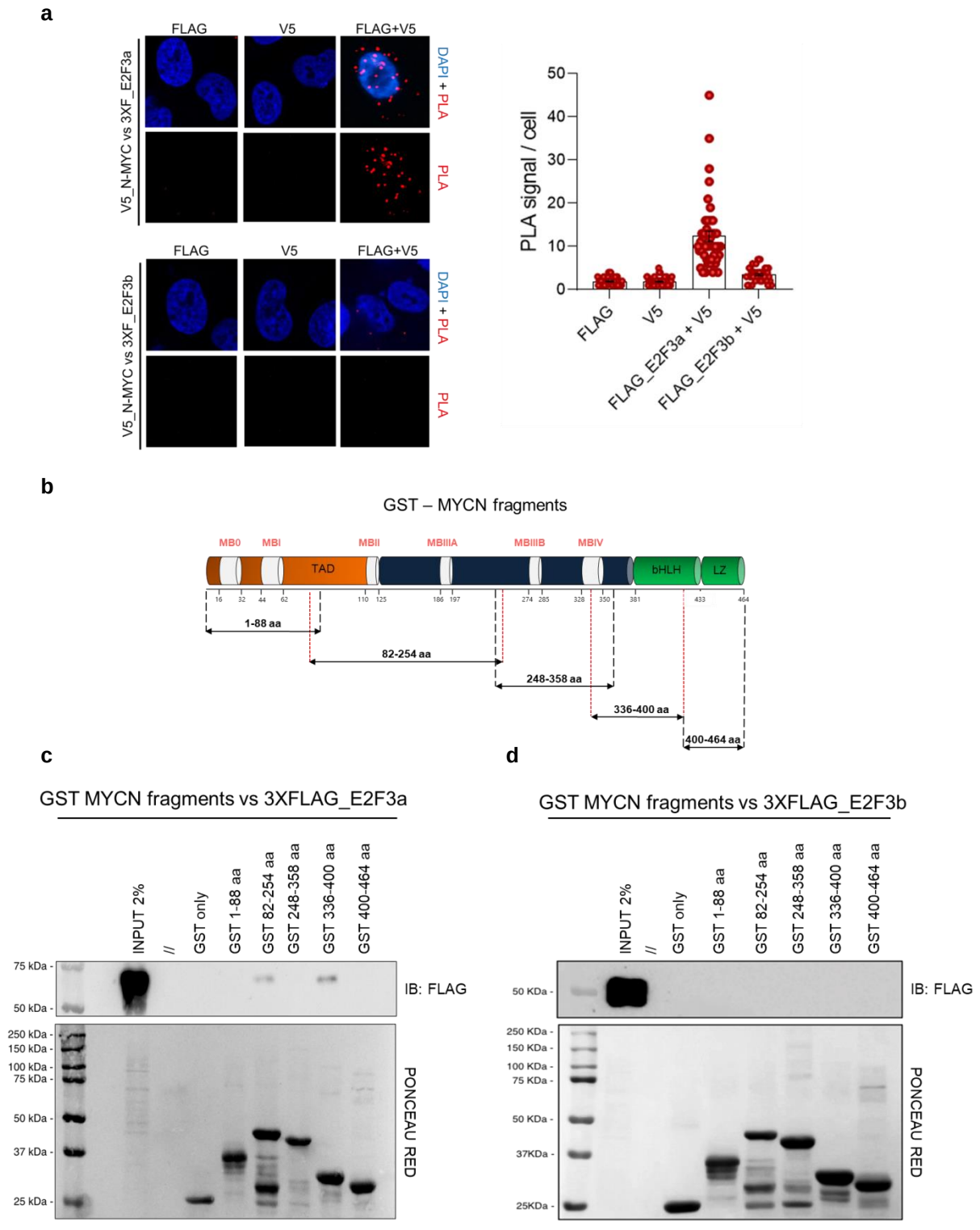

Figure 17. (**a**) SHEP cells stably overexpressing V5_N-MYC proteins were probed with V5 mouse antibody (V5_N-MYC) and/or a FLAG rabbit antibody (3XF_E2F3a or 3XF_E2F3b). The proximity of N-MYC and E2F3a/b was assayed using the Duolink Proximity Ligation Assay (PLA) In Situ Red Starter kit (Sigma-Aldrich) as per manufacturer's instructions. Representative PLA signal (red dots) and nuclear staining (DAPI; blue) are shown for cells probed with anti-FLAG alone (left row), anti-V5 alone (middle row), or anti-FLAG and anti-V5 (right row). PLA signal was quantified and shown as the median number of foci per cell with range (n = 3). (**b**) Schematic illustration of the five GST-MYCN fragments used in GST-pull down assays. Transcriptional activation domain (TAD), central domain and heterodimerization/DNA binding domains are shown in orange, dark blue, and green, respectively. (**c-d**) HEK-293T cells were transfected with either 3XF_E2F3a or 3XF_E2F3b expression construct. Total protein extract from the cells was incubated with an equal amount of different GST-MYCN protein fragments immobilized onto glutathione agarose beads, followed by immunoblot with an anti-Flag antibody. As loading controls, Ponceau stained images were detected by ChemiDoc MP. Numbers on the left refer to molecular weights.

BioID analyses revealed the huge complexity of E2F3s interactome

To determine whether MYCN expression may affect the function of E2F3a and deeper investigate the differences between E2F3a and E2F3b isoforms, we applied the *in vivo* proximity-dependent labelling technique BioID (proximity-dependent biotin identification) to examine the protein interactome of either E2F3a and E2F3b in dependency of MYCN status in neuroblastoma. BioID makes use of a mutant biotin ligase (BirA*) fused in-frame to a protein of interest. Proteins associated *in-vivo* with and proximal to the target factor are covalently labelled in a radius of ~10 nm with biotin and, after harsh lyses of the cells, they can be streptavidin pulled down and subsequently identified by mass spectrometry (LC-MS) (Roux et al., 2012).

To avoid variability due to cell-type specificity, experiments were performed using the TET21/N system, which allows the regulation of MYCN expression under tetracycline control. In particular, cells were transduced with either V5_FLAG_BirA*(control), V5_FLAG_BirA*_E2F3a and V5_FLAG_BirA*_E2F3b coding sequences using the QM812B-1 as lentiviral transfer backbone, to induce the overexpression of a protein of interest under cumate control (**Fig. 18a-c**). To limit one vector copies per cell and prevent false-positive results due to improper protein dosage, transduction was performed with a 0.3-0.5 MOI (Multiplicity Of Infection). Once selected, immunofluorescence assays were performed, confirming the chimeric proteins' proper localization, typically presented both in the nucleus and cytoplasm (**Fig. 18d**). A four days treatment with +/- tetracycline was completed to modulate MYCN expression. The next day, cells were supplemented with cumate, MG132 and biotin, triggering both protein overexpression, stabilization and biotinylation, respectively.

The experiments were performed twelve times for controls and six times for both E2F3a and E2F3b isoforms in low and high MYCN contexts.

Following mass spectrometry, the resulting data were then analyzed for a minimum spectral count and fold change over control and filtered via significance analysis of interactome (SAINT), which applies a probabilistic model to reserve a confidence score for each interaction (Choi et al., 2011).

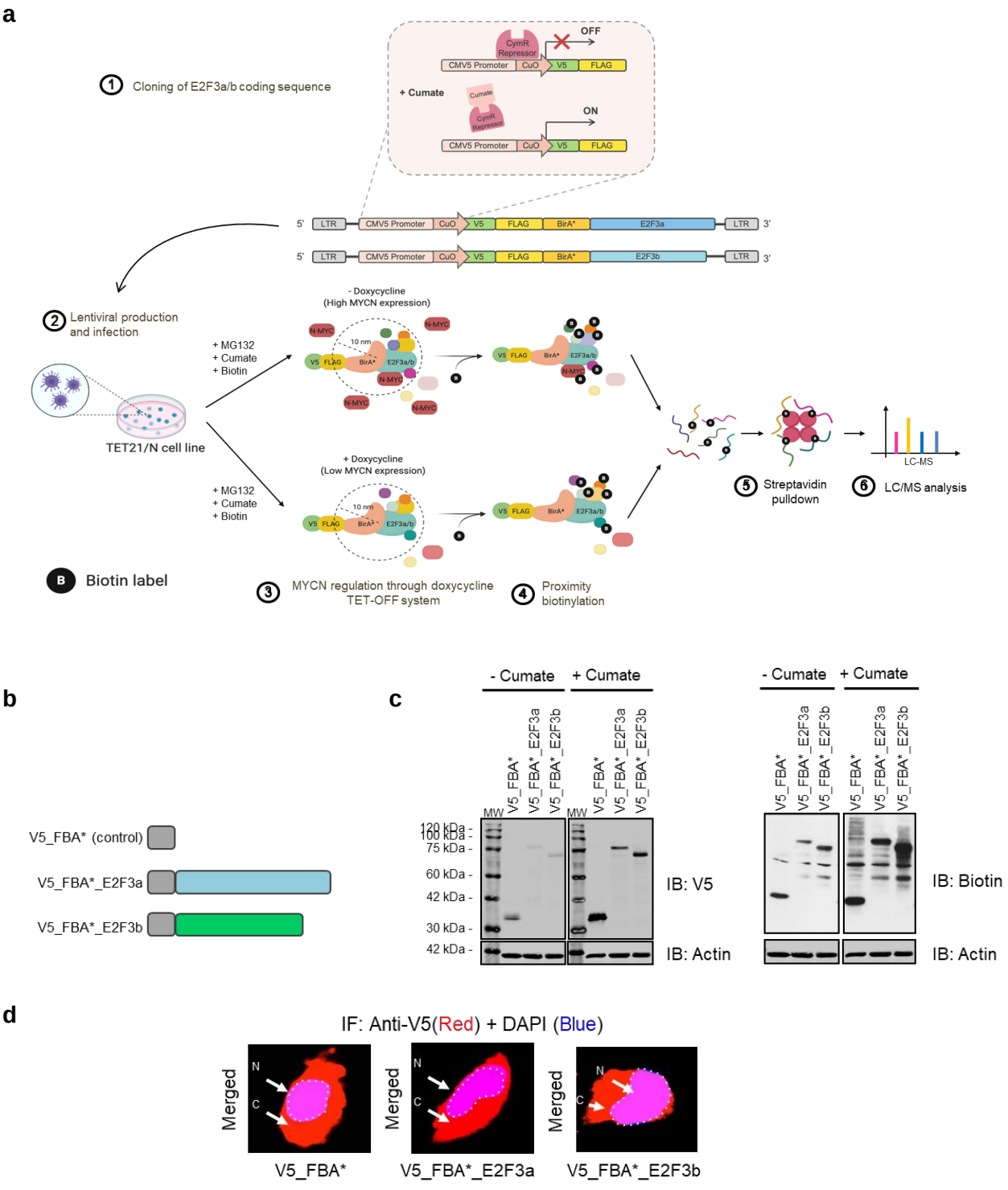

Figure 18. (a) Graphical sketch of the BioID based proteomic stategy for the identification of the E2F3 interactome in TET21/N neuroblastoma cells**. (b)** Schematic representation of the V5_FLAG_BirA* (V5_FBA*), V5_FLAG_BirA*_E2F3a (V5_FBA*_E2F3a) and V5_FLAG_BirA*_E2F3b (V5_FBA*_E2F3b) overexpressed proteins under cumate control. **(c)** Total protein extracts derived from TET21/N cells overexpressing V5_FLAG_BirA* (V5_FBA*), V5_FLAG_BirA*_E2F3a (V5_FBA*_E2F3a) and V5_FLAG_BirA*_E2F3b (V5_FBA*_E2F3b) under cumate control (cumate_ON system) were run on SDS-PAGE. Extracts were detected using anti-V5 antibodies through immunoblot analysis. Actin was used as a loading control. Proximity biotinylation activity was detected using an anti-Biotin antibody (low exp). **(d)** Immunofluorescence analysis of V5_FLAG_BirA* (V5_FBA*), V5_FLAG_BirA*_E2F3a (V5_FBA*_E2F3a) and V5_FLAG_BirA*_E2F3b (V5_FBA*_E2F3b) overexpressed proteins under cumate control. TET21/N transduced cells were prepared for immunofluorescence as described in Materials and Methods and were incubated with an anti-V5 antibody followed by an Alexa-594-conjugated secondary antibody. Nuclei were visualized using DAPI staining. Fluorescence images were acquired using the same acquisition parameters at 6 40 magnification.

BioID analyses revealed a total of 136 protein interactors, of which 96 and 99 corresponded to E2F3a and E2F3b isoforms (**Fig. 19a-d**). The investigation's validity was corroborated by identifying canonical protein interactors like RB1, RBL1, TFDP1,TFDP2 and members of the DREAM complex present in all the conditions, providing support to our results.

Strikingly, 59 proteins only were commonly bound by both E2F3a and E2F3b, while 37 and 40 interactors appear to specifically bind the isoform a and b, respectively, unveiling novel determinants required for their functional specificity.

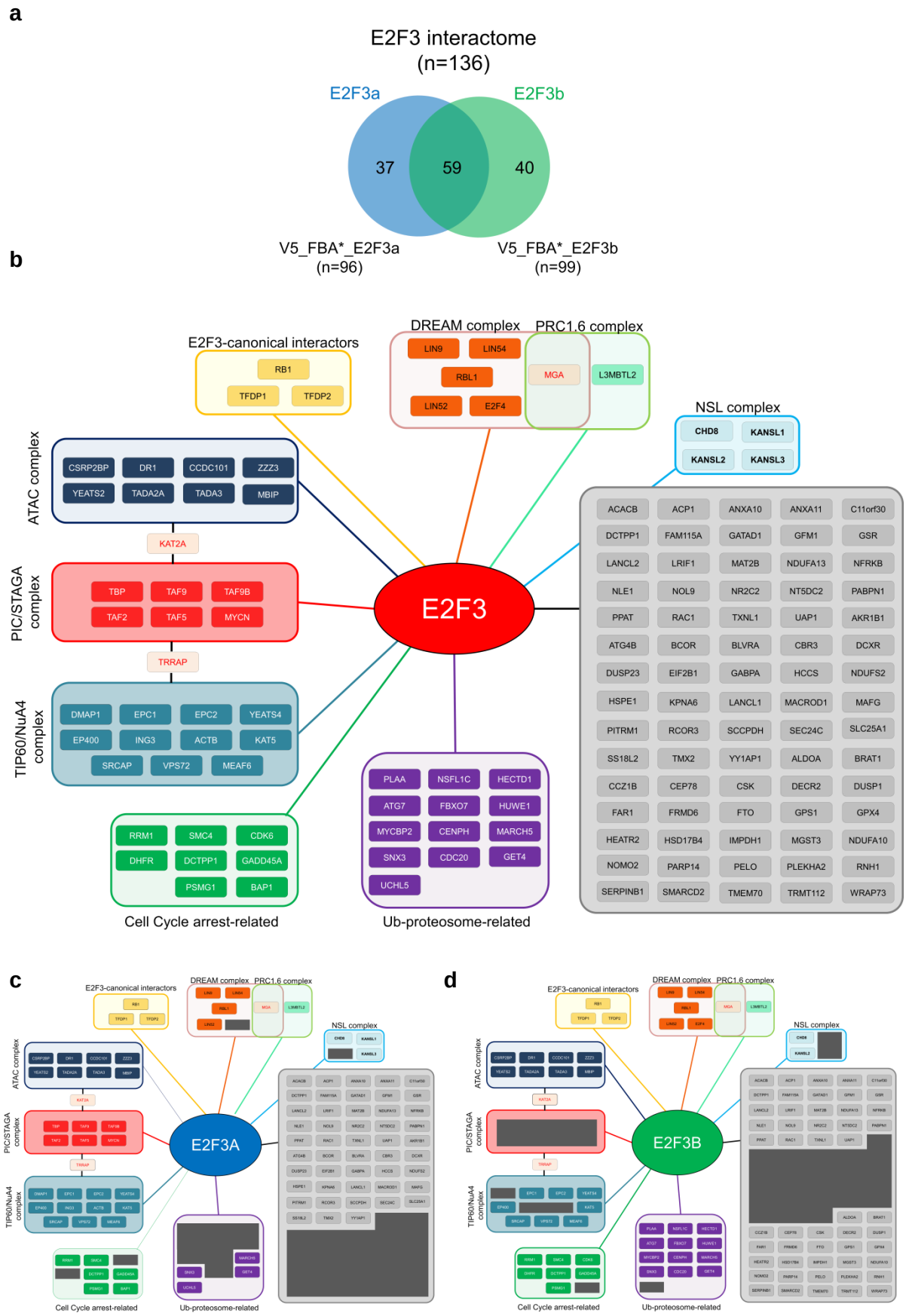

Figure 19. (a) Venn diagram showing the number of overlapping proteins identified through BioID analyses for E2F3a (blue circle) and E2F3b (green circle). Proteins were listed for common interactors, E2F3a only and E2F3b only. **(b-d)** Graphical representation of the E2F3 interactome (total, isoform A and isoform B). Protein names were imported into Cytoscape 3.8.0 using the STRING tool for visual representation and are annotated based on protein complexes membership and biological functions.

Protein network analyses coupled with gene ontologies (GO molecular functions - Fisher exact test, FDR < 0,05 -) performed using the PANTHER software showed that E2F3a interactors are mainly involved in euchromatin formation and transcriptional activation to mediate both DNA binding and transcriptional co-regulation (**Fig. 20a**).

As expected, E2F3b interactome shares a relatively quite high level of similarity compared to E2F3a interactome, even if many components of these complexes like proteins belonging to the pre-initiation complex (TBP and the TATA associated factors (TAFs)) appeared to be missing, resulting in lower regulatory capacity compared to the isoform a, as shown by GO biological processes analyses achieved using the same software described above (**Fig. 20b**). Once again, our proteomic screening revealed that only E2F3a could specifically interact with the N-MYC protein, confirming our previous PLA and GST-pull down results.

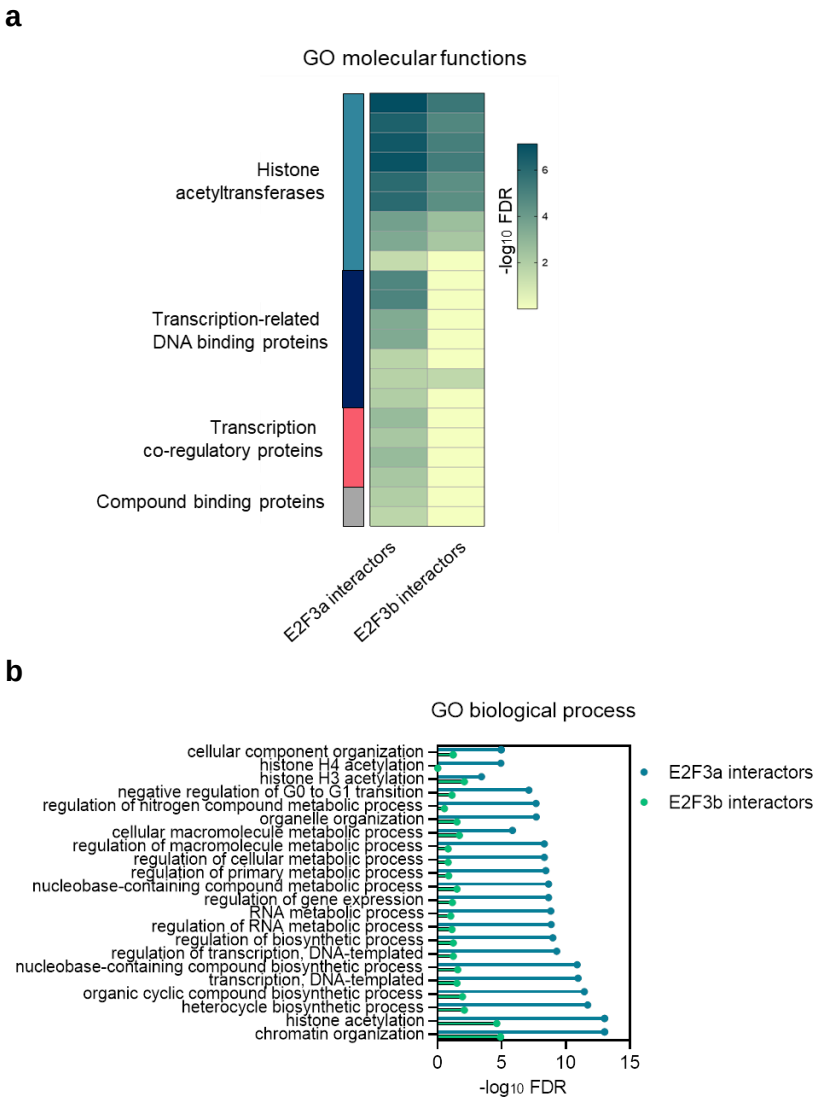

Figure 20 (a-b) Gene ontology (GO) terms for E2F3a and E2F3b interactors identified through BioID assays using the PANTHER GO Tool. GO molecular functions, and GO biological process was performed using Fisher exact test with an FDR < 0,05. GO categories considered not statistically significant are listed with -log10 FDR = 0. GO molecular functions were clusterized based on the class of membership.

High MYCN expression expands the protein interactome of E2F3a and E2F3b

Surprisingly, the interactome profiling of E2F3a and E2F3b was influenced by MYCN expression levels. Indeed, mass spectrometry analyses revealed a differential pattern of interactions as a function of MYCN levels for both E2F3a and E2F3b, suggesting the existence of a novel unreported N-MYC related mechanism dependent on its expression.

While the binding affinity of 30/96 of the E2F3a and 21/99 of the E2F3b partners was not affected by MYCN regulation, 48/96 and 59/99 interactors of E2F3a and E2F3b were detected only when TET21/N cells expressed high levels of MYCN, respectively.

The interactome of E2F3a and E2F3b appeared to be generally restricted when MYCN expression was downregulated, although 18/96 and 19/99 partners were only identified when MYCN expression was low. Indeed, high MYCN levels led E2F3a and E2F3b to expand the protein network and interact with 76 and 80 proteins compared to 48 and 40 protein partners present in low MYCN context, respectively (**Fig. 21a-b**). A subset of these factors were components of important transcriptional regulatory complexes like the pre-initiation complex (PIC), SAGA/STAGA complex, ATAC complex, TIP60/NuA4 and some canonical interactors like subunits of the DREAM complex, which drastically influence cell cycle regulation and the tumorigenic activity of neuroblastoma cells. The pattern of differentially interacting proteins generally appeared dissimilar for both E2F3a and E2F3b, although some common core elements like KAT2A (GCN5), CCDC101(SGF29), TADA2A (ADA2a), TADA3 (ADA3) and YEATS4 were always lost in the absence of MYCN expression, thus presenting consistent results. In contrast, the binding affinity of the canonical protein interactors RB1, RBL1, TFDP1 and TFDP2 was not affected by the alteration of MYCN levels (**Fig. 21c-d**).

To further explore the differences between these two transcription factors, we subjected our MS results to average percent change analyses to evaluate the peptide counts' percentile change in +/- MYCN expression for both E2F3a and E2F3b interacting proteins. Reduced MYCN levels led to a significant loss in peptide counts of several subsets of protein interactions for both E2F3a and E2F3b if compared to high MYCN expression conditions. Interestingly, E2F3a didn't show any peptide counts relative to proteins associated with cycle arrest and proteosome subgroups. Conversely, E2F3a only appears to interact with components of the PIC and SAGA/STAGA histone acetyltransferase complexes, known to induce transcriptional initiation and elongation (**Fig. 21e**).

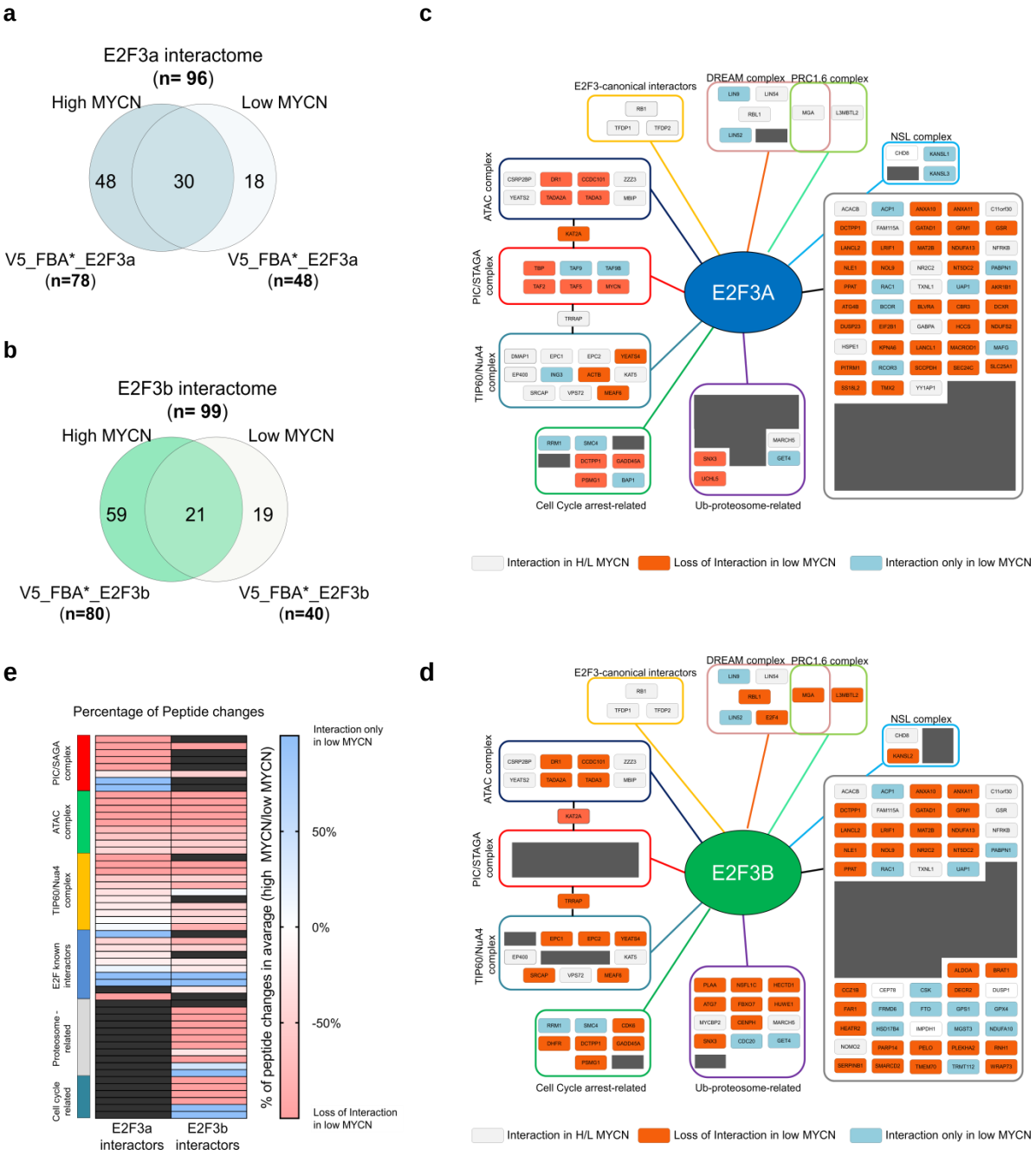

Figure 21. (a-b) Venn diagrams showing the number of overlapping proteins identified through BioID analyses for E2F3a (blue circles) and E2F3b (green circles) as a function of MYCN levels. TET21/N cells overexpressing V5_FBA*, V5_FBA*_E2F3a and V5_FBA*_E2F3b under cumate control were +/- treated with tetracycline to reduce of MYCN expression **(c-d)** Summary diagram of E2F3a and E2F3b interactors identified using BioID assays ($p < 0.05$). Proteins with peptide counts that were significantly decreased upon reduction of MYCN expression are displayed as red nodes. Proteins with peptide counts that significantly increased upon reduction of MYCN expression are displayed as blue nodes. White nodes represent interactors for which peptide counts did not significantly change in response to MYCN reduction. Protein names were imported into Cytoscape 3.8.0 using the STRING tool for visual representation and are annotated based on protein complexes membership and biological functions. **(e)** Heatmap of interactor peptide counts displayed as a percentage of peptide counts. The percentage in average of peptide changes was calculated as a ratio concerning the number of peptides of a protein of interest in high MYCN expression context divided by the number of peptides of the same protein in low MYCN expression. The results were annotated based on protein complexes membership and biological functions and visualized as a red-blue scale.

Gene Ontology (GO) was then performed using the STRING bioinformatics tool to overrepresent GO categories using Fisher's exact tests.

Multiple testing was performed for each of several 1000 GO nodes by evaluating the False Discovery Rate (FDR) for a minimum of 5%. Our analyses point out that E2F3a interactors were statistically enriched in several biological categories like histone acetylation, transcription, cellular metabolic processes and cellular organization when MYCN expression was upregulated. These groups were significantly altered by MYCN levels' downregulation, generally displaying fewer enrichments in the same sets. The trend was also consistent for E2F3b, even if lower levels were found in all the cases compared to the isoform a. Importantly, no statistically significant enrichments were found for the list of E2F3b interactors in –MYCN condition, remarking the importance of N-MYC upon E2F3 function (**Fig. 22a**). Since the N-MYC protein is known to transcriptionally regulate almost 12-15% of all human genome, the evaluation of this phenomenon was pursued by performing gene expression analyses to assess if N-MYC dysregulation impacts transcription of the E2F3a/b-interacting proteins. A subset of genes was evaluated using RT-qPCR experiments in TET21N cells expressing high and low MYCN expression levels. Although this analysis needs to be expanded to many other genes, no statistically significant differences were found in cells differentially expressing N-MYC protein levels (**Fig. 22b**).

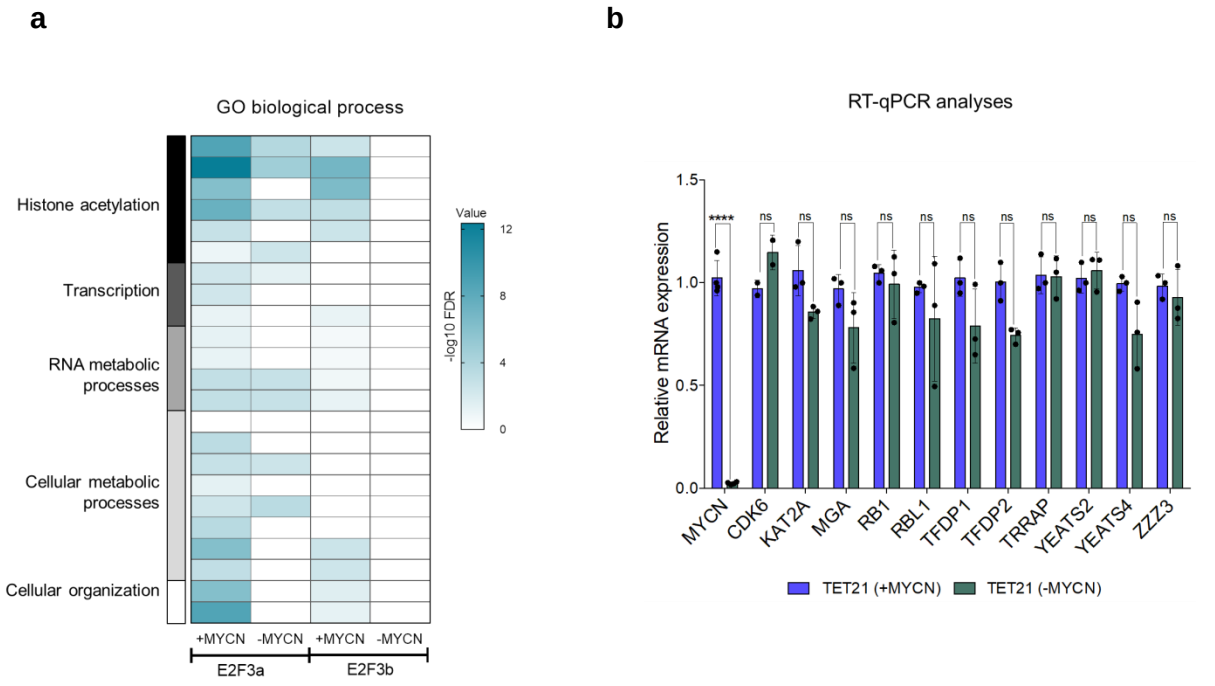

Figure 22. (a) Gene Ontology (GO) biological process performed using the STRING bioinformatics tool to overrepresent GO categories using Fisher's exact tests. Multiple testing was performed for each of several 1000 GO nodes by evaluating the False Discovery Rate (FDR) for a minimum of 5%. GO categories considered not statistically significant are listed with -log10 FDR = 0. GO were clusterized based on the class of membership. **(b)** Gene expression analyses of E2F3a/b-interacting proteins were performed using TET21/N cells (MYCN Tet-off system) after suppressing MYCN expression through tetracycline injection (+48h TETRA). Data were normalized using GUSB and TBP housekeeping genes. TET21 NT was chosen as reference. All the experiments were performed in triplicate and plotted with their respective standard deviations. Statistical analyses were performed using the Two-way ANOVA test. Error bars represent SD. *, **, *** and ns indicate P < .05, .01, .001 and no statistically significant differences, respectively.

DISCUSSION (Part II)

Neuroblastoma (NB) is the most common neurogenic-extracranial solid cancer of infancy and childhood. The most aggressive subtype of NB, which carries the worst overall prognosis, is caused by the MYCN gene amplification. Many questions concerning what discriminates MYCN-amplified from non-amplified tumours are still debated. Our data provide new insights about how high MYCN can establish a dynamic regulatory axis with the transcription factor E2F3, impacting the development of childhood neuroblastoma (NB) phenotype. High E2F3 expression is consistently associated with poor survival across different NB datasets regardless of MYCN expression, highlighting its crucial role in NB progression.

Many scientific records related to cancer diseases indicated that E2F3 appears to be a critical component for malignancy development in several types of solid tumours, including bladder cancer, ovarian cancer and melanoma (TCGA Pan-cancer data 2018). However, the frequent missing discrimination between E2F3 isoforms transcriptional activity leads only to a partial understanding of the role of E2F3 in tumour formation and progression.

Our studies revealed that N-MYC and E2F3 co-expression results in the worst scenario, even if E2F3 expression only seems to be an independent negative predictor of survival in many patients affected by NB. Notably, the application of Cox models and Kaplan-Meier analyses using the TARGET RNA-seq dataset advised the role of E2F3a, but not E2F3b, as a negative predictor of survival apart from MYCN amplification status in high-risk NB (stage 4).

Gene expression and immunoblot analysis performed using NB cells demonstrated that N-MYC regulates E2F3a but not E2F3b expression. Since E2F3a expression only was affected by MYCN variations, we first sought to investigate whether the dependence between E2F3a and N-MYC could be ascribed to direct transcriptional regulation. Gene reporter assays confirmed that E2F3a promoter activity decreases when N-MYC levels fell out, suggesting that it may promote E2F3a transcription. Our results were then verified through ChIP-seq analyses, unveiling the N-MYC protein's ability to regulate E2F3a expression directly. Given the significance of MYCN in neuroblastoma and the emerging function of E2F3 as a critical oncogene in many cancers, exploring if the presence of a link between these two genes could represent a new step for a better understanding of neuroblastoma tumorigenesis. Importantly, V. Strieder and W. Lutz previously demonstrated that E2F3a directly stimulates MYCN promoter activity both in MYCN non-amplified (SH-EP) and in MYCN-amplified (IMR-32 and Kelly) cell lines (Strieder & Lutz, 2003).

Together, these data advised the existence of a novel transcriptional circuitry between E2F3a and N-MYC, which appears to instruct a positive regulatory loop for their synergistic

transcriptional activation. To better unravel the relationship between N-MYC and E2F3a in neuroblastoma cells characterized by MYCN amplification, we then queried genome-wide occupancy on chromatin using ChIP-seq technology on SK-N-BE(2)C cells. These assays revealed that almost 16% of all the E2F3a ChIP-seq peaks overlapped N-MYC binding regions. In particular, many of these regions were close to the TSS, suggesting cooperation for the instruction of specific transcriptional programs essential for RNA post-transcriptional regulation, cell cycle, chromosome stability and organization. We speculated that in a high MYCN context, E2F3a could acquire new functions through direct interaction with N-MYC, regulating a set of genes required to promote tumorigenesis. The latter hypothesis was supported by performing *in-vivo* Proximity Ligation Assay (PLA) and *in-vitro* GST pull-down assays, confirming N-MYC/E2F3a interaction. Notably, Linda Penn's group has recently reported the exchange between c-MYC and E2F3 using proximity biotinylation assays (Kalkat et al., 2018) and, through the same technology, the interaction between N-MYC and E2F3a in neuroblastoma cells was also confirmed (personal communication). In this setting, the N-MYC/E2F3a complex may require interactions with other factors such as chromatin regulators, co-activators/co-repressors, and general transcriptional machinery components. To determine whether MYCN expression may affect the function of E2F3a and deeper investigate the differences between E2F3a and E2F3b isoforms, we applied the *in vivo* proximity-dependent labelling technique BioID. This novel technique allowed the identification of their interactome *in vivo,* unveiling respectively 96 and 99 protein candidates belonging to the comprehensive proteomics map of both E2F3a and E2F3b proteins. This unbias screening underlines for the first time the mutual dependency of MYCN status and the proteomic profiling of these two transcription factors in NB disease.

Here, we demonstrated that BioID combined with LC-MS could be applied to identify E2F3 isoforms PPIs in malignant cells and, moreover, we underscored foremost that the interactome profiling of E2F3a and E2F3b is influenced by MYCN expression levels. Strikingly, this powerful technique recognized novel potential vulnerabilities like S(T)AGA and PIC components that could associate with E2F3a only in high MYCN context, to exert the oncogenic potential upon the cells (**Overview Part II**). Our study provides for the first time a broad coverage of the E2F3 isoform's ability to interact with different effectors in neuroblastoma cells. Consequently, these studies are uncovering many potential candidate proteins that could help fill the knowledge gap in understanding the impact of MYCN on E2F3 biology, shedding light on the molecular principles that lead the MYCN/E2F3 axis to foster the oncogenic programme.

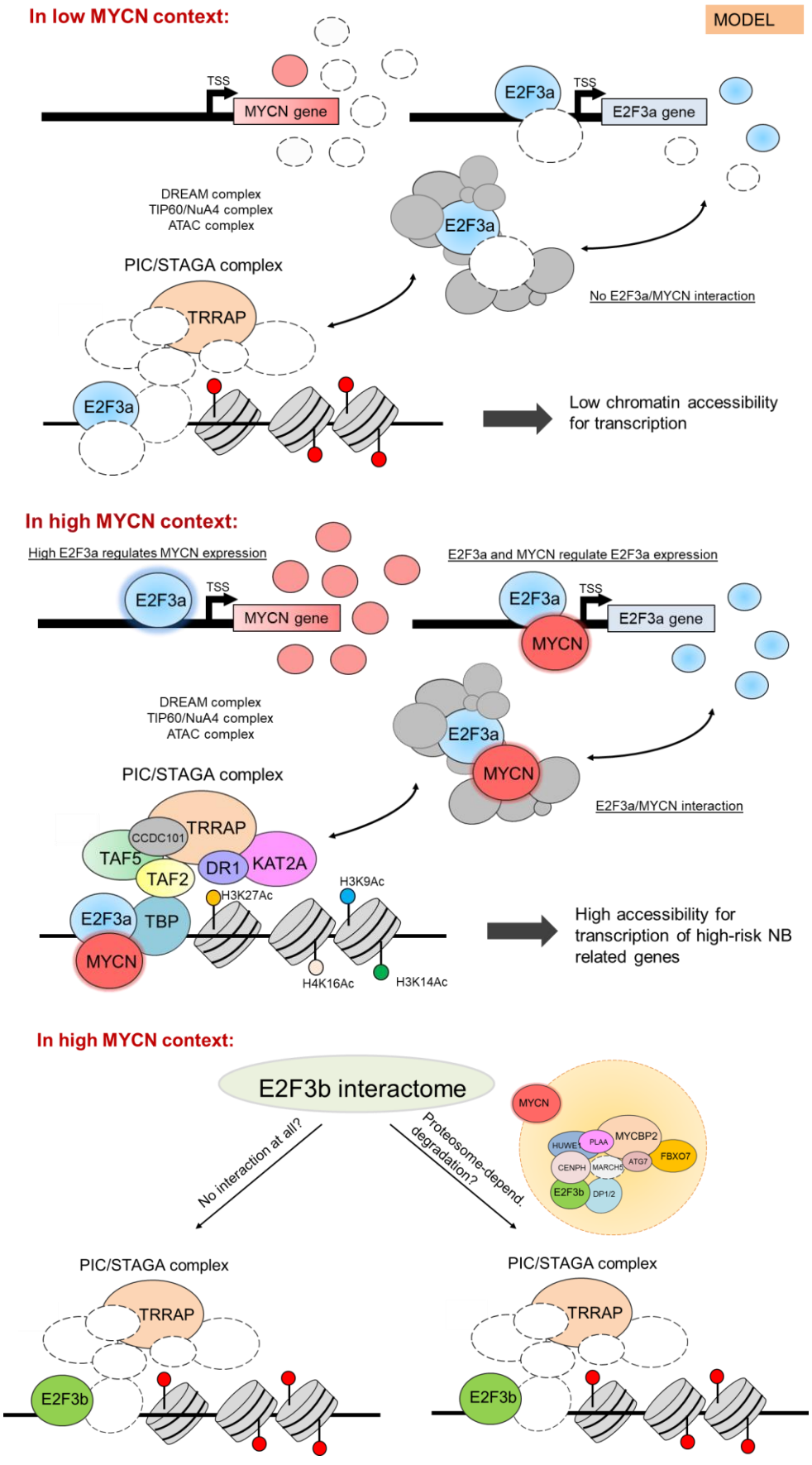

Overview Part II. Schematic representation of the role of the E2F3a and E2F3b proteins and their interactomes for the instruction of a novel functional axis with N-MYC in neuroblastoma.

THESIS CONCLUSIONS

Neuroblastoma is one of the topmost common neurogenic-extracranial solid cancers occurring in childhood and infancy. The extreme heterogeneity of this pathology is still considered a significant challenge to overcome and assumes a relevant aspect for developing novel therapeutic strategies. The vast majority of neuroblastoma patients are distinguished by multiple levels of epigenetic alterations, resulting in widespread deregulation of gene expression profiles and disruption of the signalling networks that control proliferation and cellular response. Several new pieces of evidence showed this neoplasia's critical level of plasticity, unveiling the role of numerous layers of regulation that drastically influence patient outcomes, as per MYCN gene amplification. Indeed, the N-MYC protein plays a crucial role since its gene amplification is associated with poor prognosis and advanced tumour stages and is one of the initiating events driving the transformation and progression of the high-risk cases (Matthay *et al.*, 2016; MW *et al.*, 2018). N-MYC can activate or repress many coding and non-coding genes as a pivotal oncogenic transcription factor, thereby orchestrating expression programs of several targets that cannot be ascribed to a single regulatory pathway. When deregulated, N-MYC governs the cis-regulatory landscape of the neuroblastoma cells. Consequently, loss of N-MYC leads to a reduction in global gene expression levels within the cellular transcriptome and, particularly, of its directly targeted tumour-related genes (L *et al.*, 2019), showing its determining role in maintaining both normal and altered neuroblastoma's regulatory networks. The aim of this PhD thesis focused on exploring how MYCN expression can influence the induction and maintenance of the tumorigenic phenotype in neuroblastoma to identify and characterize novel vulnerabilities that work in concert with MYCN to develop a high-risk cancer phenotype. Bioinformatic analyses of the transcriptional profiles of both MYCN amplified and non-amplified samples allowed us to unveil several molecules influencing MYCN expression and/or its dependent regulatory networks. In particular, we decided to focus our efforts on investigating the novel long non-coding RNA lncNB1 (Part I) and the cell cycle regulator E2F3a/b (Part II) since their expression is selectively higher in high MYCN cells and have the prognostic potential for this pathology. Some interesting points emerged from our analyses.

Firstly, this work allowed to discover and elucidate the molecular mechanism behind a previously unpredicted molecular target, lncNB1, relevant for neuroblastoma patophisiology. Moreover, the present study provides for the first time a broad coverage of the E2F3s

interactomes and their relationship with the N-MYC protein, also contributing to the implementation of our knowledge about cell cycle regulation and cancer biology.

Secondly, N-MYC seems to instruct a complex network of molecular interactions through transcriptional stimulation of lncNB1 and direct protein interaction with E2F3a but not E2F3b, ultimately resulting in increased protein stability (Part I) and novel regulatory potentials (Part II) to reinforce N-MYC oncogenetic program. Indeed, both lncNB1 and E2F3 proteins may establish a dynamic, positive regulatory axis through the interaction with these understudied molecules, impacting the development of the high-risk cancer phenotype.

Third, the more profound investigation of these new vulnerabilities paves the way for developing novel therapeutic approaches, bypassing the difficulties in obtaining compounds against molecules complex to targeted such as several master TFs like the same N-MYC protein. The significance of a network-based targeted therapy in neuroblastoma could be of great importance considering the standard strategies' weakening approach in treating high-risk patients (general surgery, chemotherapy, radiotherapy), distinguished by metastatic and aggressive tumours. The newly appreciated high incidence of MYC(N) amplification across adult and paediatric tumours like a small subset of Small Cell Lung Cancer, Retinoblastomas, and Medulloblastomas adds additional urgency and significance to our efforts to define MYCN-amplification driven mechanisms in neuroblastoma.

Nevertheless, the interplay between regulatory networks and oncogenesis has been unequivocally described, more in-depth research into their role in modulating cancerous-unrelated signalling pathways still needs to be carried out. According to the novel findings summarized above, discovering this intricate reticulum of interactions represents invaluable predictive factors for early-onset disease detection.

MATERIALS & METHODS

the materials and methods of Part I and II were sorted by alphabetical order, as below:

BioID in cell culture

TET21/N cells at ~70% confluency, carrying cumate-inducible V5_FLAG_BirA*, V5_FLAG_BirA*_E2F3a or V5_FLAG_BirA*_E2F3b were treated for 24 hours with 30 µg/mL of cumate (SBI – System Biosciences), 5 µM MG132 (Sigma-Aldrich), and 50 µM biotin (Sigma-Aldrich), to induce the expression of the transgene and facilitate biotin labelling. Cells were then harvested into phosphate-buffered saline (PBS) by scraping, washed twice with 50mL of PBS, and centrifuged at 1000 × *g* for 10 minutes at 4 °C. The pellets were lysed in 10 mL of cold modified RIPA buffer (w:v; 1% NP-40, 50 mM Tris–HCl pH 7.4, 150 mM NaCl, 1 mM EDTA, 1 mM EGTA, 0.1% SDS, 1:500 protease inhibitor cocktail (Sigma) 0.5% sodium deoxycholate), supplemented with 250 U of benzonase (EMD). The lysate was end-over-end rotated for 1 h at 4 °C, sonicated three × 30 s (Fisher Scientific D100 Sonic Dismembrator), and centrifuged at 27,000 × *g* for 30 min at 4 °C. Biotinylated proteins were isolated by affinity purification with 30 µg of (RIPA-equilibrated) streptavidin-sepharose beads (GE) with end-over-end rotation 3 h at 4 °C. Beads were washed 8 × 1 mL 50 mM ammonium bicarbonate (pH 8.0) before tryptic digest.

BioID: Mass spectrometry analysis

Tryptic digestion was performed with 1 µg of MS-grade TPCK trypsin (Promega, Madison, WI) dissolved in 100 µL of 50 mM ammonium bicarbonate (pH 8.0), which was added to the streptavidin-sepharose beads and incubated at 37 °C overnight. The eluate was collected and beads were washed twice in 150 µL of 50 mM ammonium bicarbonate. Eluate and washes were pooled, lyophilized and reconstituted in 0.1% formic acid. Liquid chromatography analysis was performed on an in-house analytical column (75 µm inner diameter) and pre-column (150 µm inner diameter), made from fused silica capillary tubing from InnovaQuartz (Phoenix, AZ), and packed with 100 Å C18-coated silica particles (Magic, Michrom Bioresources, Auburn, CA).

Peptides were resolved and identified using reversed phase (120 min buffer gradient 10–40% acetonitrile, 0.1% formic acid) nanoflow liquid chromatography-electrospray ionization-tandem mass spectrometry (nLC-ESI-MS/MS), running at 250 nL/min on a Proxeon EASY-nLC pump in-line with a hybrid linear quadrupole ion trap Orbitrap mass spectrometer, Velos LTQ (ThermoFisher Scientific, Waltham, MA). A parent ion scan was performed in the

Orbitrap using resolving power of 60,000. Up to 20 most intense peaks (minimum ion count of 1000) were selected for MS/MS using standard CID fragmentation. Fragment ions were detected in the LTQ. Dynamic exclusion was activated, where MS/MS of the same *m/z* (within a 10 ppm window, exclusion list size 500) detected two times within 15 s were excluded from analysis for 30 s. For protein identification, Proteowizard was used to convert Thermo.RAW files to the.mzXML, and then searched using X!Tandem against Human RefSeq Version 45 (appended with cRAP and reversed decoy database based on RefSeq v45). Search parameters specified a parent MS tolerance of 15 ppm and an MS/MS fragment ion tolerance of 0.4 Da, with up to two missed cleavages allowed for trypsin. Oxidation of methionine and ubiquitylation of lysine residues were allowed as variable modifications. Data were analyzed using trans-proteomic pipeline via the ProHits software suite. Proteins identified with ProteinProphet cut-off of 0.8 (corresponding to FDR < 2%) were analyzed with SAINT Express v. 3.3.

Cell culture

Neuroblastoma SK-N-BE(2)C, LAN5, IMR32, SH-SY5Y, SK-N-AS, SK-N-FI, SHEP and TE21/N cells were cultured in Dulbecco's modified Eagle's medium (DMEM) supplied with 10% FBS and 2 mM of glutamine and antibiotics (penicillin, 100 U/ml; streptomycin, 100 µg/ml). Kelly and CHP134 cells were cultured in Roswell Park Memorial Institute Medium (RPMI) 1640 supplemented with 10% FBS and 1% L-glutamine and 2 mM of glutamine and antibiotics (penicillin, 100 U/ml; streptomycin, 100 µg/ml). HEK-293T cells were cultured in Dulbecco's modified Eagle's medium (DMEM) supplemented with 10% FBS and 2 mM of glutamine and antibiotics (penicillin, 100 U/ml; streptomycin, 100 µg/ml). All cell lines were cultured in a humidified incubator Mycoplama-free at 37 °C and 5% CO_2. e TET21/N cells were treated with tetracycline from Sigma Aldrich (final concentration: 2 µg/ml) for the indicated time reported in the results paragraph.

Chromatin immunoprecipitation (ChIP) and ChIP-seq assays

Two 100-mm dishes are used for each immunoprecipitation. For each plate, 270 µl of formaldehyde were added from a 37% stock solution and mixed immediately. Samples were incubated on a platform shaker for 10 minutes at room temperature. For each plate, 500 ml of 2,5 M glycine were added and mixed immediately. Cells were incubated on a platform shaker for 10 minutes at room temperature and then transferred onto ice. Cells were later harvested using a scraper and then centrifuged at 230g for 10 minutes in a cold centrifuge. After washing the pellet three times with 10 ml ice-cold PBS1X containing 1 mM PMSF, cells were

centrifuged and later resuspended in 500 µl ice-cold ChIP Cell Lysis Buffer (Santa Cruz Biotechnology). After 10 minutes of incubation on ice, cells were spun down at 600g for 5 minutes at 4°C and later resuspended in 600 µl ice-cold RIPA buffer. Sonication of crosslinked cells was performed in two distinct steps. First, cells were sonicated with a Branson Sonifier 2 times for 15 seconds at 40% setting. Next, cell samples were further sonicated with the Diogene Bioruptor for 20 minutes at high potency in a tank filled with ice/water to keep cell samples at low temperature during sonication. The supernatant was transferred into a new tube, and the pre-cleared lysate was incubated with 50 µl of Immobilized Protein A for 15 minutes in the cold room at constant rotation (pre-clearing).
The pre-cleared supernatant was supplemented with 5µg of the specific antibody under-sample rotation O/N in the cold room. The next day, 50 µl of Immobilized Protein A were added to purify the antibody/protein/DNA aggregates. Beads were washed five times by incubating the samples with constant rotation for 3 minutes at room temperature. Subsequently, 10 µg of RNAse A were added to remove RNA contaminations. Once performed, Proteinase 74 K Buffer 5X and 6 µl Proteinase K (19 mg/ml) were added to eluate DNA. The immunoprecipitated DNA was purified by adding phenol/chloroform/isoamyl alcohol and later purified through a salting-out procedure. 2-4 µl of IP-DNA was used for each Real-Time PCR analysis.

Relative to Results (Part I):

Chromatin Immunoprecipitation (ChIP) assays were executed using 5 ug of a rabbit anti-E2F1 (3742S; Cell Signalling) or control rabbit antibody. qPCR was later performed to analyze if E2F1 can bind the DEPDC1B promoter region. The analysis was performed for the following genomic regions: Remote promoter region (negative control): 5'-AGAAGTCTGGGAAGGGTGCT-3' as forward and 5'-ATGCCAGCTTCTTGAGCATT-3' as reverse primer; -600bp from DEPDC1B TSS: 5'-CCCTCTGAAAGATTGCAAATCGG-3' as forward and 5'-TTAGTCCTCGGCAATAGGGTTG-3' as reverse primer; core promoter region of the *DEPDC1B* gene (DEPDC1B TSS): 5'-GTTTCGGTCGCTGGATAACA-3' as forward and 5'-CTAGGCAGGTGCGACTAAGG-3' as reverse; and +600bp from TSS with the 5'-GACGGGGTATTCGAATAAACGG-3' as forward primer and 5'-GGTGCTGACAGAAACAGAAACG -3' as reverse primer.

Relative to Results (Part II):

Chromatin Immunoprecipitation (ChIP) assays were completed using 5 ug of a mouse anti-E2F3a and anti-MYCN (E2F3a: PG30 - MYCN: B84B. Company: Santa Cruz Technology),

or control mouse antibody. Libraries for sequencing were arranged using the Rubicon Thruplex DNA-seq/FD library preparation kit. 50 ng of input DNA or more limited quantities were used, and, following ligation, libraries were amplified per the manufacturer's instructions. Libraries were then size selected using AMPure beads (Agencourt AMPure XP). Another size selection was performed using a 2% gel cassette in the Pippin Prep (SAGE Sciences) set to capture fragments of 200–700 bp in size. Libraries were multiplexed at equimolar ratios and run together either on a HiSeq 2000 (40-bp, single-end reads) or a NextSeq (75-bp, single-end reads). FASTQ.GZ files were later aligned as BAM formats for peak calling using the MACS2 tool from bedtool (Galaxy). The analysis was performed using a cutoff with a p-value < 0,0005 and an enrichment score ranging from 4 to 50 folds compared to control. The software EaSeq was used for both the tracks visualization and figure design (Lerdrup et al., 2016). The intersection between MYCN and E2F3a ChIP peaks was evaluated using the BedSect tool (Mishra et al., 2020) with an overlap size of 50bp. The same analysis was performed using the Reldist tool from the R package to evaluate the relative distances between the MYCN and E2F3a ChIP peaks (Favorov et al., 2012).

ChIP-seq (high-throughput data) from Gene Expression Omnibus – GEO -

Data contained in the GSE80154 series retrieved from the article of Zeid et al. (Zeid et al., 2018) were used to analyze the ChIP-seq tracks of MYCN and histone modification markers in neuroblastoma cells. The software EaSeq was used for both tracks visualization and figure design (Lerdrup et al., 2016).

Clinical validation of E2Fs, MYC and MYCN genes

Analyses of E2F protein expression in neuroblastoma tumours were executed through Kaplan–Meier curve analyses and Cox proportional hazards regression analyses, performed using the R "survival" package (http://cran.r-project.org/web/packages/survival/index.html following manufacturing instructions.

Clonogenic assays

Doxycycline-inducible lncNB1 shRNA cells and control shRNA cells were seeded in 6-well plates at a concentration of 500 cells/well and later treated with DMSO (vehicle treatment control) or Doxycycline (2ug/ml). After ten days, colonies were washed twice with PBS, fixed and stained with crystal violet solution (0.5% crystal violet, 50% methanol) for 30 min, washed with water and let dry for three days. Pictures of the wells were taken via the

ChemiDoc MP system (BioRad). The total surface area occupied by the colonies was determined using FigureJ software. Colonies smaller than 50 cells were excluded from the analysis. Four replicates of the experiment were performed.

Gene reporter assays

The Dual-Luciferase® Reporter (DLR) Assay System (Promega) provides an efficient means of performing dual-reporter assays. The firefly activities (Photinus pyralis) and Renilla (Renilla reniformis, also known as sea pansy) luciferases are measured sequentially from a single sample. The firefly luciferase reporter is measured first by adding Luciferase Assay Reagent II (LAR II) to generate a stabilized luminescent signal. After quantifying the firefly luminescence, this reaction is quenched, and the Renilla luciferase reaction is simultaneously initiated by adding Stop & Glo® Reagent to the same tube. The Stop & Glo® Reagent also produces a stabilized signal deriving from the Renilla luciferase, decaying slowly throughout the measurement.

Relative to Results (Part I):

Modulation of *DEPDC1B* gene promoter activity by lncNB1 was assessed through the use of this technology. pGL3 construct carrying *DEPDC1B* gene promoter (1146 bp) was obtained by directional cloning using 5'-CTCGAGTTAACTTCCACAGCTCACAAAG-3' as forward and 5'-GAGCAGCAGTTTGAATCCCAAG-3'as reverse primers. Deletion mutants of pGL3_*DEPDC1B* gene promoter were obtained by whole-around PCR technology using the following primers: 545bp promoter 5'-TCGGGGCTCCCTTCCCGC-3'(forward) and 545bp promoter: 5'-GGTACCTATCGATAGAGAAATG-3'(reverse); 75bp promoter 5'-ATTTCCGGTGACGTGCTG-3' (forward) and 75bp promoter 5'-GGTACCTATCGATAGAGAAATG-3' (reverse); 545bpPromoter+20bpDeletion 5'-GGGATTCAAACTGCTGCTCAGATCTGC-3' (forward) and 545bpPromoter+20bpDeletion 5'-TGATTGGGCGGCGCGGCA-3' (reverse). Reporter activities were mesaured using the GloMax® 20/20 luminometer (Promega). Relative percentage luciferase activity of the doxycycline treatment condition was normalized by the same reporter construct's luciferase activity under vehicle control treatment condition as a function of the pGL3-basic empty vector.

Relative to Results (Part II):

Modulation of *E2F3a* gene promoter activity as a function of N-MYC levels was assessed using this technology. pGL3 construct carrying *E2F3a* gene promoter (1263 bp) was obtained

by directional cloning using 5'- tttgctagcGGGATAGGTTTGAGTCGTTGTGTT-3' as forward and 5'- tttAAGCTTTATTTTTCCGCACCGCACAG-3'as reverse primers. Reporter activities were mesaured using the GloMax® 20/20 luminometer (Promega). Relative percentage luciferase activity of the tetracycline treatment condition was normalized by the luciferase activity of the same reporter construct under vehicle control treatment condition as a function of the pGL3-basic empty vector.

GO analysis.

Gene Ontology (GO) enrichment analyses were performed using the online software PANTHER (Protein Analysis THrough Evolutionary Relationships, http://pantherdb.org) (H. Mi et al., 2016) and STRING (Szklarczyk et al., 2019) to identify functional overrepresented GO categories in each gene group of interactors. The GREAT software was also used to evaluate the GO terms for the putative direct E2F3a/N-MYC activated or repressed genes (McLean et al., 2010). GO algorithms count and compare each category's number in the test group and the same class size in the reference group. The analysis proceeds by calculating a p-value and false discovery rate (FDR) value estimated using Fisher's exact test, which indicates the probability that the observed counts of each GO category could have resulted from the random distribution of the term between the test and reference groups. The tested groups resulting in an FDR value < 0,05 with gene counts that comprise more than two elements were examined. GO categories are shown as a function of the respective FDR value ($-\log_{10}$ FDR). GO classes considered not statistically significant are listed with $-\log_{10}$ FDR = 0. GO molecular functions, and biological processes were manually clusterized based on the class of membership.

GTEx RNA sequencing data analysis

The publicly available Genotype-Tissue Expression (GTEx) Release V7 dataset (dbGaP Accession phs000424.v7.p2) make available expression data of all transcripts from RNA sequencing of 53 normal tissue sites across nearly 1000 people. lncNB1 transcript expression levels in the normal tissues were acquired through GTEx Portal website [https://gtexportal.org/home/gene/RP1-40E16.9%20].

Immunoblot

Proteins were extracted in RIPA buffer (150 mM NaCl, 0.5% sodium deoxycholate, 1% NP-40, 1 mM PMSF, 0.1% SDS, 50 mM Tris-HCl, 2% Complete) containing protease inhibitors

(complete from Roche and PMSF distribuited by Sigma Aldrich) and phosphatase inhibitors. After 30''on/off of pulse sonication at high power using the Bioruptor standard sonicator (Diagenode), cells were spun down at 14,000 × *g* at 4 °C for 15 minutes and the supernatant was collected. Proteins were quantified using BCA assays (Bicinchoninic Acid Assay kit from Thermo Fisher Scientific). Later Protein samples have been subjected to SDS-PAGE and transfer using nitrocellulose membranes in wet condition (Transfer buffer: Tris Glycine 1x, 20% methanol, no SDS). Membranes were later blocked with 5% dried milk powder resuspended in phosphate-buffered saline (PBS), and probed with the following primary antibodies: rabbit anti-DEPDC1B (1:500) (HPA038255; Sigma), mouse anti-N-Myc (1:1000) (sc-53993; Santa Cruz Biotechnology), mouse anti-E2F1 (1:1000) (KH95; Santa Cruz Biotechnology); mouse anti-E2F3a (1:500) (PG37; Santa Cruz Biotechnology); rabbit anti-E2F3b (1:1000) (ab50917; Abcam). The membranes were incubated with a goat anti-rabbit (sc-2004) or goat anti-mouse (sc-2005) antibody conjugated to horseradish peroxidase (1:10,000) (both from Jackson ImmunoResearch), and protein bands were visualized with ECL (Bio-Rad, Hercules, CA). The membranes were probed with an anti-actin antibody (1:15000) (A5441; Sigma) as loading controls and visualized using the ChemiDoc XRS+ imager distribuited by Bio-Rad.

Immunoblot densitometry

The software ImageJ was used to analyze the profiles of each lane for the blotted nitrocellulose membrane. The size of the lane selection tool was 8 pixels wide. The lanes' shapes were represented as the average of the grayscale values or the uncalibrated optical density along a one-pixel-height horizontal lane. Protein intensity was calculated as a function of the HRP-band signal. Enrichments in percentage were assigned by normalizing on a reference control sample.

Immunofluorescence

TET21/N cells inducible overexpressing the V5_FLAG_BirA*, V5_FLAG_BirA*_E2F3a and V5_FLAG_BirA*_E2F3b proteins were grown on poly-L-Lysine (Sigma-Aldrich) coated coverslips and treated with 5 μM MG132 (Sigma Aldrich) and 30 ug/ml of cumate (System Biosciences - SBI), the latter used to lead protein overexpression. The next day, cells were fixed with 4% formaldehyde for 10 minutes and washed three times with PBS 1X + 0.25% Triton X-100. Cells were blocked in 5% bovine serum albumin (BSA) in PBS 1X for 1 hour before incubating in PBS 1X 1:1000 anti-V5 (ab27671 from Abcam) primary antibodies

overnight at 4°C. The next day, coverslips were washed three times in PBS 1X and then incubated with Alexa-594-conjugated secondary antibody (Life Technologies), used at 1:5000 at 37°C for 1 hour. After removing the solution, cells were incubated with 1 μg/ml of 4′, 6-dia-midino-2- phenylindole (DAPI) in PBS for 5 min. Coverslips were washed with PBS three times for 5 min each and mounted with ProLong Gold Antifade (Thermo Fischer Scientific). Cells were imaged using PlanApo 60× oil lens, NA 1.40 on an Olympus FV1000 confocal microscope (zoom factor between 3 and 5; Olympus America, Melville, NY). Images were processed using the Volocity Viewer v.6 and assembled using Adobe Illustrator CS6 (Adobe Systems Inc.).

Lentiviral production and infection for stable cell lines generation

Relative to Results (Part I):

The lentiviral doxycycline-inducible FH1tUTG construct from Dr. Marco Herold was used to generate control shRNA and lncNB1 shRNA expressing constructs and neuroblastoma cell lines stably expressing the constructs. lncNB1 shRNA target sequences were GCTGCAGCGTTTACCCAAAGA (shRNA-1) and GCTTCCTTCAAACCTCAAATC (shRNA-2). Sense and antisense shRNA oligonucleotides were synthesized by Sigma-Aldrich (Merck) and cloned into the backbone construct. The doxycycline-inducible control shRNA, lncNB1 shRNA-1, or lncNB1 shRNA-2 FH1tUTG construct were transfected into HEK-293T cells together with pSPAX2 and pMD2.G vectors used to permit virus packaging. Viral media were collected and used to infect neuroblastoma cells with 8ug/ml of polybrene (Santa Cruz Biotechnology, Santa Cruz, CA) for 72 hours. Fluorescence-activated cell sorting was performed with Bio-Rad's S3e Cell Sorter (Bio-Rad) to select neuroblastoma cells with high GFP protein expression (top 5%). Cells were treated with 2 μg/ml doxycycline (Sigma) or DMSO vehicle control every 24 h to or to not induce shRNA expression.

Relative to Results (Part II):

The lentiviral cumate-inducible pCDH-CuO-MCS-IRES-GFP-EF1α-CymR-T2A-Puro SparQ™ All-in-one Cloning and Expression Lentivector (QM812B-1) from System Biosciences (SBI) was used to generate plasmids expressing V5_FLAG_BirA*, V5_FLAG_BirA*_E2F3a and V5_FLAG_BirA*_E2F3b as well as TET21/N cell lines stably expressing the constructs. E2F3a and E2F3b coding sequences were previously cloned into the kanamycin-R pENTR4_V5_Flag_BirA* donor vector gently sent from Dr. Linda Z. Penn's lab. E2F3a and E2F3b were amplified from SK-N-BE(2)C cDNA library using the following primers: FW cloning E2F3a 5'-ttttGAATTCAGAAAGGGAATCCAGCCCGC-3';

FW cloning E2F3b 5'-ttttGAATTCCCCTTACAGCAGCAGGCA-3' and a common RV cloning E2F3 5'-aaaTCTAGATCAACTACACATGAAGTCTTCCACCA-3'. Oligonucleotides were synthesized by Sigma-Aldrich (Merck). Sequences were then flipped into the Ampicillin-R QM812B-1 acceptor vector through GATEWAY Cloning Technology, based on the site-specific recombination system used by phage l to integrate its DNA in the E. coli chromosome. Gateway™ LR Clonase™ II Enzyme mix (Thermo Fisher Scientific) was used following protocol specifications (Catalog number: 11791020). The recombinant QM812B-1 constructs were then transfected into HEK-293T cells together with pSPAX2 and pMD2.G vectors used to allow virus packaging. Viral media were collected and employed to infect TET21/N cells with 8 ug/ml of polybrene (Santa Cruz Biotechnology, Santa Cruz, CA) for 48 hours. Transduced cells were then selected using 1ug/ml of puromycin (Thermo Fisher Scientific – US) for 48 hours.

Patient tumour sample analysis

lncNB1, DEPDC1B, E2F1, E2F2, E2F3 (all isoforms), E2F3a and E2F3b, E2F4, E2F5, E2F6, E2F7, E2F8, MYC and MYCN RNA expression was extracted from the publicly available RNA sequencing SEQC-RPM-seqcnb1 dataset consisting of 493 human neuroblastoma samples, Kocak dataset containing 649 human neuroblastoma samples, Versteeg dataset containing 86 human neuroblastoma samples and the TARGET dataset with 161 human neuroblastoma samples with detailed information on MYCN amplification status and clinical outcome [http://r2.amc.nl].

Plasmid transfection

DP1, E2F3a, E2F3b cDNAs were amplified from SK-N-BE(2)C neuroblastoma cells using the Herculase II TAQ polymerase (Agilent Technologies, Santa Clara, CA) with the following primers: 5'-tttAAGCTTGCAAAAGATGCCGGTCTAATTGAAG-3' (DP1 forward) and 5'-ttttCTAGAGTCGTCCTCGTCATTCTCGTTG-3' (DP1 reverse); 5'-tttAAGCTTAGAAAGGGAATCCAGCCCGC-3' (E2F3a forward) and 5'-tttGGATCCTCAACTACACATGAAGTCTTCCACCA-3' (E2F3a reverse); 5'-ttttGAATTCCCCTTACAGCAGCAGGCA-3' (E2F3b forward) and 5'-tttGGATCCTCAACTACACATGAAGTCTTCCACCA-3' (E2F3b reverse) . E2F1 coding sequence was amplified from the HA-E2F1 pRcCMV construct (Addgene plasmid #21667), using the following primers: TTTAAGCTTATGGCCTTGGCCGGGGCCCCTG (pCMV14-HindIII E2F1 forward) and

TTTGAATTCTCAGAAATCCAGGGGGGTGAGGTCCCCAAAG (pCMV14-ECORI E2F1 reverse). PCR amplicons were then cloned into pCMV10 or pCMV14 (Sigma, St Louis, MO), respectively, to generate pCMV10_3× Flag-DP1, pCMV10_3× Flag-E2F3a, pCMV10_3× Flag-E2F3b and pCMV14_E2F1 constructs. Cells were transiently transfected with constructs using Effectene reagent (Qiagen) according to the manufacturer's instructions.

Proximity ligation assay (PLA)

SHEP cells stably overexpressing V5_N-MYC were grown on poly-L-Lysine (Sigma-Aldrich) coated coverslips and then transfected either with pCMV10 (empty vector), pCMV10_E2F3a (encoding for 3XFlag_E2F3a) and pCMV10_E2F3b (encoding for 3XFlag_E2F3b) using Effectene reagent (Qiagen) following manufactures' instructions.

After 48 hours, cells were fixed with 4% Paraformaldehyde at room temperature for 10 min and then washed three times with PBS + 0.25% Triton X-100. Blocking was performed using 5% of bovine serum albumin (BSA) in PBS for one hour. Anti-V5 (mouse) and Anti-Flag (rabbit) were incubated either or together in all conditions at 4°C overnight. The next day, coverslips were washed one time with PBS and two times with Wash Buffer A. PLA probes (both MINUS and PLUS) were then diluted in the Antibody diluent and placed on the slides into humidification chamber for 1 hour at 37°C. Ligation was later performed by adding Ligase into the ligation solution and using the slides in a pre-heated humidity chamber for 30 min at +37°C. After the amplification and probing processes (100 minutes at 37°C), slides were later washed five times with PBS, Wash Buffer A and Wash Buffer B and prepared for Imaging. DAPI was used to stain nuclei. Cells were imaged using PlanApo 60× oil lens, NA 1.40 on an Olympus FV1000 confocal microscope (zoom factor between 3 and 5; Olympus America, Melville, NY). Images were processed using the Volocity Viewer v.6 and assembled using Adobe Illustrator CS6 (Adobe Systems Inc).

Real-time reverse transcription PCR (RT-qPCR)

RNA was extracted from cells using 1ml of TriReagent (Sigma-Aldrich), according to the manufacturer's guidelines. RNAs were then quantified using the Nanodrop spectrophotometer ND-1000 (Thermo Fisher Scientific, Waltham, MA) to calculate the RNA concentration in microliter order. DNase Treatment was later performed to digest the contaminant genomic DNA. The reaction was carried out taking advantage of the DNAse free-kit (Ambion – Life Technologies) with 5ug of RNA and 1uL recombinant DNAse I. The reaction was conducted at 37°C for 30 minutes.

The recombinant DNase I was later inactivated with the DNase Inactivation Reagent (0.1 volume). cDNAs were then synthesized with 5X Iscript Reverse transcription supermix containing the engineered-Reverse transcriptase (RT (RNase H+), RNAse inhibitors, dNTPs, oligo (dT), random hexamers, buffer, MgCl2 and stabilizers. 1 ug of RNA was retro-transcribed for each reaction according to the manufacturer's instructions. RT-qPCR was performed using gene-specific primers and Power SYBR Green Master Mix (Bio-Rad) as the fluorescent dye in Bio-Rad CFX96 Touch Real-Time PCR Detection System. No template controls were used to detect any non-specific amplification.

Relative to Results (Part I):

The sequences of RT-qPCR primers were 5′-AATACGCCAATGTCCTGCTC-3′ (forward) and 5′-TCAGTGCCTTGGCTTGTAGA-3′ (reverse) for lncNB1; 5'-AGCTACCAGGCTGTGGAATG-3' (forward) and 5'-AGCTCTTGAAACGACAGCGA-3' (reverse) for DEPDC1B; 5′-AGCCTTGTTGGAGGAAGTCA-3′ (forward) 5′-GGACTCTTCGGAGAACTTTCAGAT-3′ (forward) and 5′-GGGCACAGGAAAACATCGAT-3′ (reverse) for E2F1; 5′-CGGTGCGGCCTCCAA-3′ (forward) and 5′-CACGGGCAATGGATTTCC-3′ (reverse) for RPL35; 5'-CCGCCGGCTGTTTAACTTC-3' (forward) and 5'-AGAAACAGTGATGCTGGGTCA-3'(reverse) for TBP; 5'- GAGCAAGACAGTGGGCTGG -3'(forward) and 5'-CCATTCGCCACGACTTTGTT-3'(reverse) for GUSB; 5'-AGGCCAACCGCGAGAAG-3'(forward) and 5'- ACAGCCTGGATAGCAACGTACA -3'(reverse) for Actin. All primers were synthesized by Sigma (Sigma-Aldrich). Following RT-qPCR, the comparative threshold cycle (▵ ▵ Ct) method was used to evaluate fold changes in target genes, relative to the figure legends' reference genes.

Relative to Results (Part II):

The sequences of RT-qPCR primers were 5′-CGACCACAAGGCCCTCAGTA-3′ (forward) and 5′-CAGCCTTGGTGTTGGAGGAG-3′ (reverse) for MYCN; 5'-ACTGCTAGCCAGCCCCG-3' (forward) and 5'-GGACTATCTGGACTTCGTAGTGCAGC-3' (reverse) for E2F3a; 5'-CCCTTACAGCAGCAGGCA-3' (forward) and 5'-GGACTATCTGGACTTCGTAGTGCAGC-3' (reverse) for E2F3b; 5'-CCTGCAGGGAAAGAAAAGTGC-3' (forward) and 5'-CCTCCTCTTCCCTCCTCGAA-3'for CDK6; 5'-CATCAAGAAGCAGAAAGAGATCAT-3' (forward) and

5’-GTAGACCTTGCGGATCTGGG-3’ (reverse) for KAT2A; 5’-GGGAAGGCTGCAGATACCAT-3’ (forward) and 5’-TCTGAAGACTAAGCCCTCCTCA-3’ (reverse) for MGA; 5’-ACTCCGTTTTCATGCAGAGACTAA-3’ (forward) and 5’-GAGGAATGTGAGGTATTGGTGACA-3’ (reverse) for RB1; 5’-TCTAACAATGGCCACAGCCC-3’ (forward) and 5’-GCATCATTTGCGACACCATGT-3’ (reverse) for RBL1; 5’-ATGGCTCAGGGAACTGTTGG-3’ (forward) and 5’-TTGGTCAGGTCACTGGCAGA-3’ (reverse) for TFDP1; 5’-GAAGTCGCTGATGAGCTGGT-3’ (forward) and 5’-TTCTGATCATAAGCCTGCGAA-3’ (reverse) for TFDP2; 5’-ACGCTACAAGAGCGATCCAG-3’ (forward) and 5’-GAAGACAGAAGGGTGGGGTG-3’ (reverse) for TRRAP ; 5’-CCATTCCAGCCCCAGTGAAA-3’ (forward) and 5’-AGCTGGGAATCCTGCTTTCT-3’ (reverse) for YEATS2; 5’-TACTGAAACAGGATGGGGTGA-3’ (forward) and 5’-GCAAATGATACAGGGTTACAGGTC-3’ (reverse) for YEATS4 ; 5’-TGGGACCAATATACCCATAGCC-3’ (forward) and 5’-TCTAGCAGGTAAACCTACTTTATC-3’ (reverse) for ZZZ3; 5’-CCGCCGGCTGTTTAACTTC -3’ (forward) and 5’-AGAAACAGTGATGCTGGGTCA-3’(reverse) for TBP; 5’- GAGCAAGACAGTGGGCTGG -3’(forward) and 5’- CCATTCGCCACGACTTTGTT -3’(reverse) for GUSB; 5’- AGGCCAACCGCGAGAAG-3’(forward) and 5’- ACAGCCTGGATAGCAACGTACA -3’(reverse) for Actin. All primers were synthesized by Sigma (Sigma-Aldrich). Following RT-qPCR, the comparative threshold cycle ($\Delta\Delta$Ct) method was used to evaluate fold changes in target genes, relative to the reference genes described in the figure legends.

RNA fractionation assays

LncNB1 RNA localization was assessed using cytoplasmic/nuclear RNA fractionations assays (Carneiro & Schibler, 1984) coupled with RT-qPCR analyses with some modifications. 1*107 BE(2)-C cells were harvested and collected with 5 ml of DMEM in a polypropylene tube, centrifuged at 230g for 5 minutes and subsequently washed twice with 1 ml of ice-cold phosphate-buffered saline (PBS 1X). Cells were later resuspended again with 1 ml of PBS 1X and dived in two aliquots of 500 uL each to perform Total RNA purification

(using Tri-reagent protocol by Sigma Aldrich company) and Cytoplasmic/nuclear RNA fractionation. To perform the subcellular fractionation, cells were centrifuged and later gently resuspended with 300 uL of Lysis Buffer (see Carneiro & Schibler, 1984) for 20 times and sedimented 4 minutes at 800g (4°C). The supernatant (cytoplasmic fraction) was collected and next resuspended with 1 ml of Tri-reagent to perform Cytoplasmic RNA purification, while pellet (nuclei) were resuspended in 500 uL of Lysis buffer and leave on ice for 30 minutes. Nuclei were then washed by two consecutive centrifugations through 350 ul sucrose cushions in lysis buffer 20% and 30% (w/w) and span at 900g (4°C) for 10 minutes. The purified nuclei were resuspended with 500 ul of Tri-reagent solution to perform nuclear RNA purification. Total-cytoplasmic-nuclear RNA integrity was then verified by Agarose gel electrophoresis (gel concentration: 1,5%) using Ethidium bromide as an intercalating agent.
1 ug of RNA was later treated with DNase I using the DNA-free™ Kit From Ambion (Thermofisher - Invitrogen company) and subsequently re-quantified to evaluate the Cytoplasmic and nuclear quantity ratio compared to the Total RNA, which could be previously distorted by DNA contamination. An equal amount of DNA-free RNAs were retro-transcribed using iScript RT (Bio-Rad company) and then amplified by RT-qPCR using SSO Advanced (Bio-Rad), CFX96 thermocycler (Bio-Rad company) and the same amounts of cDNA to evaluate lncNB1 localization. The target enrichment was evaluated as follow:

STEP I: qPCR efficiency calculation of all primers used in the experiment;

STEP II: Fold Ct difference calculation based on the RNA quantities after DNase I treatment. Comparison between Total RNA vs Cytoplasmic RNA and Total RNA vs Nuclear RNA;

STEP III: Ct raw data acquisition at the end of the RT-qPCR;

STEP IV: Ct raw data shift based on STEP II for nuclear and cytoplasmic fractions;
STEP V: RT-qPCR analyses based on the primer efficiency^ - (Total cDNA – fraction of interest cDNA) formula.

MALAT1 (Forward: 5'-GAATTGCGTCATTTAAAGCCTAGTT-3' and Reverse 5'-GTTTCATCCTACCACTCCCAATTAAT-3') and GAPDH (Forward: 5'-ACAGTCAGCCGCATCTTCTT-3' and Reverse 5'-GACAAGCTTC CCGTTCTCAG-3') have been used as internal controls for nuclear and cytoplasmic RNA fractionation purity, respectively.

RNA sequencing

On an excellent sequencing performance, ribosomal RNA was removed using the Ribo-Zero™ rRNA Removal Magnetic kit (Illumina, San Diego, CA). RNA purity was assessed using a BioSpec-nano spectrophotometer, and integrity was evaluated through Bioanalyzer separation chips (Agilent Technologies) with A260/A280 ratios of >2.0 for all samples and a minimum RNA Integrity Number (RIN) of 6. RNA sequencing was performed in collaboration with Tao Liu's research group (Australian facility), which completed the bioinformatics analysis.

siRNA transfection

SK-N-BE(2)C neuroblastoma cells were transfected with siRNAs using Lipofectamine 2000 (Life Technologies, Grand Island, NY), conforming to the manufacturer's guidelines and plated onto 6-well plates. Transfected cells were harvested for RNA extraction. siRNA sequences used for the mRNA silencing were 5′-CAGCTGCAGCGTTTACCCAAA-3′ (siRNA-1) and 5′-CACAGCGAATGCTAACTGATA-3′ (siRNA-2) (Qiagen, Hamburg, Germany) for lncNB1; 5′-GAGGAGCGTGTGGCTCATCTA-3′ (siRNA-1) (Qiagen) and 5′-GAGTTATTAGCTGCTAGATTGGTAA-3′ (siRNA-2) (Invitrogen, Carlsbad, CA) for DEPDC1B; Negative control siRNAs did not target any human genes (All-Stars Negative Control siRNA, Qiagen).

TCGA RNA sequencing data analysis

RNA sequencing data from TCGA was complemented using RNA sequencing data from 493 primary neuroblastoma tumours. cBioPortal was used to extract all the information relative to the tumours tested (https://www.cbioportal.org/).

GST pull-down assay

Five different N-Myc protein fragments (1–88aa, 82–254aa, 248–358aa, 336–400aa, and 400–464 aa) were cloned into the pGEX-2T construct (GE Healthcare Life Sciences), in frame with N-terminal GST and later used as baits. The constructs were transformed into BL-21 *E. Coli*, leading to the controlled-overexpression of the induced the T7-driven transcriptionally activated proteins under the control of Isopropyl β-D-1-thiogalactopyranoside (IPTG) injection. Bacteria were grown 4 hours at 30°C under shaking conditions (200 rpm). GST-N-

Myc fragments were then purified using glutathione-agarose resin (Sigma Aldrich - G4510) after 4 hours of incubation at 4°C in a cold room. HEK-293T cells were transiently transfected with pCMV10_E2F3a and pCMV10_E2F3b to overexpress the 3XFlag_E2F3a and 3XFlag_E2F3b proteins, respectively. Total protein lysates were completed after two days from transfection, and an equal amount of different GST-N-Myc protein fragments immobilized onto glutathione agarose beads were used to pull-down the overexpressed prey proteins. Pulled-down complexes were analyzed by immunoblot with a monoclonal anti-Flag antibody (F1804, Sigma Aldrich), and Ponceau staining detected by ChemiDoc MP (Bio-Rad) was used as loading controls.

Statistical analysis

Experiments for statistical interpretation were conducted at least three times. Data were analyzed using Graphpad Prism 8 program and showed a mean ± standard error. Differences were examined for significance with a two-sided unpaired t-test for two groups or ANOVA among groups. Correlation of lncNB1, MYCN, E2F3a and E2F3b, DEPDC1B in human neuroblastoma tissues was tested using a two-sided Pearson's correlation. Overall survival was established from diagnosis until death or until the last meeting if the patient did not die. According to Kaplan and Meier's method, survival analyses were completed using GraphPad Prism 8.0, and comparisons of survival curves were performed using two-sided log-rank tests. Probabilities of survival and hazard ratios (HRs) were provided with 95% confidence intervals (CIs). Proportionality was validated by visual examination of the plots of log(2 log(S(time))) versus log(time), which were determined to remain parallel. A probability value of 0.05 or less was considered statistically significant. All statistical tests were two-sided.

REFERENCES

1. A, B., E, W. and M, E. (2020) 'Target gene-independent functions of MYC oncoproteins', *Nature reviews. Molecular cell biology*, 21(5), pp. 255–267. doi: 10.1038/S41580-020-0215-2.
2. A, H. *et al.* (2016) 'Targeting MYCN-Driven Transcription By BET-Bromodomain Inhibition', *Clinical cancer research : an official journal of the American Association for Cancer Research*, 22(10), pp. 2470–2781. doi: 10.1158/1078-0432.CCR-15-1449.
3. AD, D. *et al.* (2018) 'Selective gene dependencies in MYCN-amplified neuroblastoma include the core transcriptional regulatory circuitry', *Nature genetics*, 50(9), pp. 1240–1246. doi: 10.1038/S41588-018-0191-Z.
4. AD, P. *et al.* (2008) 'High-dose rapid and standard induction chemotherapy for patients aged over 1 year with stage 4 neuroblastoma: a randomised trial', *The Lancet. Oncology*, 9(3), pp. 247–256. doi: 10.1016/S1470-2045(08)70069-X.
5. AE, T. *et al.* (2020) 'Combination therapy with the CDK7 inhibitor and the tyrosine kinase inhibitor exerts synergistic anticancer effects against MYCN-amplified neuroblastoma', *International journal of cancer*, 147(7), pp. 1928–1938. doi: 10.1002/IJC.32936.
6. Allis, C. D. and Jenuwein, T. (2016) 'The molecular hallmarks of epigenetic control', *Nature Reviews Genetics*. Nature Publishing Group, pp. 487–500. doi: 10.1038/nrg.2016.59.
7. Araki, K. *et al.* (2019) 'Mitochondrial protein E2F3d, a distinctive E2F3 product, mediates hypoxia-induced mitophagy in cancer cells', *Communications Biology*, 2(1). doi: 10.1038/s42003-018-0246-9.
8. Arand, J. *et al.* (2012) 'In vivo control of CpG and non-CpG DNA methylation by DNA methyltransferases', *PLoS Genetics*, 8(6). doi: 10.1371/journal.pgen.1002750.
9. Arrowsmith, C. H. *et al.* (2012) 'Epigenetic protein families: A new frontier for drug discovery', *Nature Reviews Drug Discovery*. Nat Rev Drug Discov, pp. 384–400. doi: 10.1038/nrd3674.
10. AS, F. and RC, S. (2014) 'MYC degradation', *Cold Spring Harbor perspectives in medicine*, 4(3). doi: 10.1101/CSHPERSPECT.A014365.
11. Atanassov, B. S., Koutelou, E. and Dent, S. Y. (2011) 'The role of deubiquitinating enzymes in chromatin regulation', *FEBS Letters*. NIH Public Access, pp. 2016–2023. doi: 10.1016/j.febslet.2010.10.042.
12. B, G. *et al.* (2017) 'A Phase I Study of the CDK4/6 Inhibitor Ribociclib (LEE011) in Pediatric Patients with Malignant Rhabdoid Tumors, Neuroblastoma, and Other Solid Tumors', *Clinical cancer research : an official journal of the American Association for Cancer Research*, 23(10), pp. 2433–2441. doi: 10.1158/1078-0432.CCR-16-2898.
13. Bai, X. *et al.* (2008) 'Overexpression of myocyte enhancer factor 2 and histone hyperacetylation in hepatocellular carcinoma', *Journal of Cancer Research and Clinical Oncology*, 134(1), pp. 83–91. doi: 10.1007/s00432-007-0252-7.
14. Balas, M. M. and Johnson, A. M. (2018) 'Exploring the mechanisms behind long noncoding RNAs and cancer', *Non-coding RNA Research*. KeAi Communications Co., pp. 108–117. doi: 10.1016/j.ncrna.2018.03.001.
15. Barrera, L. O. *et al.* (2008) 'Genome-wide mapping and analysis of active promoters in mouse embryonic stem cells and adult organs', *Genome Research*, 18(1), pp. 46–59. doi: 10.1101/gr.6654808.
16. Bartonicek, N., Maag, J. L. V. and Dinger, M. E. (2016) 'Long noncoding RNAs in cancer: Mechanisms of action and technological advancements', *Molecular Cancer*. BioMed Central Ltd. doi: 10.1186/s12943-016-0530-6.
17. Batta, K. *et al.* (2011) 'Genome-wide function of H2B ubiquitylation in promoter and genic regions', *Genes and Development*, 25(21), pp. 2254–2265. doi: 10.1101/gad.177238.111.
18. Becker, J. S., Nicetto, D. and Zaret, K. S. (2016) 'H3K9me3-Dependent Heterochromatin: Barrier to Cell Fate Changes', *Trends in Genetics*. Elsevier Ltd, pp. 29–41. doi: 10.1016/j.tig.2015.11.001.
19. Bell, E., Lunec, J. and Tweddle, D. A. (2007) 'Cell cycle regulation targets of MYCN identified by gene expression microarrays', *Cell Cycle*, 6(10), pp. 1249–1256. doi: 10.4161/cc.6.10.4222.
20. Betters, E. *et al.* (2010) 'Analysis of early human neural crest development', *Developmental Biology*, 344(2), pp. 578–592. doi: 10.1016/j.ydbio.2010.05.012.
21. Bianco-Miotto, T. *et al.* (2016) 'Recent progress towards understanding the role of DNA methylation in human placental development', *Reproduction*. BioScientifica Ltd., pp. R23–R30. doi: 10.1530/REP-16-0014.
22. Blackwell, T. K. *et al.* (1990) 'Sequence-specific DNA binding by the c-Myc protein', *Science*, 250(494), pp. 1149–1151. doi: 10.1126/science.2251503.
23. Blackwood, E. M. and Eisenman, R. N. (1991) 'Max: A helix-loop-helix zipper protein that forms a sequence-specific DNA-binding complex with Myc', *Science*, 251(4998), pp. 1211–1217. doi: 10.1126/science.2006410.
24. Bown, N. (2001) 'Neuroblastoma tumour genetics: Clinical and biological aspects', *Journal of Clinical Pathology*. BMJ Publishing Group, pp. 897–910. doi: 10.1136/jcp.54.12.897.
25. Brownell, J. E. *et al.* (1996) 'Tetrahymena histone acetyltransferase A: A homolog to yeast Gcn5p linking histone acetylation to gene activation', *Cell*, 84(6), pp. 843–851. doi: 10.1016/S0092-8674(00)81063-6.
26. Buechner, J. and Einvik, C. (2012) 'N-myc and noncoding RNAs in neuroblastoma', *Molecular Cancer Research*. Mol Cancer Res, pp. 1243–1253. doi: 10.1158/1541-7786.MCR-12-0244.
27. Bywater, M. J. *et al.* (2020) 'Reactivation of Myc transcription in the mouse heart unlocks its proliferative capacity', *Nature Communications*, 11(1). doi: 10.1038/s41467-020-15552-x.
28. C, B. *et al.* (2001) 'Regulation of cyclin D2 gene expression by the Myc/Max/Mad network: Myc-dependent TRRAP recruitment and histone acetylation at the cyclin D2 promoter', *Genes & development*, 15(16), pp. 2042–2047. doi: 10.1101/GAD.907901.
29. C, L. *et al.* (2021) 'MYC protein interactors in gene transcription and cancer', *Nature reviews. Cancer*, 21(9). doi: 10.1038/S41568-021-00367-9.
30. Castel, V. *et al.* (2007) 'Molecular biology of neuroblastoma', *Clinical and Translational Oncology*, 9(8), pp. 478–

483. doi: 10.1007/s12094-007-0091-7.
31. Castelnuovo, M. *et al.* (2010) 'An Alu-like RNA promotes cell differentiation and reduces malignancy of human neuroblastoma cells', *FASEB Journal*, 24(10), pp. 4033–4046. doi: 10.1096/fj.10-157032.
32. Chan, J. C. and Maze, I. (2020) 'Nothing Is Yet Set in (Hi)stone: Novel Post-Translational Modifications Regulating Chromatin Function', *Trends in Biochemical Sciences*. Elsevier Ltd, pp. 829–844. doi: 10.1016/j.tibs.2020.05.009.
33. Charron, J. *et al.* (1992) 'Embryonic lethality in mice homozygous for a targeted disruption of the N-myc gene', *Genes and Development*, 6(12 A), pp. 2248–2257. doi: 10.1101/gad.6.12a.2248.
34. Chen, H., Liu, H. and Qing, G. (2018) 'Targeting oncogenic Myc as a strategy for cancer treatment', *Signal Transduction and Targeted Therapy*. Springer Nature. doi: 10.1038/s41392-018-0008-7.
35. Cheng, J. *et al.* (2014) 'A role for H3K4 monomethylation in gene repression and partitioning of chromatin readers', *Molecular Cell*, 53(6), pp. 979–992. doi: 10.1016/j.molcel.2014.02.032.
36. Cheng, X. (2014) 'Structural and functional coordination of dna and histone methylation', *Cold Spring Harbor Perspectives in Biology*, 6(8). doi: 10.1101/cshperspect.a018747.
37. Cheung, N. K. V. and Dyer, M. A. (2013) 'Neuroblastoma: Developmental biology, cancer genomics and immunotherapy', *Nature Reviews Cancer*. NIH Public Access, pp. 397–411. doi: 10.1038/nrc3526.
38. Clarke, S. (1993) 'Protein methylation', *Current Opinion in Cell Biology*, 5(6), pp. 977–983. doi: 10.1016/0955-0674(93)90080-A.
39. Clavería, C. *et al.* (2013) 'Myc-driven endogenous cell competition in the early mammalian embryo', *Nature*, 500(7460), pp. 39–44. doi: 10.1038/nature12389.
40. CM, van G. *et al.* (2003) 'N-Myc overexpression leads to decreased beta1 integrin expression and increased apoptosis in human neuroblastoma cells', *Oncogene*, 22(17), pp. 2664–2673. doi: 10.1038/SJ.ONC.1206362.
41. Cole, K. A. *et al.* (2011) 'RNAi screen of the protein kinome identifies checkpoint kinase 1 (CHK1) as a therapeutic target in neuroblastoma', *Proceedings of the National Academy of Sciences of the United States of America*, 108(8), pp. 3336–3341. doi: 10.1073/pnas.1012351108.
42. Costa, V. *et al.* (2010) 'Uncovering the complexity of transcriptomes with RNA-Seq', *Journal of Biomedicine and Biotechnology*. Hindawi Limited. doi: 10.1155/2010/853916.
43. Creyghton, M. P. *et al.* (2010) 'Histone H3K27ac separates active from poised enhancers and predicts developmental state', *Proceedings of the National Academy of Sciences of the United States of America*, 107(50), pp. 21931–21936. doi: 10.1073/pnas.1016071107.
44. D, M.-V. and L, S. (2020) 'Blocking Myc to Treat Cancer: Reflecting on Two Decades of Omomyc', *Cells*, 9(4). doi: 10.3390/CELLS9040883.
45. D, N. *et al.* (2002) 'N-Myc and Bcl-2 coexpression induces MMP-2 secretion and activation in human neuroblastoma cells', *Oncogene*, 21(29), pp. 4549–4557. doi: 10.1038/SJ.ONC.1205552.
46. Davis, A. C. *et al.* (1993) 'A null c-myc mutation causes lethality before 10.5 days of gestation in homozygotes and reduced fertility in heterozygous female mice', *Genes and Development*, 7(4), pp. 671–682. doi: 10.1101/gad.7.4.671.
47. DeGregori, J. and Johnson, D. (2012) 'Distinct and Overlapping Roles for E2F Family Members in Transcription, Proliferation and Apoptosis', *Current Molecular Medicine*, 6(7), pp. 739–748. doi: 10.2174/1566524010606070739.
48. Diaz-Lagares, A. *et al.* (2016) 'Epigenetic inactivation of the p53-induced long noncoding RNA TP53 target 1 in human cancer', *Proceedings of the National Academy of Sciences of the United States of America*, 113(47), pp. E7535–E7544. doi: 10.1073/pnas.1608585113.
49. Dominissini, D. *et al.* (2016) 'The dynamic N1 -methyladenosine methylome in eukaryotic messenger RNA', *Nature*, 530(7591), pp. 441–446. doi: 10.1038/nature16998.
50. Doolittle, W. F. (2013) 'Is junk DNA bunk? A critique of ENCODE', *Proceedings of the National Academy of Sciences of the United States of America*. Proc Natl Acad Sci U S A, pp. 5294–5300. doi: 10.1073/pnas.1221376110.
51. E, C. *et al.* (2014) 'CDK7 inhibition suppresses super-enhancer-linked oncogenic transcription in MYCN-driven cancer', *Cell*, 159(5), pp. 1126–1139. doi: 10.1016/J.CELL.2014.10.024.
52. E, P. *et al.* (2020) 'Orally bioavailable CDK9/2 inhibitor shows mechanism-based therapeutic potential in MYCN-driven neuroblastoma', *The Journal of clinical investigation*, 130(11), pp. 5875–5892. doi: 10.1172/JCI134132.
53. Engreitz, J. M., Ollikainen, N. and Guttman, M. (2016) 'Long non-coding RNAs: Spatial amplifiers that control nuclear structure and gene expression', *Nature Reviews Molecular Cell Biology*. Nature Publishing Group, pp. 756–770. doi: 10.1038/nrm.2016.126.
54. Ewens, K. G. *et al.* (2017) 'Phosphorylation of pRb: mechanism for RB pathway inactivation in MYCN-amplified retinoblastoma', *Cancer Medicine*, 6(3), pp. 619–630. doi: 10.1002/cam4.1010.
55. F, F. *et al.* (2020) 'Corrigendum to: "MAX to MYCN intracellular ratio drives the aggressive phenotype and clinical outcome of high risk neuroblastoma" [Biochim. Biophys. Acta, Gene Regul. Mech. 1861 (2018) 235-245]', *Biochimica et biophysica acta. Gene regulatory mechanisms*, 1863(11). doi: 10.1016/J.BBAGRM.2020.194645.
56. F, W. *et al.* (2008) 'Distinct transcriptional MYCN/c-MYC activities are associated with spontaneous regression or malignant progression in neuroblastomas', *Genome biology*, 9(10). doi: 10.1186/GB-2008-9-10-R150.
57. Feinberg, A. P., Koldobskiy, M. A. and Göndör, A. (2016) 'Epigenetic modulators, modifiers and mediators in cancer aetiology and progression', *Nature Reviews Genetics*. Nature Publishing Group, pp. 284–299. doi: 10.1038/nrg.2016.13.
58. Feinberg, A. P., Ohlsson, R. and Henikoff, S. (2006) 'The epigenetic progenitor origin of human cancer', *Nature Reviews Genetics*. Nat Rev Genet, pp. 21–33. doi: 10.1038/nrg1748.
59. Feingold, E. A. *et al.* (2004) 'The ENCODE (ENCyclopedia of DNA Elements) Project', *Science*. Science, pp. 636–640. doi: 10.1126/science.1105136.
60. Fischedick, G. *et al.* (2014) 'Nanog induces hyperplasia without initiating tumors', *Stem Cell Research*, 13(2), pp.

300–315. doi: 10.1016/j.scr.2014.08.001.
61. Flavahan, W. A., Gaskell, E. and Bernstein, B. E. (2017) 'Epigenetic plasticity and the hallmarks of cancer', *Science*. American Association for the Advancement of Science. doi: 10.1126/science.aal2380.
62. G, M., FW, A. and P, E. (1988) 'N-myc proto-oncogene expression during organogenesis in the developing mouse as revealed by in situ hybridization', *The Journal of cell biology*, 107(4), pp. 1325–1335. doi: 10.1083/JCB.107.4.1325.
63. Gayther, S. A. *et al.* (2000) 'Mutations truncating the EP300 acetylase in human cancers', *Nature Genetics*, 24(3), pp. 300–303. doi: 10.1038/73536.
64. Gil, R. S. and Vagnarelli, P. (2019) 'Protein phosphatases in chromatin structure and function', *Biochimica et Biophysica Acta - Molecular Cell Research*. Elsevier B.V., pp. 90–101. doi: 10.1016/j.bbamcr.2018.07.016.
65. Gillette, T. G. and Hill, J. A. (2015) 'Readers, writers, and erasers: Chromatin as the whiteboard of heart disease', *Circulation Research*. Lippincott Williams and Wilkins, pp. 1245–1253. doi: 10.1161/CIRCRESAHA.116.303630.
66. Grant, P. A. *et al.* (1997) 'Yeast Gcn5 functions in two multisubunit complexes to acetylate nucleosomal histones: Characterization of an ada complex and the saga (spt/ada) complex', *Genes and Development*, 11(13), pp. 1640–1650. doi: 10.1101/gad.11.13.1640.
67. Greenberg, M. V. C. and Bourc'his, D. (2019) 'The diverse roles of DNA methylation in mammalian development and disease', *Nature Reviews Molecular Cell Biology*. Nature Publishing Group, pp. 590–607. doi: 10.1038/s41580-019-0159-6.
68. GT, H. *et al.* (2017) 'Sequence Specificity in the Entropy-Driven Binding of a Small Molecule and a Disordered Peptide', *Journal of molecular biology*, 429(18), pp. 2772–2779. doi: 10.1016/J.JMB.2017.07.016.
69. Guenatri, M. *et al.* (2004) 'Mouse centric and pericentric satellite repeats form distinct functional heterochromatin', *Journal of Cell Biology*, 166(4), pp. 493–505. doi: 10.1083/jcb.200403109.
70. Gupta, R. A. *et al.* (2010) 'Long non-coding RNA HOTAIR reprograms chromatin state to promote cancer metastasis', *Nature*, 464(7291), pp. 1071–1076. doi: 10.1038/nature08975.
71. H, K. *et al.* (2013) 'Hox-C9 activates the intrinsic pathway of apoptosis and is associated with spontaneous regression in neuroblastoma', *Cell death & disease*, 4(4). doi: 10.1038/CDDIS.2013.84.
72. H, Y. *et al.* (2014) 'miR-329 suppresses the growth and motility of neuroblastoma by targeting KDM1A', *FEBS letters*, 588(1), pp. 192–197. doi: 10.1016/J.FEBSLET.2013.11.036.
73. Hamilton, M. J. *et al.* (2015) 'The interplay of long non-coding RNAs and MYC in cancer', *AIMS Biophysics*. American Institute of Mathematical Sciences, pp. 794–809. doi: 10.3934/biophy.2015.4.794.
74. Harrow, J. *et al.* (2009) 'Identifying protein-coding genes in genomic sequences.', *Genome biology*. BioMed Central, p. 201. doi: 10.1186/gb-2009-10-1-201.
75. Helm, M. and Motorin, Y. (2017) 'Detecting RNA modifications in the epitranscriptome: Predict and validate', *Nature Reviews Genetics*. Nature Publishing Group, pp. 275–291. doi: 10.1038/nrg.2016.169.
76. Henley, S. A. and Dick, F. A. (2012) 'The retinoblastoma family of proteins and their regulatory functions in the mammalian cell division cycle', *Cell Division*. BioMed Central, p. 10. doi: 10.1186/1747-1028-7-10.
77. Howk, C. L. *et al.* (2013) 'Genetic diversity in normal cell populations is the earliest stage of oncogenesis leading to intra-tumor heterogeneity', *Frontiers in Oncology*, 3 APR. doi: 10.3389/fonc.2013.00061.
78. Huarte, M. (2015) 'The emerging role of lncRNAs in cancer', *Nature Medicine*. Nature Publishing Group, pp. 1253–1261. doi: 10.1038/nm.3981.
79. I, M. *et al.* (2014) 'Targeting of the MYCN protein with small molecule c-MYC inhibitors', *PloS one*, 9(5). doi: 10.1371/JOURNAL.PONE.0097285.
80. Iaquinta, P. J. and Lees, J. A. (2007) 'Life and death decisions by the E2F transcription factors', *Current Opinion in Cell Biology*. NIH Public Access, pp. 649–657. doi: 10.1016/j.ceb.2007.10.006.
81. Ishihama, K. *et al.* (2007) 'Expression of HDAC1 and CBP/p300 in human colorectal carcinomas', *Journal of Clinical Pathology*, 60(11), pp. 1205–1210. doi: 10.1136/jcp.2005.029165.
82. Issa, J. P. (2000) 'CpG-island methylation in aging and cancer', *Current Topics in Microbiology and Immunology*. Springer Verlag, pp. 101–118. doi: 10.1007/978-3-642-59696-4_7.
83. J, K. *et al.* (2019) 'Drugging MYCN Oncogenic Signaling through the MYCN-PA2G4 Binding Interface', *Cancer research*, 79(21), pp. 5652–5667. doi: 10.1158/0008-5472.CAN-19-1112.
84. J, P. *et al.* (2001) 'The ATM-related domain of TRRAP is required for histone acetyltransferase recruitment and Myc-dependent oncogenesis', *Genes & development*, 15(13), pp. 1619–1624. doi: 10.1101/GAD.900101.
85. J, R. *et al.* (2013) 'Dual CDK4/CDK6 inhibition induces cell-cycle arrest and senescence in neuroblastoma', *Clinical cancer research : an official journal of the American Association for Cancer Research*, 19(22), pp. 6173–6182. doi: 10.1158/1078-0432.CCR-13-1675.
86. Jin, B., Li, Y. and Robertson, K. D. (2011) 'DNA methylation: Superior or subordinate in the epigenetic hierarchy?', *Genes and Cancer*. Genes Cancer, pp. 607–617. doi: 10.1177/1947601910393957.
87. JJ, M. *et al.* (2012) 'Sequencing of neuroblastoma identifies chromothripsis and defects in neuritogenesis genes', *Nature*, 483(7391), pp. 589–593. doi: 10.1038/NATURE10910.
88. JL, H. *et al.* (2017) 'Corrigendum: Transcriptomic profiling of 39 commonly-used neuroblastoma cell lines', *Scientific data*, 4, p. 170183. doi: 10.1038/SDATA.2017.183.
89. JM, G. *et al.* (2015) 'Histone acetyltransferase inhibitors block neuroblastoma cell growth in vivo', *Oncogenesis*, 4(2). doi: 10.1038/ONCSIS.2014.51.
90. JR, H. *et al.* (2014) 'Inhibitor of MYC identified in a Kröhnke pyridine library', *Proceedings of the National Academy of Sciences of the United States of America*, 111(34), pp. 12556–12561. doi: 10.1073/PNAS.1319488111.
91. K, K. *et al.* (1990) 'Screening for respiratory syncytial virus and assignment to a cohort at admission to reduce nosocomial transmission', *The Journal of pediatrics*, 116(6), pp. 894–898. doi: 10.1016/S0022-3476(05)80646-8.
92. Kalkat, M. *et al.* (2018) 'MYC Protein Interactome Profiling Reveals Functionally Distinct Regions that Cooperate to Drive Tumorigenesis', *Molecular Cell*, 72(5), pp. 836-848.e7. doi: 10.1016/j.molcel.2018.09.031.
93. Kent, L. N. and Leone, G. (2019) 'The broken cycle: E2F dysfunction in cancer', *Nature Reviews Cancer*. Nature

Publishing Group, pp. 326–338. doi: 10.1038/s41568-019-0143-7.
94. Khalil, A. M. *et al.* (2009) 'Many human large intergenic noncoding RNAs associate with chromatin-modifying complexes and affect gene expression', *Proceedings of the National Academy of Sciences of the United States of America*, 106(28), pp. 11667–11672. doi: 10.1073/pnas.0904715106.
95. Kim, E. D. and Sung, S. (2012) 'Long noncoding RNA: Unveiling hidden layer of gene regulatory networks', *Trends in Plant Science*. Trends Plant Sci, pp. 16–21. doi: 10.1016/j.tplants.2011.10.008.
96. Kim, T. *et al.* (2015) 'Role of MYC-Regulated long noncoding RNAs in cell cycle regulation and tumorigenesis', *Journal of the National Cancer Institute*, 107(4). doi: 10.1093/jnci/dju505.
97. Kimura, A., Matsubara, K. and Horikoshi, M. (2005) 'A decade of histone acetylation: Marking eukaryotic chromosomes with specific codes', *Journal of Biochemistry*. J Biochem, pp. 647–662. doi: 10.1093/jb/mvi184.
98. Knoepfler, P. S. *et al.* (2006) 'Myc influences global chromatin structure', *EMBO Journal*, 25(12), pp. 2723–2734. doi: 10.1038/sj.emboj.7601152.
99. Kollenstart, L. *et al.* (2019) 'Gcn5 and esa1 function as histone crotonyltransferases to regulate crotonylation-dependent transcription', *Journal of Biological Chemistry*, 294(52), pp. 20122–20134. doi: 10.1074/jbc.RA119.010302.
100. Kouzarides, T. (2007) 'Chromatin Modifications and Their Function', *Cell*. Cell, pp. 693–705. doi: 10.1016/j.cell.2007.02.005.
101. Krebs, A. R. *et al.* (2011) 'SAGA and ATAC histone acetyl transferase complexes regulate distinct sets of genes and ATAC defines a class of p300-independent enhancers', *Molecular Cell*, 44(3), pp. 410–423. doi: 10.1016/j.molcel.2011.08.037.
102. Kugel, J. F. and Goodrich, J. A. (2013) 'The regulation of mammalian mRNA transcription by lncRNAs: Recent discoveries and current concepts', *Epigenomics*, 5(1), pp. 95–102. doi: 10.2217/epi.12.69.
103. L, C. *et al.* (2018) 'CRISPR-Cas9 screen reveals a MYCN-amplified neuroblastoma dependency on EZH2', *The Journal of clinical investigation*, 128(1), pp. 446–462. doi: 10.1172/JCI90793.
104. L, W. *et al.* (2019) 'ASCL1 is a MYCN- and LMO1-dependent member of the adrenergic neuroblastoma core regulatory circuitry', *Nature communications*, 10(1). doi: 10.1038/S41467-019-13515-5.
105. L, W. and SY, D. (2014) 'Functions of SAGA in development and disease', *Epigenomics*, 6(3), pp. 329–339. doi: 10.2217/EPI.14.22.
106. Lang, S. E. *et al.* (2001) 'E2F Transcriptional Activation Requires TRRAP and GCN5 Cofactors', *Journal of Biological Chemistry*, 276(35), pp. 32627–32634. doi: 10.1074/jbc.M102067200.
107. Lengner, C. J. *et al.* (2007) 'Oct4 Expression Is Not Required for Mouse Somatic Stem Cell Self-Renewal', *Cell Stem Cell*, 1(4), pp. 403–415. doi: 10.1016/j.stem.2007.07.020.
108. Leone, G. *et al.* (2000) 'Identification of a Novel E2F3 Product Suggests a Mechanism for Determining Specificity of Repression by Rb Proteins', *Molecular and Cellular Biology*, 20(10), pp. 3626–3632. doi: 10.1128/mcb.20.10.3626-3632.2000.
109. Levayer, R., Hauert, B. and Moreno, E. (2015) 'Cell mixing induced by myc is required for competitive tissue invasion and destruction', *Nature*, 524(7566), pp. 476–480. doi: 10.1038/nature14684.
110. Lin, C. Y. *et al.* (2012) 'Transcriptional amplification in tumor cells with elevated c-Myc', *Cell*, 151(1), pp. 56–67. doi: 10.1016/j.cell.2012.08.026.
111. Ling, H. *et al.* (2015) 'Junk DNA and the long non-coding RNA twist in cancer genetics', *Oncogene*. Nature Publishing Group, pp. 5003–5011. doi: 10.1038/onc.2014.456.
112. Liu, B. L. *et al.* (2010) 'Global histone modification patterns as prognostic markers to classify glioma patients', *Cancer Epidemiology Biomarkers and Prevention*, 19(11), pp. 2888–2896. doi: 10.1158/1055-9965.EPI-10-0454.
113. Liu, G. *et al.* (2019) 'Architecture of Saccharomyces cerevisiae SAGA complex', *Cell Discovery*, 5(1), p. 25. doi: 10.1038/s41421-019-0094-x.
114. Liu, P. Y. *et al.* (2014) 'Effects of a novel long noncoding RNA, lncUSMycN, on N-Myc expression and neuroblastoma progression', *Journal of the National Cancer Institute*, 106(7). doi: 10.1093/jnci/dju113.
115. Liu, P. Y. *et al.* (2019) 'The long noncoding RNA lncNB1 promotes tumorigenesis by interacting with ribosomal protein RPL35', *Nature Communications*, 10(1). doi: 10.1038/s41467-019-12971-3.
116. LM, M. *et al.* (2020) 'Targeting the SAGA and ATAC Transcriptional Coactivator Complexes in MYC-Driven Cancers', *Cancer research*, 80(10), pp. 1905–1911. doi: 10.1158/0008-5472.CAN-19-3652.
117. Lorenzin, F. *et al.* (2016) 'Different promoter affinities account for specificity in MYC-dependent gene regulation', *eLife*, 5(JULY). doi: 10.7554/eLife.15161.
118. Louis, C. U. and Shohet, J. M. (2015) 'Neuroblastoma: Molecular pathogenesis and therapy', *Annual Review of Medicine*, 66, pp. 49–63. doi: 10.1146/annurev-med-011514-023121.
119. LS, H. *et al.* (2017) 'Preclinical Therapeutic Synergy of MEK1/2 and CDK4/6 Inhibition in Neuroblastoma', *Clinical cancer research : an official journal of the American Association for Cancer Research*, 23(7), pp. 1785–1796. doi: 10.1158/1078-0432.CCR-16-1131.
120. Luger, K., Dechassa, M. L. and Tremethick, D. J. (2012) 'New insights into nucleosome and chromatin structure: An ordered state or a disordered affair?', *Nature Reviews Molecular Cell Biology*. Nat Rev Mol Cell Biol, pp. 436–447. doi: 10.1038/nrm3382.
121. Luo, Y. B. *et al.* (2018) 'Advances in the Surgical Treatment of Neuroblastoma', *Chinese Medical Journal*. Wolters Kluwer Medknow Publications, pp. 2332–2337. doi: 10.4103/0366-6999.241803.
122. M, H. and WA, W. (2013) 'Neuroblastoma and MYCN', *Cold Spring Harbor perspectives in medicine*, 3(10). doi: 10.1101/CSHPERSPECT.A014415.
123. Martello, G. and Smith, A. (2014) 'The Nature of Embryonic Stem Cells', *Annual Review of Cell and Developmental Biology*. Annual Reviews Inc., pp. 647–675. doi: 10.1146/annurev-cellbio-100913-013116.
124. Matthay, K. K. *et al.* (2016) 'Neuroblastoma', *Nature Reviews Disease Primers*, 2. doi: 10.1038/nrdp.2016.78.
125. Medema, J. P. (2013) 'Cancer stem cells: The challenges ahead', *Nature Cell Biology*. Nat Cell Biol, pp. 338–344. doi: 10.1038/ncb2717.

126. Mestdagh, P. *et al.* (2010) 'An integrative genomics screen uncovers ncRNA T-UCR functions in neuroblastoma tumours', *Oncogene*, 29(24), pp. 3583–3592. doi: 10.1038/onc.2010.106.
127. Meyer, N. and Penn, L. Z. (2008) 'Reflecting on 25 years with MYC', *Nature Reviews Cancer*. Nat Rev Cancer, pp. 976–990. doi: 10.1038/nrc2231.
128. Mi, W. *et al.* (2017) 'YEATS2 links histone acetylation to tumorigenesis of non-small cell lung cancer', *Nature Communications*, 8(1). doi: 10.1038/s41467-017-01173-4.
129. Michalak, E. M. *et al.* (2019) 'The roles of DNA, RNA and histone methylation in ageing and cancer', *Nature Reviews Molecular Cell Biology*. Nature Publishing Group, pp. 573–589. doi: 10.1038/s41580-019-0143-1.
130. Milazzo, G. *et al.* (2020) 'Histone deacetylases (HDACs): Evolution, specificity, role in transcriptional complexes, and pharmacological actionability', *Genes*. MDPI AG. doi: 10.3390/genes11050556.
131. Morandi, F. *et al.* (2018) 'Novel immunotherapeutic approaches for neuroblastoma and malignant melanoma', *Journal of Immunology Research*. Hindawi Limited. doi: 10.1155/2018/8097398.
132. Mosse, Y. P. *et al.* (2007) 'Neuroblastomas have distinct genomic DNA profiles that predict clinical phenotype and regional gene expression', *Genes Chromosomes and Cancer*, 46(10), pp. 936–949. doi: 10.1002/gcc.20477.
133. Musselman, C. A. *et al.* (2012) 'Perceiving the epigenetic landscape through histone readers', *Nature Structural and Molecular Biology*. Nat Struct Mol Biol, pp. 1218–1227. doi: 10.1038/nsmb.2436.
134. Muth, D. *et al.* (2010) 'Transcriptional repression of SKP2 is impaired in MYCN-amplified neuroblastoma', *Cancer Research*, 70(9), pp. 3791–3802. doi: 10.1158/0008-5472.CAN-09-1245.
135. MW, Z. *et al.* (2018) 'MYC Drives a Subset of High-Risk Pediatric Neuroblastomas and Is Activated through Mechanisms Including Enhancer Hijacking and Focal Enhancer Amplification', *Cancer discovery*, 8(3), pp. 320–335. doi: 10.1158/2159-8290.CD-17-0993.
136. N, Z. *et al.* (2014) 'MYC interacts with the human STAGA coactivator complex via multivalent contacts with the GCN5 and TRRAP subunits', *Biochimica et biophysica acta*, 1839(5), pp. 395–405. doi: 10.1016/J.BBAGRM.2014.03.017.
137. Ng, H. H. *et al.* (2003) 'Lysine-79 of histone H3 is hypomethylated at silenced loci in yeast and mammalian cells: A potential mechanism for position-effect variegation', *Proceedings of the National Academy of Sciences of the United States of America*, 100(4), pp. 1820–1825. doi: 10.1073/pnas.0437846100.
138. Nie, Z. *et al.* (2012) 'c-Myc is a universal amplifier of expressed genes in lymphocytes and embryonic stem cells.', *Cell*, 151(1), pp. 68–79. doi: 10.1016/j.cell.2012.08.033.
139. O, T. *et al.* (2016) 'HAUSP deubiquitinates and stabilizes N-Myc in neuroblastoma', *Nature medicine*, 22(10), pp. 1180–1186. doi: 10.1038/NM.4180.
140. Olsen, R. R. *et al.* (2017) 'MYCN induces neuroblastoma in primary neural crest cells', *Oncogene*, 36(35), pp. 5075–5082. doi: 10.1038/onc.2017.128.
141. Pandey, G. K. and Kanduri, C. (2015) 'Long noncoding RNAs and neuroblastoma', *Oncotarget*, 6(21), pp. 18265–18275. doi: 10.18632/oncotarget.4251.
142. Papai, G. *et al.* (2020) 'Structure of SAGA and mechanism of TBP deposition on gene promoters', *Nature*, 577(7792), pp. 711–716. doi: 10.1038/s41586-020-1944-2.
143. Patel, J. H. *et al.* (2004) 'The c-MYC Oncoprotein Is a Substrate of the Acetyltransferases hGCN5/PCAF and TIP60', *Molecular and Cellular Biology*, 24(24), pp. 10826–10834. doi: 10.1128/mcb.24.24.10826-10834.2004.
144. Ping, Z. *et al.* (2012) 'APC/CCdh1 controls the proteasome-mediated degradation of E2F3 during cell cycle exit', *Cell Cycle*, 11(10), pp. 1999–2005. doi: 10.4161/cc.20402.
145. Piunti, A. and Shilatifard, A. (2016) 'Epigenetic balance of gene expression by polycomb and compass families', *Science*. American Association for the Advancement of Science. doi: 10.1126/science.aad9780.
146. Pokholok, D. K. *et al.* (2005) 'Genome-wide map of nucleosome acetylation and methylation in yeast', *Cell*, 122(4), pp. 517–527. doi: 10.1016/j.cell.2005.06.026.
147. Poli, V. *et al.* (2018) 'MYC-driven epigenetic reprogramming favors the onset of tumorigenesis by inducing a stem cell-like state', *Nature Communications*, 9(1). doi: 10.1038/s41467-018-03264-2.
148. Prasad, M. S., Sauka-Spengler, T. and LaBonne, C. (2012) 'Induction of the neural crest state: Control of stem cell attributes by gene regulatory, post-transcriptional and epigenetic interactions', *Developmental Biology*. Academic Press Inc., pp. 10–21. doi: 10.1016/j.ydbio.2012.03.014.
149. Pray-Grant, M. G. *et al.* (2005) 'Chd1 chromodomain links histone H3 methylation with SAGA- and SLIK-dependent acetylation', *Nature*, 433(7024), pp. 434–438. doi: 10.1038/nature03242.
150. De Pretis, S. *et al.* (2017) 'Integrative analysis of RNA polymerase II and transcriptional dynamics upon MYC activation', *Genome Research*, 27(10), pp. 1658–1664. doi: 10.1101/gr.226035.117.
151. Pui, C. H. *et al.* (2011) 'Challenging issues in pediatric oncology', *Nature Reviews Clinical Oncology*. NIH Public Access, pp. 540–549. doi: 10.1038/nrclinonc.2011.95.
152. Puissant, A. *et al.* (2013) 'Targeting MYCN in neuroblastoma by BET bromodomain inhibition', *Cancer Discovery*, 3(3), pp. 309–323. doi: 10.1158/2159-8290.CD-12-0418.
153. Qiao, H. *et al.* (2007) 'Human TFDP3, a novel DP protein, inhibits DNA binding and transactivation by E2F', *Journal of Biological Chemistry*, 282(1), pp. 454–466. doi: 10.1074/jbc.M606169200.
154. R, C. and PS, K. (2009) 'N-Myc regulates expression of pluripotency genes in neuroblastoma including lif, klf2, klf4, and lin28b', *PloS one*, 4(6). doi: 10.1371/JOURNAL.PONE.0005799.
155. Rickman, D. S., Schulte, J. H. and Eilers, M. (2018) 'The expanding world of N-MYC-driven tumors', *Cancer Discovery*. American Association for Cancer Research Inc., pp. 150–164. doi: 10.1158/2159-8290.CD-17-0273.
156. Rinn, J. L. and Chang, H. Y. (2012) 'Genome regulation by long noncoding RNAs', *Annual Review of Biochemistry*, 81, pp. 145–166. doi: 10.1146/annurev-biochem-051410-092902.
157. Robertson, K. D. and Wolffe, A. P. (2000) 'DNA methylation in health and disease', *Nature Reviews Genetics*. European Association for Cardio-Thoracic Surgery, pp. 11–19. doi: 10.1038/35049533.
158. Rogers, C. D., Saxena, A. and Bronner, M. E. (2013) 'Sip1 mediates an E-cadherin-to-N-cadherin switch during cranial neural crest EMT', *Journal of Cell Biology*, 203(5), pp. 835–847. doi: 10.1083/jcb.201305050.

159. Rushlow, D. E. *et al.* (2013) 'Characterisation of retinoblastomas without RB1 mutations: Genomic, gene expression, and clinical studies', *The Lancet Oncology*, 14(4), pp. 327–334. doi: 10.1016/S1470-2045(13)70045-7.
160. Ryl, T. *et al.* (2017) 'Cell-Cycle Position of Single MYC-Driven Cancer Cells Dictates Their Susceptibility to a Chemotherapeutic Drug', *Cell Systems*, 5(3), pp. 237-250.e8. doi: 10.1016/j.cels.2017.07.005.
161. S, A. *et al.* (2011) 'Polo-like kinase 1 is a therapeutic target in high-risk neuroblastoma', *Clinical cancer research : an official journal of the American Association for Cancer Research*, 17(4), pp. 731–741. doi: 10.1158/1078-0432.CCR-10-1129.
162. S, A. and M, E. (2005) 'Transcriptional regulation and transformation by Myc proteins', *Nature reviews. Molecular cell biology*, 6(8), pp. 635–645. doi: 10.1038/NRM1703.
163. S, F. and EV, P. (2015) 'Small-molecule inhibitors of the Myc oncoprotein', *Biochimica et biophysica acta*, 1849(5), pp. 525–543. doi: 10.1016/J.BBAGRM.2014.03.005.
164. S, W. *et al.* (2014) 'Activation and repression by oncogenic MYC shape tumour-specific gene expression profiles', *Nature*, 511(7510), pp. 483–487. doi: 10.1038/NATURE13473.
165. SA, P.-P. *et al.* (2019) 'Phase 1 Study of Molibresib (GSK525762), a Bromodomain and Extra-Terminal Domain Protein Inhibitor, in NUT Carcinoma and Other Solid Tumors', *JNCI cancer spectrum*, 4(2). doi: 10.1093/JNCICS/PKZ093.
166. Sabò, A. *et al.* (2014) 'Selective transcriptional regulation by Myc in cellular growth control and lymphomagenesis', *Nature*, 511(7510), pp. 488–492. doi: 10.1038/nature13537.
167. Santos-Rosa, H. *et al.* (2002) 'Active genes are tri-methylated at K4 of histone H3', *Nature*, 419(6905), pp. 407–411. doi: 10.1038/nature01080.
168. SB, M. *et al.* (1998) 'The novel ATM-related protein TRRAP is an essential cofactor for the c-Myc and E2F oncoproteins', *Cell*, 94(3), pp. 363–374. doi: 10.1016/S0092-8674(00)81479-8.
169. SB, M., MA, W. and MD, C. (2000) 'The essential cofactor TRRAP recruits the histone acetyltransferase hGCN5 to c-Myc', *Molecular and cellular biology*, 20(2), pp. 556–562. doi: 10.1128/MCB.20.2.556-562.2000.
170. Scaruffi, P. *et al.* (2009) 'Transcribed-ultra conserved region expression is associated with outcome in high-risk neuroblastoma', *BMC Cancer*, 9. doi: 10.1186/1471-2407-9-441.
171. Schaub, F. X. *et al.* (2018) 'Pan-cancer Alterations of the MYC Oncogene and Its Proximal Network across the Cancer Genome Atlas', *Cell Systems*, 6(3), pp. 282-300.e2. doi: 10.1016/j.cels.2018.03.003.
172. Schmitt, A. M. and Chang, H. Y. (2016) 'Long Noncoding RNAs in Cancer Pathways', *Cancer Cell*. Cell Press, pp. 452–463. doi: 10.1016/j.ccell.2016.03.010.
173. Schmitz, S. U., Grote, P. and Herrmann, B. G. (2016) 'Mechanisms of long noncoding RNA function in development and disease', *Cellular and Molecular Life Sciences*. Birkhauser Verlag AG, pp. 2491–2509. doi: 10.1007/s00018-016-2174-5.
174. Serman, L. *et al.* (2014) 'Epigenetic alterations of the Wnt signaling pathway in cancer: A mini review', *Bosnian Journal of Basic Medical Sciences*, 14(4), pp. 191–194. doi: 10.17305/bjbms.2014.4.205.
175. Seruggia, D. *et al.* (2019) 'TAF5L and TAF6L Maintain Self-Renewal of Embryonic Stem Cells via the MYC Regulatory Network', *Molecular Cell*, 74(6), pp. 1148-1163.e7. doi: 10.1016/j.molcel.2019.03.025.
176. SG, D. *et al.* (2016) 'Phase I Study of the Aurora A Kinase Inhibitor Alisertib in Combination With Irinotecan and Temozolomide for Patients With Relapsed or Refractory Neuroblastoma: A NANT (New Approaches to Neuroblastoma Therapy) Trial', *Journal of clinical oncology : official journal of the American Society of Clinical Oncology*, 34(12), pp. 1368–1375. doi: 10.1200/JCO.2015.65.4889.
177. Siegel, R. L., Miller, K. D. and Jemal, A. (2016) 'Cancer statistics, 2016', *CA: A Cancer Journal for Clinicians*, 66(1), pp. 7–30. doi: 10.3322/caac.21332.
178. SK, M. *et al.* (2021) 'Taking the Myc out of cancer: toward therapeutic strategies to directly inhibit c-Myc', *Molecular cancer*, 20(1). doi: 10.1186/S12943-020-01291-6.
179. Soshnev, A. A., Josefowicz, S. Z. and Allis, C. D. (2016) 'Greater Than the Sum of Parts: Complexity of the Dynamic Epigenome', *Molecular Cell*. Cell Press, pp. 681–694. doi: 10.1016/j.molcel.2016.05.004.
180. Spedale, G., Timmers, H. T. M. and Pijnappel, W. W. M. P. (2012) 'ATAC-king the complexity of SAGA during evolution', *Genes and Development*, 26(6), pp. 527–541. doi: 10.1101/gad.184705.111.
181. SR, F. *et al.* (2003) 'MYC recruits the TIP60 histone acetyltransferase complex to chromatin', *EMBO reports*, 4(6), pp. 575–580. doi: 10.1038/SJ.EMBOR.EMBOR861.
182. Sterner, D. E. and Berger, S. L. (2000) 'Acetylation of Histones and Transcription-Related Factors', *Microbiology and Molecular Biology Reviews*, 64(2), pp. 435–459. doi: 10.1128/mmbr.64.2.435-459.2000.
183. Strahl, B. D. and Allis, C. D. (2000) 'The language of covalent histone modifications', *Nature*. Nature, pp. 41–45. doi: 10.1038/47412.
184. Strieder, V. and Lutz, W. (2003) 'E2F proteins regulate MYCN expression in neuroblastomas', *Journal of Biological Chemistry*, 278(5), pp. 2983–2989. doi: 10.1074/jbc.M207596200.
185. SW, C. *et al.* (1999) 'c-MYC interacts with INI1/hSNF5 and requires the SWI/SNF complex for transactivation function', *Nature genetics*, 22(1), pp. 102–105. doi: 10.1038/8811.
186. T, B. *et al.* (2002) 'Small-molecule antagonists of Myc/Max dimerization inhibit Myc-induced transformation of chicken embryo fibroblasts', *Proceedings of the National Academy of Sciences of the United States of America*, 99(6), pp. 3830–3835. doi: 10.1073/PNAS.062036999.
187. T, O. *et al.* (2009) 'Stabilization of N-Myc is a critical function of Aurora A in human neuroblastoma', *Cancer cell*, 15(1), pp. 67–78. doi: 10.1016/J.CCR.2008.12.005.
188. Tee, A. E. *et al.* (2014) 'The histone demethylase JMJD1A induces cell migration and invasion by up-regulating the expression of the long noncoding RNA MALAT1', *Oncotarget*, 5(7), pp. 1793–1804. doi: 10.18632/oncotarget.1785.
189. Tee, A. E. *et al.* (2016) 'The long noncoding RNA MALAT1 promotes tumor-driven angiogenesis by up-regulating pro-angiogenic gene expression', *Oncotarget*, 7(8), pp. 8663–8675. doi: 10.18632/oncotarget.6675.
190. Theissen, J. *et al.* (2014) 'Chromosome 17/17q gain and unaltered profiles in high resolution array-CGH are

prognostically informative in neuroblastoma', *Genes Chromosomes and Cancer*, 53(8), pp. 639–649. doi: 10.1002/gcc.22174.
191. Trojer, P. and Reinberg, D. (2007) 'Facultative Heterochromatin: Is There a Distinctive Molecular Signature?', *Molecular Cell*. Cell Press, pp. 1–13. doi: 10.1016/j.molcel.2007.09.011.
192. Tsai, M. C. *et al.* (2010) 'Long noncoding RNA as modular scaffold of histone modification complexes', *Science*, 329(5992), pp. 689–693. doi: 10.1126/science.1192002.
193. Tweddle, D. A. *et al.* (2001) 'p53 cellular localization and function in neuroblastoma: Evidence for defective G1 arrest despite WAF1 induction in MYCN-amplified cells', *American Journal of Pathology*, 158(6), pp. 2067–2077. doi: 10.1016/S0002-9440(10)64678-0.
194. Utley, R. T. and Côté, J. (2003) 'The MYST family of histone acetyltransferases', *Current Topics in Microbiology and Immunology*. Springer Verlag, pp. 203–236. doi: 10.1007/978-3-642-55747-7_8.
195. V, M.-C. *et al.* (2012) 'N-Myc and GCN5 regulate significantly overlapping transcriptional programs in neural stem cells', *PloS one*, 7(6). doi: 10.1371/JOURNAL.PONE.0039456.
196. Veal, G. J. *et al.* (2013) 'Adaptive dosing approaches to the individualization of 13-cis-retinoic acid (isotretinoin) treatment for children with high-risk neuroblastoma', *Clinical Cancer Research*, 19(2), pp. 469–479. doi: 10.1158/1078-0432.CCR-12-2225.
197. Vella, S. *et al.* (2015) 'Perhexiline maleate enhances antitumor efficacy of cisplatin in neuroblastoma by inducing over-expression of NDM29 ncRNA', *Scientific Reports*, 5(1), p. 18144. doi: 10.1038/srep18144.
198. Verdin, E. and Ott, M. (2015) '50 years of protein acetylation: From gene regulation to epigenetics, metabolism and beyond', *Nature Reviews Molecular Cell Biology*. Nature Publishing Group, pp. 258–264. doi: 10.1038/nrm3931.
199. Waddington, C. H. (2012) 'The epigenotype. 1942.', *International journal of epidemiology*, 41(1), pp. 10–13. doi: 10.1093/ije/dyr184.
200. Walz, S. *et al.* (2014) 'Activation and repression by oncogenic MYC shape tumour-specific gene expression profiles', *Nature*, 511(7510), pp. 483–487. doi: 10.1038/nature13473.
201. Wang, H. *et al.* (2020) 'Structure of the transcription coactivator SAGA', *Nature*, 577(7792), pp. 717–720. doi: 10.1038/s41586-020-1933-5.
202. Wang, X. and He, C. (2014) 'Dynamic RNA modifications in posttranscriptional regulation', *Molecular Cell*. Cell Press, pp. 5–12. doi: 10.1016/j.molcel.2014.09.001.
203. Wang, Y. *et al.* (2017) 'KAT2A coupled with the α-KGDH complex acts as a histone H3 succinyltransferase', *Nature*, 552(7684), pp. 273–277. doi: 10.1038/nature25003.
204. Wang, Z. *et al.* (2008) 'Combinatorial patterns of histone acetylations and methylations in the human genome', *Nature Genetics*, 40(7), pp. 897–903. doi: 10.1038/ng.154.
205. Watters, K. M. *et al.* (2013) 'Expressional alterations in functional ultra-conserved non-coding rnas in response to all-trans retinoic acid - induced differentiation in neuroblastoma cells', *BMC Cancer*, 13(1), p. 184. doi: 10.1186/1471-2407-13-184.
206. WC, G. *et al.* (2014) 'Drugging MYCN through an allosteric transition in Aurora kinase A', *Cancer cell*, 26(3), pp. 414–427. doi: 10.1016/J.CCR.2014.07.015.
207. Welch, C., Chen, Y. and Stallings, R. L. (2007) 'MicroRNA-34a functions as a potential tumor suppressor by inducing apoptosis in neuroblastoma cells', *Oncogene*, 26(34), pp. 5017–5022. doi: 10.1038/sj.onc.1210293.
208. Wilusz, J. E., Sunwoo, H. and Spector, D. L. (2009) 'Long noncoding RNAs: Functional surprises from the RNA world', *Genes and Development*. Cold Spring Harbor Laboratory Press, pp. 1494–1504. doi: 10.1101/gad.1800909.
209. Wong, M. *et al.* (2019) 'JMJD6 is a tumorigenic factor and therapeutic target in neuroblastoma', *Nature Communications*, 10(1). doi: 10.1038/s41467-019-11132-w.
210. Woo, C. W. *et al.* (2008) 'Use of RNA interference to elucidate the effect of MYCN on cell cycle in neuroblastoma', *Pediatric Blood and Cancer*. Pediatr Blood Cancer, pp. 208–212. doi: 10.1002/pbc.21195.
211. Wu, L. *et al.* (2015) 'Selective roles of E2Fs for ErbB2- and Myc-mediated mammary tumorigenesis', *Oncogene*, 34(1), pp. 119–128. doi: 10.1038/onc.2013.511.
212. Wu, T. P. *et al.* (2016) 'DNA methylation on N6-adenine in mammalian embryonic stem cells', *Nature*, 532(7599), pp. 329–333. doi: 10.1038/nature17640.
213. X, Y. *et al.* (2003) 'Low molecular weight inhibitors of Myc-Max interaction and function', *Oncogene*, 22(40), pp. 6151–6159. doi: 10.1038/SJ.ONC.1206641.
214. Xuan, J. J. *et al.* (2018) 'RMBase v2.0: Deciphering the map of RNA modifications from epitranscriptome sequencing data', *Nucleic Acids Research*, 46(D1), pp. D327–D334. doi: 10.1093/nar/gkx934.
215. Yoon, J. H. *et al.* (2013) 'Scaffold function of long non-coding RNA HOTAIR in protein ubiquitination', *Nature Communications*, 4. doi: 10.1038/ncomms3939.
216. You, J. S. and Jones, P. A. (2012) 'Cancer Genetics and Epigenetics: Two Sides of the Same Coin?', *Cancer Cell*. NIH Public Access, pp. 9–20. doi: 10.1016/j.ccr.2012.06.008.
217. Yu, M. *et al.* (2009) 'High expression of ncRAN, a novel non-coding RNA mapped to chromosome 17q25.1, is associated with poor prognosis in neuroblastoma', *International Journal of Oncology*, 34(4), pp. 931–938. doi: 10.3892/ijo_00000219.
218. Zeid, R. *et al.* (2018) 'Enhancer invasion shapes MYCN-dependent transcriptional amplification in neuroblastoma', *Nature Genetics*, 50(4), pp. 515–523. doi: 10.1038/s41588-018-0044-9.
219. Zhang, C. *et al.* (2009) 'PF-00477736 mediates checkpoint kinase 1 signaling pathway and potentiates docetaxel-induced efficacy in xenografts', *Clinical Cancer Research*, 15(14), pp. 4630–4640. doi: 10.1158/1078-0432.CCR-08-3272.
220. Zimmerman, K. A. *et al.* (1986) 'Differential expression of myc family genes during murine development', *Nature*, 319(6056), pp. 780–783. doi: 10.1038/319780a0.